Interaction between limbic circuits and basal ganglia in behaviour inhibition

by

Ashik Banstola

A thesis submitted for the degree of

Doctor of Philosophy

at the University of Otago, Dunedin,

New Zealand

21 December, 2018

Abstract

Changing behaviour in response to changing internal and external situations is crucial for survival. In particular, we need to inhibit ongoing, unwanted or inappropriate behaviour. Behavioural inhibition includes inhibition of an ongoing action, thought or emotion (in the basal ganglia; BG). But it can also involve inhibition of goals (in the limbic system) – which is much slower. A better understanding of the neural mechanisms controlling inhibition of behaviour is important for cognitive neuroscience, particularly in relation to problems of impulsivity. This thesis aims to fill a gap in our understanding of behavioural inhibition and to elucidate the parallel circuits that control its different types.

Several lesion, neuroimaging, and electrophysiological studies have been conducted to understand the role of brain regions in behavioural inhibition. Previous research has identified roles for the BG, orbitofrontal cortex (OFC) and hippocampus (HPC) in generation of various frequencies of rhythmicity during behavioural inhibition. However, the interaction between these regions has not been studied in rats during simple learning, simple action inhibition and complex behavioural inhibition. The stop signal task (SST) is the most commonly used paradigm to study simple behavioural inhibition. In this study, I recorded local field potentials (LFPs) simultaneously from BG (particularly striatum; STR and subthalamic nucleus; STN), OFC and HPC while rats performed the SST to assess how simple action inhibition differs from complex behavioural inhibition linked to goal-conflict.

The data show increases in the STN LFP spectral beta power and coherence with OFC after stopping an ongoing action (simple stopping). In contrast, stop failure increased HPC-STN coherent activity in the theta frequency band. In addition to the HPC, goal-conflict also activates OFC and STN during high conflict at higher theta frequency (11-12 Hz). In contrast, the conflict induced coherence effect was seen at lower theta frequencies (5-8 Hz) between two pairs of STN (HPC-STN and OFC-STN).

The results from the various experiments suggest that part of BG (STR and STN) and limbic system work in parallel and in a dynamic way for learning, response inhibition and complex behavioural inhibition (approach-avoidance conflict). The HPC is not involved in simple motor learning but may receive motivational information form STR and OFC. Simple inhibition involves mainly cortex and BG, while complex inhibition during goal-conflict also involves HPC, OFC and STN. Interestingly, goal inhibition appears to access circuits involved in simple stopping via OFC. In conclusion, functional connections between limbic and BG provides an adaptive control, so that goal selection (limbic structures) and programming of motor action (BG) can operate in parallel.

Acknowledgements

This work was carried out in the McNaughton's Lab, Department of Psychology, University of Otago, during the years 2015-2018. First and foremost I would like to thank my supervisor Prof. Neil McNaughton and co-supervisor Dr Louise Par-Brownlie for taking me as their doctoral student. Before I joined the Lab I had very limited knowledge in neuroscience as I majored in Pharmacology. I am forever indebted to my supervisors for what I have achieved while under their supervision. I greatly appreciate the effort with which Prof. McNaughton helped me learn how to plan and perform the experiments described here. I express my sincere thanks to Dr Louise Par-Brownlie for agreeing to act as my co-supervisor. Her guidance, support, and training for optogenetic was unforgettable. Prof McNaughton and Dr Brownlie not only help me to perform the study but also to discuss and present the data. Without their continual support and advice throughout my studies I would not have been able to finish my project. Prof. McNaughton's broad experience, expertise, wisdom and kindness never ceased to impress and educate me. Despite his never-ending hectic schedule, his door was always open to me. Thank you, I could not have asked for a better mentor.

Special thanks to Dr. Ming Ruan for teaching me the basics of stereotaxic surgery, and Rose Smither for viral training. I would like to thank Dr. Calvin Young for helping me setting up optogenetics and for supplying the Matlab code and reading resources. Calvin's technical knowledge in electrophysiology, data processing and signal analysis helped me a lot for the experimental work done here. I am thankful to all my lab members in both rat lab and human lab: my fellow colleague in the lab Carlos, Shabah, Tame, Bede and Ralph.

The technicians in the department of psychology were amazing people. Their continuous support made my project so much easier. I will never forget D-maze, Labjack and jig, which were key for my project. Thanks to all techs especially to Richard, Lindsay, Jeremy,

Willy, Russel, and Paul. I would also like to thank the animal technicians and vets. Natasha and Sara were of great help and I have lots of respect for their hard work.

Many thanks to Neurological Foundation of New Zealand for funding that helped me to present my preliminary result at Society for Neuroscience. Also thanks to Wayne, Rishi, and Rob for taking care of my rats while I was away. Thank you Faya and Anurag for all the support, encouragement, coffees in the staff room and the great advice. I would like to remember all my rats, especially Ash, Amt, Jam, Bal, Sabi, Poka, Katman, Hemj and Evrst for good behaviour.

Finally, I would like thank my parents, wife, brother, my wife Acika's family, who have supported us coming abroad to further my education. When I come home tired, there is nothing better than seeing my son Ajax smile. I could not have achieved what I have without Acika's support. She worked hard at her night job to financially support us, cook food and take good care of us.

Dedication

To my parents, my wife who have made it possible for me to come this far and my son. To all the rats used in this thesis.

Table of Contents

CHAPTER 1. INTRODUCTION 1

1.1 IMPULSIVITY AS A PROBLEM 1

1.2 OVERVIEW OF THE KEY REGIONS AND CIRCUITS FOR INHIBITORY PROCESSES 4

1.3 LOCAL FIELD POTENTIAL OSCILLATORY ACTIVITY IN RELATION TO BEHAVIOUR 6

1.4 ANATOMY AND FUNCTION OF STRUCTURES INVOLVED IN ACTION AND GOAL INHIBITION 7

1.4.1 Basal Ganglia (BG) 9

1.4.2 Orbitofrontal Cortex (OFC) 13

1.4.3 Hippocampus (HPC) 15

1.4.4 Network connections of basal ganglia, orbitofrontal cortex and hippocampus 18

1.5 SIMPLE INHIBITION - CURRENT MODELS OF SIMPLE STOPPING 20

1.5.1 Types of stopping 21

1.5.2 Mechanisms of simple motor stopping 22

1.5.3 Summary 25

1.6 COMPLEX INHIBITION - THE BEHAVIOURAL INHIBITION SYSTEM (BIS) 25

1.6.1 Simple versus complex inhibition 25

1.6.2 Gray's Behavioural Inhibition System Theory 26

1.6.3 Simple and complex inhibition – a number of possible networks 28

1.6.4 Hippocampus as the main node in the BIS 29

1.6.5 Hippocampal rhythmic slow activity 29

1.6.6 Neural circuitry involved in hippocampal rhythmicity 31

1.6.7 Summary 33

1.7 HYPOTHESES OF THE CURRENT THESIS 34

CHAPTER 2. GENERAL METHODS 37

2.1 SUBJECTS/PERMISSIONS 37

2.2 ELECTRODE ARRAY CONSTRUCTION 38

2.2.1 Reference Electrode and Earth electrode 38

2.2.2 Construction of electrodes for 28-channel recordings 39

2.3 SURGERIES AND ELECTRODE IMPLANTATION 43

2.3.1 Surgery 43

2.3.2 Electrode Implantation 46

2.3.3 Recovery from Surgery 48

2.4 GENERAL EXPERIMENTAL PROCEDURE 49

2.4.1 Food Restriction Scheme 49

2.4.2 D-Maze Apparatus 49

2.4.3 Experimental Procedure 50

2.4.3.1 Pre-training 50
2.4.3.2 Light 0 training: Sensor 0 (two sessions per day, 15 min each) 51
2.4.3.3 Light 1 Training: Sensor 1 (one session per day, 20 min each) 51
2.4.3.4 GO Training: Sensor 1 and then 5 (one session per day, 20 min each) 51
2.4.3.5 STOP Training 52
2.5 Local field potentials 53
2.6 Behaviour and LFP Recording 54
2.7 Data processing and Electrophysiological Analysis 55
2.8 Statistical Analysis 56
CHAPTER 3. ASSESSMENT OF ELECTRODE POSITIONING 58
3.1 Introduction 58
3.2 Histological methods 58
3.3 Results 59
3.3.1 Assessment of OFC electrode positioning 59
3.3.2 Assessment of striatum electrode positioning 60
3.3.3 Assessment of hippocampus-subthalamic electrode positioning 61
3.4 Conclusion 61
CHAPTER 4. ELECTROPHYSIOLOGICAL INVESTIGATION OF STRIATAL, ORBITOFRONTAL AND HIPPOCAMPAL DYNAMIC INTERACTIONS DURING SIMPLE MOTOR LEARNING 62
4.1 Introduction 62
4.1.1 The role of the striatum and orbitofrontal cortex in simple motor learning 62
4.1.2 The role of the hippocampus in simple motor learning 63
4.1.3 Interaction between striatum, orbitofrontal cortex and hippocampus in motor learning 63
4.2 Methods 64
4.2.1 GO Task 65
4.2.2 Data processing 66
4.2.2.1 Behavioural data 66
4.2.2.2 Event triggered power spectra – Go task 66
4.2.2.3 Event triggered coherence spectra – Go task 67
4.2.3 Statistical analysis 67
4.3 Results 67
4.3.1 Behavioural Data 67
4.3.2 Electrophysiological Analysis of task events (S1, S5 and S0) 70
4.3.2.1 Description: Power spectrograms for striatum, orbitofrontal cortex and hippocampus 70
4.3.2.2 Analysis: STR, OFC and HPC LFP power are modulated with task events during early and late period of learning 71
4.3.2.3 Description: Cohereogram between hippocampal-striatal, orbitofrontal-hippocampal and orbitofrontal-striatal during successive task events 75

4.3.2.4 Analysis: STR, OFC and HPC shows task dependent patterns of coherence at four frequency bands, during learning of GO task 75
4.4 DISCUSSION 79
4.4.1 Behaviour *80*
4.4.2 Striatal, orbitofrontal and hippocampus LFPs oscillations have different task-dependent coherence and power patterns 80

CHAPTER 5. INVOLVEMENT OF SUBTHALAMIC, ORBITOFRONTAL AND HIPPOCAMPAL OSCILLATIONS IN THE STOP SIGNAL TASK 84

5.1 INTRODUCTION 84
5.1.1 Role of subthalamic nucleus, orbitofrontal cortex and hippocampus in response inhibition *84*
5.1.2 Cortico-subthalamic and Cortico-hippocampal interaction for behavioural inhibition *85*
5.2 MATERIALS AND METHODS 86
5.2.1 Stop Signal Task *86*
5.2.2 Electrophysiological Analysis *87*
5.2.3 Stop Signal Reaction Time (SSRT) Estimation *87*
5.2.4 Statistical analysis *88*
5.3 RESULTS 89
5.3.1 Behavioural data *89*
5.3.2 Neurophysiological data *91*
5.3.2.1 Description: Power spectrum between correct Go, correct Stop and failed Stop trials 91
5.3.2.2 Analysis: Mean power between STN, OFC and HPC for four frequency bands during SST task 92
5.3.2.3 Description: Comparison between correct Stop and correct Go trials 94
5.3.2.4 Description: Comparison between correct Stop and failed Stop trials 95
5.3.2.5 Description: Comparison between failed Stop and correct Go trials 96
5.3.2.6 Analysis: Stop-Go power differences (i.e. changes due to Stop signal) in correct and incorrect stopping for four frequency bands during SST task 97
5.3.2.7 Description: Coherence spectrum between correct Go, correct Stop and failed Stop trials 98
5.3.2.8 Analysis: Mean coherence between HPC-OFC, HPC-STN and OFC-STN for four frequency bands during SST task 99
5.3.2.9 Analysis: Stop-Go coherence differences (i.e. changes due to Stop signal) for correct and incorrect stopping for four different bands 101
5.4 DISCUSSION 102

CHAPTER 6. DYNAMIC INTERACTION BETWEEN HIPPOCAMPUS, ORBITOFRONTAL CORTEX AND SUBTHALAMIC NUCLEUS DURING GOAL-CONFLICT IN THE STOP SIGNAL TASK 105

6.1 INTRODUCTION 105
6.1.1 The Role of the HPC, OFC and BG during conflict *105*
6.1.2 Is goal conflict a separate process from simple behavioural inhibition? *106*
6.2 METHODS 107

6.2.1 Data processing *107*
6.2.1.1 Separating low, intermediate and high delay stop trials 107
6.2.1.2 Spectral power and coherence post-processing – Stop and Go trials 107
6.2.2 Data Analysis *107*
6.3 RESULTS 108
6.3.1 Mean power of OFC, HPC and STN theta LFPs at three correct stopping values (25%, 50% and 75%) during SST *108*
6.3.2 Quadratic and linear effects of percent correct stopping on power *109*
6.3.3 Mean coherence of OFC, HPC and STN theta LFPs at three correct stopping values (25%, 50%, 75%) during the SST *110*
6.3.4 Quadratic and linear effects of percent correct stopping on coherence *111*
6.4 DISCUSSION 113
6.4.1 Goal-conflict related HPC, OFC and STN theta power *113*
6.4.2 Goal-conflict related HPC, OFC and STN theta coherence *114*

CHAPTER 7. GENERAL DISCUSSION 116

7.1 ELECTROPHYSIOLOGY OF STR, OFC AND HPC DURING SIMPLE MOTOR LEARNING/ APPROACH BEHAVIOUR 117
7.1.1 The role of STR in simple motor learning *117*
7.1.2 The role of OFC in simple motor learning *118*
7.1.3 HPC involvement in simple motor learning *119*
7.2 ELECTROPHYSIOLOGY OF STN, OFC AND HPC DURING SIMPLE RESPONSE INHIBITION (STOPPING) 119
7.2.1 STN and OFC involvement in response inhibition *120*
7.2.2 HPC involvement in response inhibition *120*
7.3 ELECTROPHYSIOLOGY OF STN, OFC AND HPC DURING COMPLEX INHIBITION (APPROACH-AVOIDANCE / GOAL-CONFLICT) .122
7.3.1 Conflict activations in OFC *122*
7.3.2 Conflict activations in HPC *123*
7.3.3 Conflict activations in the STN *123*
7.4 IMPLICATIONS FOR MOTIVATION, RESPONSE INHIBITION AND BEHAVIOURAL INHIBITION 125
7.4.1 Implications for motivation *125*
7.4.2 Implications for response inhibition *127*
7.4.3 Implications for complex behavioural inhibition (goal-conflict) *128*
7.5 IMPLICATIONS FOR THE FUTURE RESEARCH 130
7.6 FINAL REMARKS 131

List of Figures

Figure 1.1 Frontal, BG and hippocampal connectivity for motor cognitive interaction. 9
Figure 1.2 Cortico-basal ganglia-thalamo-cortical circuit mediating goal selection, action selection and motor act selection through limbic, associative and sensorimotor circuit respectively. 11
Figure 1.3 Schematic diagram showing OFC inputs. 14
Figure 1.4 Cortical and subcortical connections of HPC. 16
Figure 1.5 Proposed neural connection between BG, OFC and STN for going and stopping and their links to the BIS (shaded box). 20
Figure 1.6 Graphic representation of the assumptions and predictions of the horse-race model. 23
Figure 1.7 A fronto-basal ganglia model of response control in A. Go and B. Stop trials. 24
Figure 1.8 An updated model for the relationship of approach (BAS = behavioural approach/activation system), avoidance (FFFS = fight, freeze, flee), and conflict (BIS = behavioural inhibition systems)— an updated model. 27
Figure 1.9 Neural circuitry involved in the generation of theta oscillations. 32
Figure 2.1 Procedure for 28 channel electrode construction. 40
Figure 2.2 Jig for implanting the array. 42
Figure 2.3 shows final multi electrode arrays with electrode tip for HPC-STN array. 43
Figure 2.4 The location for unilateral stereotaxic electrode implantation into HPC-STN, BG and OFC. X; location of reference electrode. The recording sites mapped from Paxinos and Watson (2007). 47
Figure 2.5 Rat with 32pin-3 array implant. 48
Figure 2.6 Schematic diagram of D-maze. 50
Figure 2.7 Flow chart showing contingencies for the Stop signal task. 52
Figure 2.8 Experimental setup and LFP recordings 55
Figure 3.1 Histological placements of OFC electrodes. 59
Figure 3.2 Histological placements of STR recording electrodes. 60
Figure 3.3 Histological placements of HPC-STN recording electrodes. 61
Figure 4.1 Photographic representation of animal performing Go Task. 65
Figure 4.2 Early and late response on the Go trials. 68
Figure 4.3 Pictorial representation of movement profiles across early and late period of learning sessions. 69
Figure 4.4 Average time frequency power spectra over all sessions across rats (n=5). 70
Figure 4.5 STR, OFC and HPC power at four frequency bands are differentially modulated during learning of D-maze GO task before sensor triggered. 72
Figure 4.6 STR, OFC and HPC power at four frequency bands are differentially modulated during learning of D-maze GO task after sensor triggered. 73
Figure 4.7 STR, OFC and HPC mean power at four frequency bands are differentially modulated during learning of GO task after-before sensor triggered. 74
Figure 4.8 Coherogram average over all sessions across rats (n=5). 75

Figure 4.9 The mean coherence between HPC-STR, OFC-HPC and OFC-STR LFP oscillations before sensor triggered for successive task events at early and late period of training.....76
Figure 4.10 Distinct frequency bands exhibit different coherence variations in task events of after sensor triggered at early and late period of learning. 77
Figure 4.11 Mean coherence between HPC-STR, OFC-HPC and OFC-STR LFPs oscillations during 0.5s before and after sensor triggered for successive task events at early and late period of learning. 78
Figure 5.1 Rat performing Stop signal task.....86
Figure 5.2 Behavioural measures across SSDs 89
Figure 5.3 Average time-frequency plot showing LFP activity of correct Go trials (left panels) and matching correct Stop (center panels) and failed Stop (right panels). 91
Figure 5.4 Mean power during Stop-signal task performance comparing correct Go, correct Stop, and fail stop before (left panels) and after (middle panels) event marker triggered. The right panels shows the difference between them. 93
Figure 5.5 Average time-frequency plot showing LFP activity of correct Go trials (left panels) and latency-matched correct Stop (center panels) and their differences (right panels). 94
Figure 5.6 Average time-frequency plot showing LFP activity of correct Stop trials (left panels) and failed Stop (center panels) and their differences (right panels). 95
Figure 5.7 Average time-frequency plot showing LFP activity of failed Stop trials (left panels) and latency-matched correct Go (center panels) and their differences (right panels).....96
Figure 5.8 Changes in mean power during Stop signal task performance, comparing correct Stop-correct Go (CSt-CGo), correct Stop-failed Go (CSt-FGo) and failed Go-correct Go (FGo-CGo) at four frequency bands.....98
Figure 5.9 Time-frequency plot showing coherence between brain areas during correct Go, correct Stop and failed Stop. CGo; correct Go, CSt; correct Stop and FSt; failed Stop. 99
Figure 5.10 Mean coherence during Stop-signal task performance comparing correct GO (CGo), correct Stop (CSt) and Stop failure (FSt) before, after and difference (after-before). 100
Figure 5.11 Changes in mean coherence during Stop signal task performance, comparing correct Stop-correct Go (CSt-CGo), correct Stop-failed Go (CSt-FGo) and failed Go- correct Go (FGo-CGo) at four frequency bands. 102
Figure 6.1 mean theta power during correct Stop, correct Go and Stop-Go differences.....108
Figure 6.2 Power in Stop trials relative to Go trials. 110
Figure 6.3 mean theta coherence during correct Stop, correct Go and Stop-Go differences. 111
Figure 6.4 Coherence in Stop trials relative to Go trials. 112
Figure 7.1 proposed neural connection between BG, OFC and STN for going and stopping and their links to the BIS (shaded box). 124

List of Tables

Table 2.1 List of drugs used for surgeries and their designated concentrations and dose rate. **44**
Table 2.2 Amount of Isoflurane anesthesia in different surgical periods **45**
Table 4.1 Performance on the Go task. Data presented are average across rats across sessions. **68**
Table 5.1 Performance on the Stop Signal Task in Experiment 2 .....**89**

List of Abbreviations

ACC	anterior cingulate cortex
AP	anterior posterior
ADHD	attention deficit hyperactivity disorder
ANOVA	analysis of variance
ATN	anterior thalamic nucleus
AV	ventral anterior nucleus
BAS	behavioural approach system
BIS	behavioural inhibition system
BG	basal ganglia
CA1	cornu ammonis subfield 1
CA3	cornu ammonis subfield 3
CGo	correct GO
CN	caudate nucleus
CSt	correct Stop
-d	dorsal
DA	dopamine
DBS	deep brain stimulation
DG	dentate gyrus
DLPFC	dorsolateral prefrontal cortex
DM	dorsalis medialis
dPM	dorsal premotor cortex
EEG	electroencephalography
ERHC	entorhinal cortex
FGo	failed go

FSt	failed Stop
GABA	gamma amino butyric acid
GORT	go reaction time
GPe	globus pallidus pars externa
GPi	globus pallidus pars interna
HF	hippocampal formation
HPC	hippocampus
Hz	hertz
i.p	intraperitoneal
ICD	impulse control disorder
IFG	inferior frontal gyrus
IL	infralimbic
kg	kilogram
-lat	lateral
LH	limit hold
LFP	local field potentials
-m	medial
M1	primary motor cortex
MDTN	medial dorsal thalamic nuclei
MEAs	microelectrode arrays
MFB	medial forebrain bundle
mg	milligram
ms	millisecond
mRT	mean reaction time
MS	medial septum

NAcc	nucleus accumbens core
NegR	negative reinforcer
OFC	orbitofrontal cortex
PCS	percent correct stopping
PD	Parkinson’s disease
PFC	prefrontal cortex
PL	prelimbic
PreSMA	pre-supplementary motor areas
PosR	positive reinforcer
PUT	putamen
rIFG	right inferior frontal gyrus
RSA	rhythmic slow activity
s	second
s.c	subcutaneous
SMA	supplementary motor area
SNc	substantia nigra pars compact
SNr	Substantia nigra pars reticulate
SSD	stop signal delay
SSRT	signal reaction time
SST	stop signal task
STN	subthalamic nucleus
STR	striatum
SUB	subiculum
Subst. nigra	substantia nigra
TEO	inferior temporal cortical areas

-v	ventral
vGP	ventral pallidum
VLm	ventral lateral nucleus pars medialis
VLo	ventral lateral nucleus pars oralis

Chapter 1. Introduction

1.1 Impulsivity as a problem

Adaptive behaviour in response to changing internal and external situations is crucial for survival. We need to adapt our behaviour based on previous experiences, by continuously monitoring and updating our actions in response to changes in the environment. In particular, to adapt, we need to inhibit ongoing or pre-potent unwanted or inappropriate behaviour. A better understanding of the neural mechanisms of the generation, and particularly inhibition, of behaviour, is essential for cognitive neuroscience. In this thesis, I will assess the possible interactions between limbic structures and basal ganglia (BG) in the generation of inhibitory processes that contribute to cognitive control.

Cognitive control involves a set of processes by which goals or plans influence behaviour. It helps us to initiate, coordinate, monitor and update our behavioural strategies. Cognitive functions depend on interconnected networks of anatomical components. Each network system has a different role, with some elements more central to network function. For the selection of behaviour in complex situations, inhibition of unwanted response is arguably central given that many behaviours could be elicited simultaneously. There are many questions about inhibitory processes that have not been answered and require further investigation.

Upcoming behaviour may need to change, or ongoing behaviour stop, because it is inappropriate given the current situation in daily life. Response inhibition – the ability to suppress or cancel future actions that are unsafe, no longer relevant, or not required – is crucial. Failure of response inhibition leads to impulsive behaviour. Impulsivity is a tendency to do things suddenly without any planning and without considering the future effects of our actions. Moderate levels of impulsivity can be beneficial, helping us to gain valuable experience. However, excessive impulsivity is dysfunctional and generates symptoms of psychiatric disorders including attention deficit hyperactivity disorder (ADHD), bipolar disorder (Mason,

O'Sullivan, Montaldi, Bentall, & El-Deredy, 2014), personality disorder, Parkinson's disease (Gauggel, Rieger, & Feghoff, 2004), impulse control disorder, substance use disorder (Najt et al., 2007; Winstanley, 2011), and antisocial behaviour (Dalley, Everitt, & Robbins, 2011).

Impulsivity is multifaceted (Donnelly et al., 2014). Impulsive choice (decision making) and impulsive action (motor disinhibition) are two primary components of the purest form of impulsivity (Jupp, Caprioli, & Dalley, 2013) that may occur due to deficits in selective attention to relevant information and inhibitory control (Evenden, 1999). Most studies of impulsivity focus on impulsive choice rather than action. Impulsive action occurs due to failure to stop or cancel an inappropriate response to a pre-potent stimulus (Broos et al., 2012). Suppression of actions supports flexible and goal-directed behaviour in changing environments. To achieve a goal, one must use previous experience or knowledge to plan appropriate steps and then keep on task. This behaviour allows us to not just react to the world but act upon it to obtain the desired outcome (Buschman & Miller, 2014).

Impulsive behaviour results from various independent neurochemical mechanisms that can interact to change the behaviour of individuals (Evenden, 1999). The behavioural and neurobiological analysis defines different forms of impulsivity depending on the distinct dysfunctions they produce in fronto-striatal circuits (Dalley et al., 2011). Both subcortical and cortical structures are associated with impulsivity (Balasubramani, Chakravarthy, Ali, Ravindran, & Moustafa, 2015). More recently it has been found that impulsive behaviour may occur due to an imbalance between "top-down" control by frontal cortex and "bottom-up" control by limbic regions (Sala et al., 2011; Siever, 2008). Dysfunction and imbalance of neuromodulators such as dopamine (DA) and serotonin in the fronto-striatal circuitry may play a role in impulsivity (Aron, 2011; Dalley, Mar, Economidou, & Robbins, 2008; Jahanshahi, Obeso, Rothwell, & Obeso, 2015). Bari et al. (2011) found distinct monoaminergic contributions that modulate action inhibition: noradrenergic inputs selectively impaired

stopping and dopaminergic inputs prolonged go reaction time. Depletion of DA in the frontal cortex, limbic cortex, and striatum (STR) could, therefore, affect impulsivity.

The thesis aims to examine the possible interactions between fronto-BG and limbic structures, especially the hippocampus (HPC) when stopping or cancelling an inappropriate response (actions and thoughts) to a stimulus. We believe limbic interaction with fronto-BG circuitry supports flexible and goal-directed behaviour in response to changing environments. In addition to the fast simple-action stopping that explicitly involves the motor system, slower goal inhibition is vital for the execution of more complex plans including limbic structures. Therefore, the involvement of inhibitory networks depends on time pressure and affect (McNaughton & Corr, 2004). For instance, the frontal-BG network is recruited for quick but simple action stopping, while limbic-BG system connections might play a vital role for slower but more accurate goal inhibition. Hence, goal inhibition could result in selective inhibitory control.

Limbic control characteristically involves brain rhythmicity. The functions of such rhythmicity vary with types of oscillatory activity, events during behavioural tasks and the specific brain region included. I will try to answer; how heavily interconnected BG-limbic system allows precise behavioural control in simple and complicated processes. I will examine various frequencies of rhythmicity that bind parts of the BG-limbic system into different functional circuits on different occasions of stopping or cancelling inappropriate responses.

In the following sections, section 1.2 will provide an overview of how BG, orbitofrontal cortex (OFC) and HPC are linked to inhibitory processes. Section 1.3 will give a general overview of how brain oscillations are important for regulating information flow across brain areas. It also provides some examples of LFPs oscillatory activity to behaviour. Section 1.4 then discusses in detail the anatomy of BG, OFC and HPC and links their connectivity to function. Section 1.5 describes in detail current models of simple action inhibition. In section

1.5, I will regularly highlight the STN, which is a crucial node in the BG, and may play a particularly important role in stopping and impulsivity because it is well placed to suppress the "direct" fronto-striatal pathway that is activated by response initiation. Action stopping is in general motoric and focused on reaction to a cue or event in the environment that occurs after the response has been initiated. However, impulses are not only motoric, but they are also emotional and motivational as well. It is likely that inhibitory control may extend to the limbic domain to implement inhibition of goals for action. So, in section 1.6 I will discuss Gray's Behavioural Inhibition System (BIS) theory that provides a model of complex inhibition. Finally, section 1.7 presents resultant hypotheses, research questions and the overview of the experiments to be performed.

1.2 Overview of the key regions and circuits for inhibitory processes

Past studies have reported that inhibitory control depends on circuits and brain structures such as BG (Jentsch & Taylor, 1999), frontal cortex (Dalley, Theobald, Eagle, Passetti, & Robbins, 2002; Deng et al., 2017) and HPC (Abela, Dougherty, Fagen, Hill, & Chudasama, 2013). Their detailed anatomy and functions are described in later sections, but first I provide a brief overview of these areas that are jointly involved in inhibitory control.

For adaptive behaviour (for instance, motor inhibition) the BG are centrally involved. The STR responds to the Go cue, while stop-related activity develops in STN (N. Mallet et al., 2016). STN is activated by stopping or pausing in a wide range of species as shown in neuroimaging in humans (Aron & Poldrack, 2006), non-human primates (Isoda & Hikosaka, 2008), and in vivo recordings in rodents (Schmidt, Leventhal, Mallet, Chen, & Berke, 2013). Evidence from STN-deep brain stimulation (DBS) for Parkinson's disease suggests that STN stimulation facilitates the selection and inhibition of motor responses (Ray et al., 2012; van den Wildenberg et al., 2006). Furthermore, studies have shown that conflict (Zavala, Zaghloul, &

Brown, 2015), unexpected (Wessel & Aron, 2017) or surprising events (Fife et al., 2017; Wessel et al., 2016) also recruit the STN for pausing or stopping.

The OFC may be necessary for inhibiting unwanted consequences. Dysfunction in OFC has been linked to inhibitory control disorders (Dillon & Pizzagalli, 2007; Eagle & Baunez, 2010; Leventhal et al., 2012). It acts as an important area for suppression of behaviour (Bryden & Roesch, 2015) and conflict-induced executive control adjustment (Mansouri, Buckley, & Tanaka, 2014). OFC is heavily connected with cortical (frontal cortex, sensory cortex and premotor areas), subcortical (STR, hypothalamus, periaqueductal grey matter, basal forebrain) and other limbic structures. Among the limbic regions, connections with the HPC and parahippocampal areas are important (Cavada, Company, Tejedor, Cruz-Rizzolo, & Reinoso-Suarez, 2000). OFC receives direct projections from the HPC (Cavada et al., 2000; Haber & Calzavara, 2009). Moreover, HPC and STR (particularly the caudate nucleus) are functionally distinct regions, but both have anatomical links with the OFC (Brown, Ross, Tobyne, & Stern, 2012).

In addition to the BG and OFC, there is a well-established role of the HPC in active inhibition of goal-directed responses (Gray & McNaughton, 2000). It has been shown that lesions in both ventral and dorsal HPC produce inhibitory control deficits in rats (Abela et al., 2013; Chudasama, Doobay, & Liu, 2012), and disrupt normal context specific inhibition during discrimination learning (McDonald, Devan, & Hong, 2004). Suppression of unwanted thoughts also engages HPC through a fronto-hippocampal inhibitory control pathway (Schmitz, Correia, Ferreira, Prescot, & Anderson, 2017). These observations raise the possibility that HPC is recruited for inhibitory control of adaptive behaviour. Historically, the HPC has been viewed as a critical area where function depends on low frequency rhythmic ("theta") oscillations (Buzsáki, 2002; Gray & McNaughton, 2000; Vertes & Kocsis, 1997). However, more recently theta and related rhythms have been seen as necessary for other areas such as frontal cortex

(Amarante, Caetano, & Laubach, 2017; O'Neil et al., 2015). This thesis will focus on task-related rhythmicity in each of BG, OFC and HPC – and assess the relationships among these areas.

1.3 Local field potential oscillatory activity in relation to behaviour

Brain oscillations (brain waves) are rhythmic or repetitive patterns of neural activity. Oscillations are generated either by single neurons or due to an interaction between neuronal populations. Brain rhythms are ubiquitous phenomena of complex brain dynamics (Cannon et al., 2014). Oscillations can be divided into microscopic (membrane potential oscillations), mesoscopic (local field potential) or macroscopic oscillations (scalp or epidural) (C. K. Young & Eggermont, 2009). Oscillations are important features of neuronal activity. Various spectral dynamics of oscillations such as phase, amplitude, frequency and degree of rhythmicity are essential for regulating information flow across brain areas. In general, neuronal oscillations are investigated through the measures of coherence and power (Fransen, van Ede, & Maris, 2015).

LFP are summed electrical activity recorded extracellularly from the neuronal population around the electrode tip (Pani et al., 2014). It has been argued that LFPs represent relatively slow current fluctuations (e.g. synaptic currents, sodium and calcium spikes, ionic fluxes through voltage-and ligand-gated ion channel) in the extracellular matrix rather than local spiking activity (Buzsaki, Anastassiou, & Koch, 2012).

Rhythmicity has been separated into conventional frequency bands in human electroencephalography (EEG): delta = 1-4 Hz; theta = 4-7 Hz; alpha = 8-12 Hz; beta = 12-30 Hz; gamma = 30-100 Hz. The human and rat theta terminology are different. Despite human theta, rodent hippocampal “theta band” is more extensive, 4-12 Hz, rhythmic oscillatory activity (see page 31 for more details). These have been implicated in distinct cognitive processes. For instance, alpha (8-12 Hz) and beta (13-35 Hz) in the dorsal premotor cortex of

monkey promotes motor coordination (Pani et al., 2014). Increased alpha oscillation (11-13Hz) is implicated in volitional inhibition of acquired motor programmes over sensorimotor area (Knyazev, 2007). Human studies show that behavioural disinhibition and cognitive deficits (emotional and motivational) are also associated with increased slow-wave activity and deficient alpha oscillation (Knyazev, 2007; Knyazev & Slobodskaya, 2003).

Network oscillations have a role in communication across brain structures (Fujisawa & Buzsaki, 2011). Most brain systems are circuits: the output of one computation can become the input for the next many times over. Such “recursive processing” progressively refines signals, massively increases computational power (Eagle & Robbins, 2003a), and results in rhythmicity, which is functional and not a mere epiphenomenon (McNaughton, Ruan, & Woodnorth, 2006). Rhythmicity appears to be important both for the production of relatively simple motor responses and for the control of the action by goal processing in, for example, the Papez circuit. As described by James Papez in 1937, the limbic system is complex and consists of both cortical and subcortical structures such as the cingulate gyrus, the hypothalamus, the anterior thalamic nucleus, the HPC and their connections. The limbic system plays a significant role in emotional and motivational activity among others (Morgane, Galler, & Mokler, 2005).

Rhythmicity also provides knowledge of normal as well as pathological brain function. For instance, excessive synchronisation occurs during a seizure in epilepsy. Thus, brain rhythms are essential for information processing across brain areas. In the next section, I will discuss in detail the anatomy of BG, OFC and HPC and link their connectivity to function.

1.4 Anatomy and function of structures involved in action and goal inhibition

In the neuroscience literature, the term "inhibition" has a wide range of meanings with its subtypes belonging to different levels of analysis described by different authors. Inhibition can refer to the form of observed acts/actions/behaviours or to neural inhibition, i.e. at a

synapse. Importantly, inhibition at a synapse can release action. Inhibition may also refer to forms of control that do not engage the motor system for instance, control of impulses, thoughts, and emotions. Successful behavioural or cognitive inhibition involves monitoring performance and then adjusting response strategies. “Inhibition is therefore not an occasional accident; it is an essential and unremitting element of our cerebral life" (James, 1890). Hence, the relationship between inhibition of physical responses (involving the motor system) and mental processes (with no explicit motor system involvement) is not entirely clear.

Information requiring stopping of current behaviour is quickly sent to prefrontal cortex and a stopping command is generated. Two main regions of prefrontal cortex are involved in stopping: the dorsomedial frontal cortex (pre-supplementary motor areas; PreSMA) and the right inferior frontal gyrus (rIFG). The rIFG includes several distinct areas of lateral prefrontal cortex: Brodmann’s areas 44 (opercularis), 45 (triangularis), and 47/12(orbitalis) (Aron, 2011). Due to their strong functional similarities, rIFG in humans is thought to be a homologous region to OFC in rats (Birrell & Brown, 2000; Eagle et al., 2008). Cortical input in relation to the stopping command is then sent to BG. Among BG structures, the STR is a major input nucleus for going and the STN is a major target for the production of action stopping.

For successful adaptation to the environment we require control over thoughts and behaviours. It is easy to conclude when motor inhibition has occurred because a motor response is withheld or withdrawn. By contrast, cognitive inhibition is often more diverse and complicated. This cognitive control is especially important for processing of goal-relevant information (Miller & Cohen, 2001).

Stopping of action can get more complicated when there is an involvement of thoughts, goals or competing goals. In such cases, the simple action stopping circuit may need inputs from brain areas involved in goal inhibition. For stopping goals, subjects must have information on what to stop and use it on how and when inhibition should be implemented. This likely

involves brain areas responsible for motivation, including the limbic system and particularly the HPC. As seen in Figure 1.1, the BG have connections with frontal areas and the HPC for attention, memory and executive function (Leisman, Braun-Benjamin, & Melillo, 2014). The involvement of the limbic system could result in selective inhibitory control. However, the mechanisms of such selective effects of the limbic system are not clear yet. Hence, it is important to differentiate behavioural inhibition in the sense of action stopping and goal inhibition. Behaviourally, both of these can look quite similar; nevertheless neurally, functionally, and in terms of speed, they can be different.

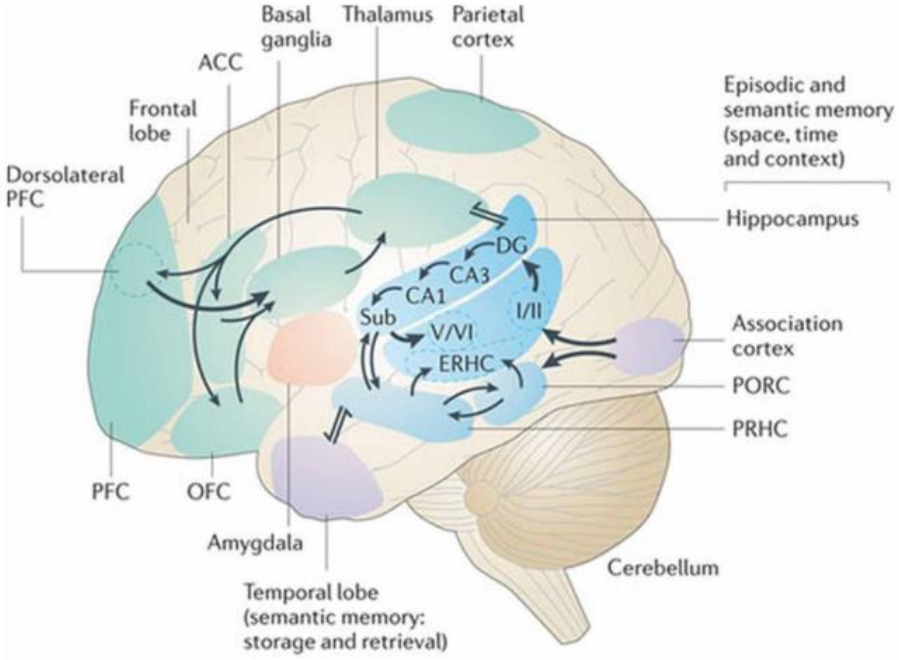

Figure 1.1 Frontal, BG and hippocampal connectivity for motor cognitive interaction.

Specific connectivity of the BG with other brain areas for attention, working memory, and executive function. ACC: anterior cingulate cortex; PFC: prefrontal cortex; DG: dentate gyrus. CA1: cornu ammonis subfield 1; CA3: cornu ammonis subfield 3; Sub: subiculum; ERHC: entorhinal cortex; PORC: postrhinal cortex; PRHC: perirhinal cortex; I/II, V/VI: layers of the entorhinal cortex. Figure copied with permission from Leisman et al. (2014).

1.4.1 Basal Ganglia (BG)

The BG are a group of subcortical nuclei, located at the base of the forebrain and highly connected to the thalamus and cerebral cortex. The BG and related nuclei can be divided into input, output and intrinsic nuclei (Lanciego, Luquin, & Obeso, 2012).

1. Input Nuclei (STR) – caudate nucleus (CN), putamen (Put), nucleus accumbens core (NAcc), STN– receive information from different sources, mainly from cortical, thalamic and nigral regions.
2. Intrinsic Nuclei – globus pallidus pars externa (GPe), STN (also an input nucleus), substantia nigra pars compacta (SNc) – relay information between input and output nuclei.
3. Output Nuclei – globus pallidus pars interna (GPi), substantia nigra pars reticulata (SNr) – send BG information to the thalamus.

Figure 1.1 shows the important BG connections with other regions of the brain such as the cortex, thalamus, HPC and amygdala (through limbic circuits) (Haegelen, Rouaud, Darnault, & Morandi, 2009). The BG receive most of their afferent input from cerebral cortex, mainly from the frontal lobe (premotor, SMA, area8, DLPFC, lat/mOFC and ACC) and thalamus (also see figure 1.2). This input is directed to both the STR and the STN. The STR is the major input nucleus of BG and consists of both dorsal STR (CN, Put) and ventral STR (NAcc) (Jahanshahi, Obeso, Rothwell, & Obeso, 2015; Schmidt, Leventhal, Mallet, Chen, & Berke, 2013). Being a part of the extrapyramidal motor system BG is thought to be involved mainly in higher order movement initiation, execution, inhibition and voluntary control of eye movement (Leisman et al., 2014).

Figure 1.2 shows the BG circuitry mediating motor act selection, action selection and goal selection through parallel sensorimotor, associative, and limbic circuits, respectively. The sensorimotor circuit involves connections to the supplementary motor area (SMA), pre-motor cortex, and primary motor cortex (M1); while the oculomotor circuit projects to the frontal eye field and supplementary eye field. The associative circuit includes dorsolateral prefrontal cortex (DLPFC) and lateralOFC (Manes et al., 2014). Lastly, the limbic circuit is connected to the dACC, mOFC , prelimbic and infralimbic areas (Haegelen et al., 2009). Individual

networks seem to be engaged in specific behavioural functions. Damage to the BG loop within motor areas of the cortex leads to motor symptoms, whereas higher order deficits are due to damage to the subcortical components of circuits within non-motor areas (Leisman et al., 2014).

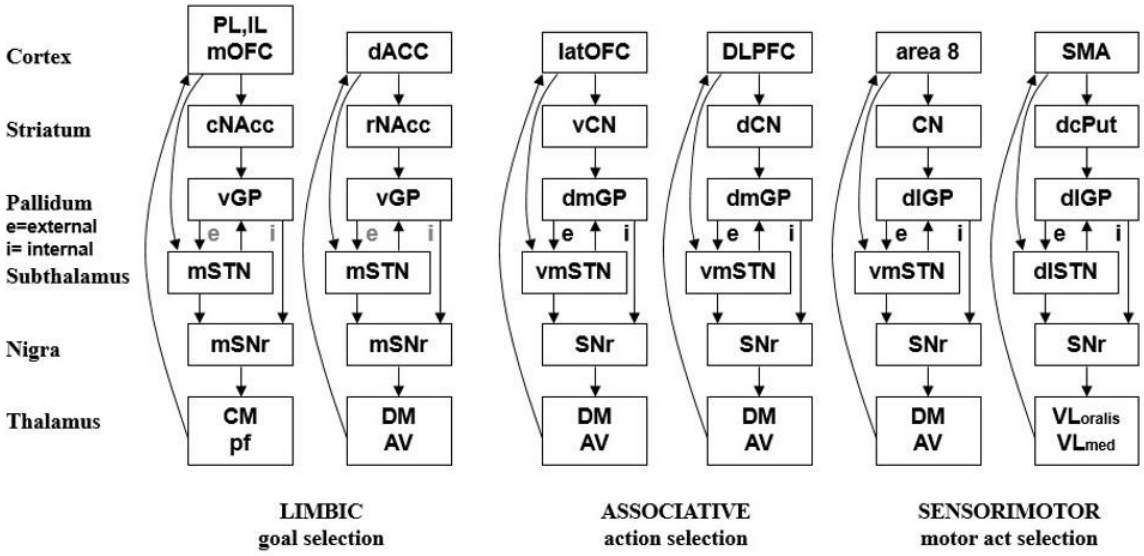

Figure 1.2 Cortico-basal ganglia-thalamo-cortical circuit mediating goal selection, action selection and motor act selection through limbic, associative and sensorimotor circuit respectively.

The STN is in central position within cortico-basal ganglia thalamo-cortical circuit. ACC: anterior cingulate cortex; CN: caudate nucleus; PL: prelimbic; IL: infralimbic; NAcc: nucleus accumbens core; -r: rostral; -m: medial: -d: dorsal; -v: ventral; -lat: lateral; -dm: dorsomedial; -dl: dorsolateral; -vm: ventromedial; DLPFC: dorsolateral prefrontal cortex; GPi/e: globus pallidus pars interna/externa; OFC: orbitofrontal cortex; Put: putamen; STN: subthalamic nucleus; SMA: supplementary motor area; SNr: substantia nigra pars reticulata; SNr: substantia nigra; AV: ventral anterior nucleus; VLo: ventral lateral nucleus pars oralis; VLm: ventral lateral nucleus pars medialis; DM: dorsalis medialis; CM: centromedian; pf: parafascicular. Unpublished figure provided by Neil McNaughton based on previous work (Chambers, Garavan, & Bellgrove, 2009; Haber & Calzavara, 2009; Haegelen et al., 2009; Humphries & Prescott, 2010).

The BG has a complex internal network and neurochemical organisation. DA is a key neurotransmitter in the BG. The primary ascending dopaminergic neurons originate from the SNc – a BG structure, located in the midbrain, which is the main source of striatal DA. In addition, DA is also released from other midbrain structures such as ventral tegmental areas (VTA) which have large projection to the brain region involved in goal directed and reward

processing, for instance NAcc and ventral STR giving rise to mesolimbic pathway (Sesack & Grace, 2010). Nevertheless, SNc has an extensive connection with the dorsal STR giving rise to the nigrostriatal pathway and involved in the regulation of impulse control (Dalley & Roiser, 2012). DA is implicated in normal brain functioning such as motivation, reinforcement learning and motor control as well as brain pathology, for instance Parkinsons disease. DA and agonists of dopaminergic receptors could also contribute to the development of impulsivity.

The role of the BG in motor control has been extensively studied (Leisman et al., 2014; Nambu, Tokuno, & Takada, 2002; Schmidt et al., 2013). It also contributes to other functions such as learning, visual selective attention (Tommasi et al., 2015), human linguistic activity, reasoning and reward-related behaviour and emotions (Lanciego et al., 2012). Cognitive functions of the BG depend on a neuronal circuit between the BG and frontal cortex. Fronto-basal ganglia-thalamo-cortical circuits mediate social behaviour and motivation, executive functions, motor activity and eye movements. BG is also implicated in decision making allowing an individuals to respond appropriately to environmental cues through information that flows from limbic, to cognitive to motor circuits (Haber & Calzavara, 2009). Redgrave, Prescott, and Gurney (1999) have proposed that the BG are a centralized selection device, specialized to resolve action conflicts over access to limited motor and cognitive resources.

The STN is a small biconvex nucleus of the BG located ventral to the zona incerta and dorsal to the cerebral peduncle (Nambu et al., 2002; Temel, Blokland, Steinbusch, & Visser-Vandewalle, 2005). Previously, it was believed to be a relay station (serving as a "gate") for cortico-basal ganglia-thalamocortical circuits; but now is considered both as a main motor regulating centre (Temel et al., 2005) and a key structure for limbic-BG function (Haegelen et al., 2009). The STN has long been known to composed of excitatory (glutamatergic) neurons (Albin, Young, & Penney, 1989; Temel et al., 2005) with little evidence for involvement of

inhibitory effects (via GABA) on its target nuclei (Baufreton, Atherton, Surmeier, & Bevan, 2005; Galvan, Kuwajima, & Smith, 2006; Guridi & Obeso, 2001; Temel et al., 2005).

The STN is an important area for motor control as it is the only node in the BG that receives glutamatergic input from frontal cortex (especially the pre-SMA) (Isoda & Hikosaka, 2008; Nambu et al., 2002) mainly from rIFG (Aron et al., 2007). The STN is anatomically connected with the direct pathway (STN➔GPe➔STR➔SNr/GPi), the indirect pathway (STN➔GPe➔SNr/Gpi) and hyper-direct pathway (cortical areas➔STN➔GPi/SNr) (Chambers et al., 2009; Temel et al., 2005).

STN is considered an input station within the BG, and sends outputs to the GPi/SNr (Nambu et al., 2002). In primates, cortico-basal ganglia-thalamocortical circuits consists of the limbic, associative and the sensorimotor circuits. Among these circuits, the STN has a central position (See Figure 1.2).

STN is implicated in the ability to stop or inhibit an already initiated response, highlighting its potential role in impulse control disorders (Aron & Poldrack, 2006; Eagle et al., 2008). Other, non-motor, functions of STN involve cognition, emotion (Mallet et al., 2007; Temel et al., 2005), decision making (Frank, 2006), and switching from automatic to controlled eye movement (Isoda & Hikosaka, 2008).

1.4.2 Orbitofrontal Cortex (OFC)

The OFC is located in the ventral surface of the prefrontal cortex and is one of the three main divisions of prefrontal cortex (Fuster, 2001). OFC is reciprocally connected with major cortical areas of prefrontal, motor, limbic and sensory cortex by cortico-cortical connections. The OFC projects densely to the ventromedial STR. Other subcortical connections of OFC are with thalamus, hypothalamus and amygdala (Cavada, Company, Tejedor, Cruz-Rizzolo, & Reinoso-Suarez, 2000). These heterogeneous patterns of connectivity make OFC a convergence zone for afferents from limbic and association areas (Elliott, Dolan, & Frith, 2000). Detailed understanding of the anatomy of OFC is difficult because it is connected to a

wide range of regions. The OFC can be further subdivided cytoarchitectonically according to Brodmann (see numbers) into areas 10, 11, 13 and 47.

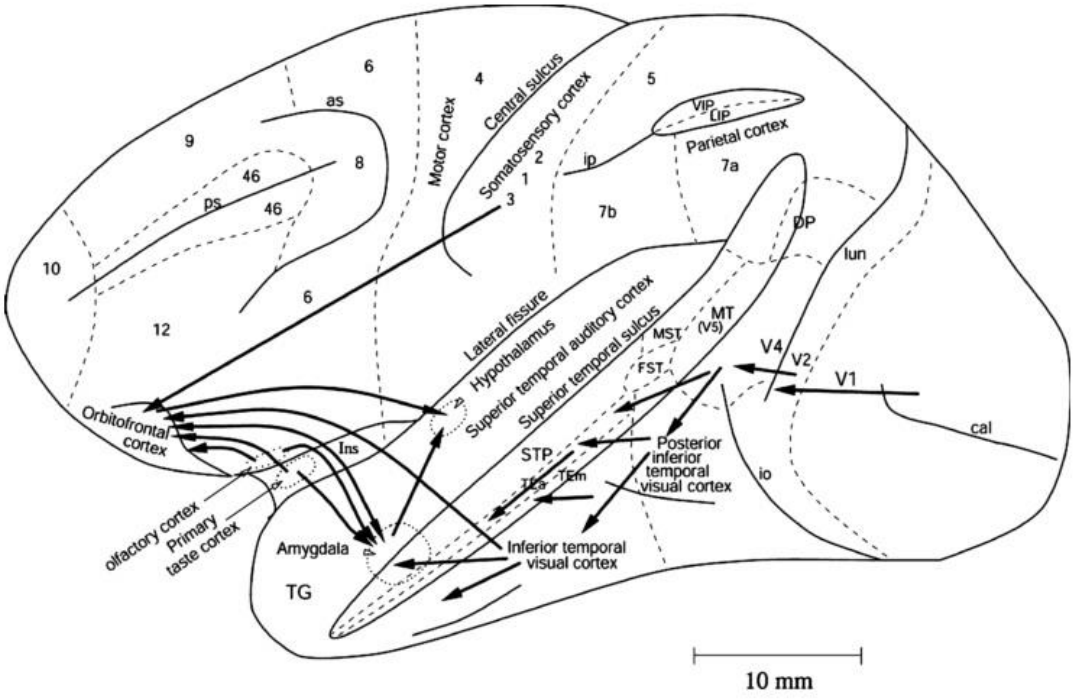

Figure 1.3 Schematic diagram showing OFC inputs.

From gustatory (from primary taste cortex), olfactory (from olfactory cortex), visual (from inferior temporal visual cortex) and sensation (somatosensory) pathways in primates. V1- primary visual cortex, V4- Visual cortical areas V4. Figure adapted with permission from Rolls (2004).

As seen in Figure 1.3 OFC receives input from all sensory modalities: somatosensory, taste, auditory, visual and olfactory inputs (Kringelbach, 2005). OFC has distinct medial and lateral portions (Winstanley, Theobald, Cardinal, & Robbins, 2004). The lateral portion has connections with sensory areas, premotor regions, midline thalamus, temporal lobe, primary gustatory cortex and amygdala (Cavada et al., 2000). The medial portion of OFC (mOFC) is connected with the HPC, posterior parahippocampal cortex, and associated areas of the cingulate cortex, entorhinal cortices, anterior thalamus, septum/diagonal band (Elliott et al., 2000; Winstanley et al., 2004), and ventral and dorsal STR (Kringelbach, 2005). OFC consists

of association cortex that has a role in the cognitive processes of decision making, though it is relatively poorly developed in rodents compared to humans (Rolls & Grabenhorst, 2008).

The famous case of Phineas Gage showed that lesion of OFC leads to changes of personality (Harlow, 1993), indicating its role in preventing impulsive behaviour (Fuster, 2001; Rudebeck, Walton, Smyth, Bannerman, & Rushworth, 2006). Despite many studies, the functions of OFC have remained relatively poorly understood. The OFC has been implicated in higher order functions, sensory integration and autonomic reactions (Kringelbach, 2005). Distinct sub-regions of OFC may have different functions. mOFC has been implicated in making stimulus-reward associations and with the reinforcement of behaviour, monitoring incentive values of stimuli (Elliott et al., 2000; Kringelbach, 2005), performance in the guessing task (Elliott et al., 2000). Lateral OFC is involved in stimulus-outcome associations, suppression of previously rewarded response (Elliott et al., 2000), expectation about punishment (Mar, Walker, Theobald, Eagle, & Robbins, 2011), inhibiting or filtering out cognitive information (Fuster, 2001; Kringelbach, 2005). It has a vital role in emotion, suppressing negative emotion (Fuster, 2001; Kringelbach, 2005), and goal directed behaviour (Kringelbach, 2005). Interestingly, OFC also has a role in suppressing actions that are inappropriate to the current context (Aron et al., 2007; Eagle et al., 2008; Stalnaker, Cooch, & Schoenbaum, 2015; Wikenheiser & Schoenbaum, 2016).

1.4.3 Hippocampus (HPC)

The hippocampus is one of the most extensively studied brain structures. It is an elongated brain structure shaped like a C, sea horse, banana, or curved tube; and is located in the medial temporal lobe of both hemispheres. The septal area and the HPC are closely connected. The HPC can be removed from the brain intact as ventricles separate the bulk of the two hippocampi from the rest of the brain. The medial septal area projects to the HPC and the lateral septal area receives a projection from HPC. As described by Gray and McNaughton, 2000, the septo-hippocampal system includes the hippocampus proper, the dentate gyrus, the

entorhinal cortex, the subicular area, and the posterior cingulate cortex. Viewed in cross-section, HPC consists of two interlocking cell layers: hippocampus proper (consisting of CA1, CA2 and CA3) and the dentate gyrus (DG). Both the CA regions and the DG have clear layers that are a combination of primary cells, afferent and efferent fibres, and interneurons. The parahippocampal region lies adjacent to the hippocampal formation (HF) and includes pre- and para-subiculum, entorhinal cortex (EC, medial and lateral areas), perirhinal cortex (PER, Brodman areas 35 and 36) and postrhinal cortex (van Strien, Cappaert, & Witter, 2009).

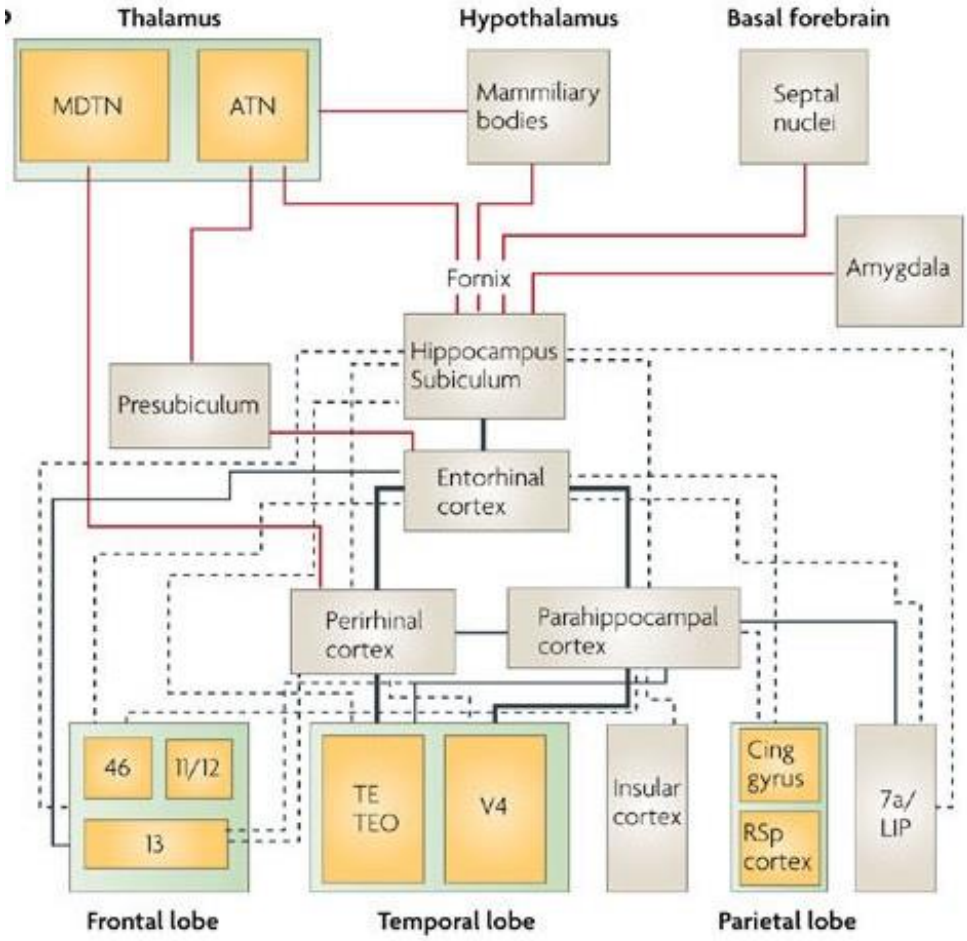

Figure 1.4 Cortical and subcortical connections of HPC.

Cortical and subcortical structures connected to HPC. MDTN: Medial dorsal thalamic nucleus; ATN: anterior thalamic nucleus; Cing gyrus: cingulate gyrus, TE & TEO: inferior temporal cortical areas TE and TEO; 7a/LIP: lateral intraparietal area; RSp: retrosplenial cortices; V4: visual area 4. Figure adapted with permission from Bird and Burgess (2008). Red lines: cortical connections; Black lines: subcortical connection; thickness of lines: strength of connections.

As shown in Figure 1.4 (compare also Figure 1.2), the HPC is part of Papez's circuit, connected to several cortical and subcortical structures. Subcortical structures include the thalamus (anterior thalamic nuclei/ATN, the medial dorsal thalamic nuclei/MDTN), hypothalamus (the mammillary bodies), basal forebrain (the septal nuclei), and amygdala. Cortical structures include prefrontal cortex (areas 11, 12, 13 and 46), temporal lobe (inferior temporal cortical areas, TEO and TE), parietal lobe, and cingulate gyrus and retrosplenial cortices/RSp (Bird & Burgess, 2008). Most of the HPC's neocortical inputs are relayed by the entorhinal cortex from the perirhinal and parahippocampal cortices (which lie at the end of the central visual processing areas) via the perforant path. And most of its neocortical output is relayed by the subiculum, which also projects back to the entorhinal cortex (Bird & Burgess, 2008). The HF can also be viewed as an essentially linear, unidirectional set of modules (EC➔DG ➔CA3 ➔CA1 ➔SUB ➔posterior cingulate) embedded in systems that have largely bidirectional connections (Gray & McNaughton, 2000). The HF forms a feed-forward loop of connections that starts and ends in EC (Fox et al., 2009). Representation of complex objects and the processing of visuospatial information have been linked with perirhinal cortex and parahippocampal cortex respectively.

Connectivity in the CA3 subfield of the HPC has been studied in much detail. CA3 receives input from EC directly via the perforant pathway or indirectly from the DG via mossy fibre (Cherubini & Miles, 2015). CA3 pyramidal cells then send output to the mammillary bodies through the lateral septum and, simultaneously, through the Schaffer collaterals to CA1. The CA1/subiculum area also send a projection through alveus and fimbria to the lateral septum and mammillary bodies of the hypothalamus (Gray & McNaughton, 2000). The HPC is viewed primarily as memory and spatial cognition structure. Connections between the HF and parahippocampal regions are involved in memory formation (S. H. Wang & Morris, 2010), memory consolidation (Battaglia, Benchenane, Sirota, Pennartz, & Wiener, 2011), memory

reconsolidation (McKenzie & Eichenbaum, 2011) and spatial navigation (Moser et al., 2014; O'Mara, 2005). Involvement of the HPC in associating places with the rewards available at different spatial locations implicates it in association (object-place event) memory (Rolls & Xiang, 2005). The principal neurons in the HPC can fire when subjects traverse distinct locations in space providing a neural code for spatial navigation (Kay et al., 2016) thus providing a role in spatial coding. The HPC has been theorized to be a "cognitive map" of the external world in humans and animals because it contains information about the environment and mental representations of physical locations (O'Keefe & Nadel, 1978). The HPC has also been implicated in learning (Jarrard, 1993), social emotions (Immordino-Yang & Singh, 2013), flexible cognition, social behaviour (Rubin, Watson, Duff, & Cohen, 2014), approach-avoidance conflict processing and decision making (Gray & McNaughton, 2000; Ito & Lee, 2016; O'Neil et al., 2015).

1.4.4 Network connections of basal ganglia, orbitofrontal cortex and hippocampus

Integrated networks within the brain interact and communicate with each other. Each of BG, OFC and HPC has been implicated in inhibitory control. It would be interesting to see if there exists a neuronal circuit that connects each with the others. In particular, is there functional connectivity between BG and limbic cortical structures (OFC and HPC) for behavioural inhibition?

The limbic system is a complex network that consists of both cortical and subcortical systems including major areas of medial prefrontal cortex (the dACC, the mOFC and the septal areas), the HF, amygdala, hypothalamus, limbic STR (NAcc), limbic pallidum (ventral pallidum), medial tip of the SNr and the medial tip of the STN (mSTN), ventral tegmental area, and limbic midbrain areas (Haegelen et al., 2009; Morgane, Galler, & Mokler, 2005).

The CA1/subiculum regions of HPC receive input from PFC/ACC through the parahippocampal projections. mSTN is connected with the PFC/ACC, entorhinal cortex, dentate gyrus, CA3, CA1 area and subiculum. Mainly, NAcc – the ventral part of the limbic

STR – receives projections from neurons of the CA1/subiculum areas of HPC (Haegelen et al., 2009; Silkis, 2008). As can be seen in Figure 1.2, NAcc then sends projections to mSTN through the ventral pallidum (vGP). Finally, mSTN send projections to mSNr and then to dorsomedial thalamus before reaching dACC. mOFC is an interface between limbic and neocortical areas (Jin & Maren, 2015; Vertes, Hoover, & Viana Di Prisco, 2004). Thus, the HF forms a closed loop with BG-thalamic-frontal circuitry. This limbic loop may play a vital role in inhibition of thoughts, emotions and motivation. This closed loop runs in parallel with sensorimotor and associative circuitry for motor act and action selection respectively (See Figure 1.2). Figure 1.5 shows simplified possible network connections between BG and limbic structures for going and stopping.

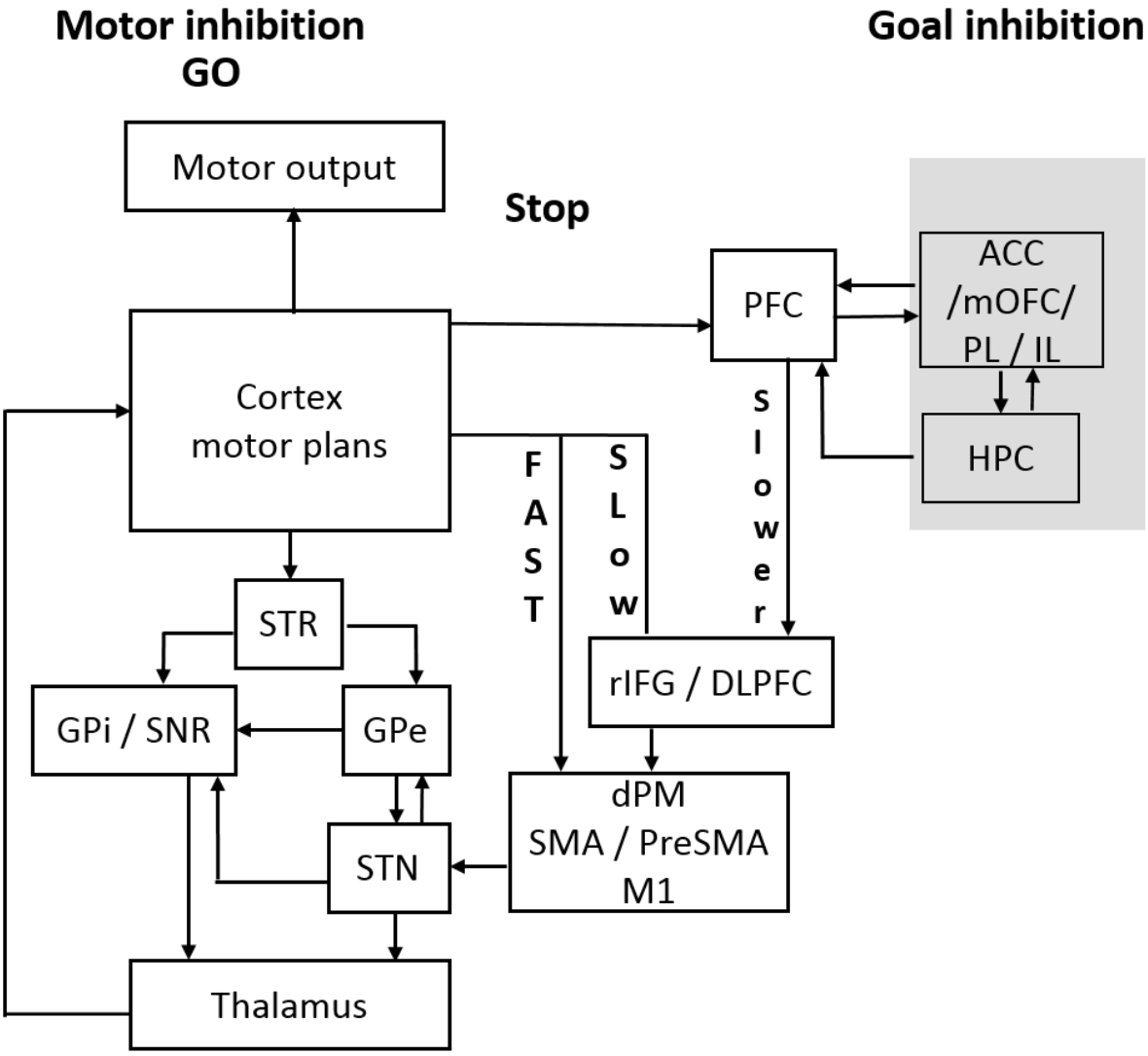

Figure 1.5 Proposed neural connection between BG, OFC and STN for going and stopping and their links to the BIS (shaded box).

We propose that goal inhibition circuitry involves the HPC and OFC, in addition to fast and slow routes motor inhibition circuits, to modulate the go circuit. To simplify the neural connections other structures in the BIS are omitted. PFC: prefrontal cortex; ACC: anterior cingulate cortex; mOFC: medial orbitofrontal cortex; PL: prelimbic; IL: infralimbic, HPC: hippocampus; STR: striatum; GPi/e: globus pallidus interna/externa; STN: subthalamic nucleus; dPM: dorsal premotor cortex; SMA: supplementary motor areas; preSMA: pre supplementary motor area; M1: primary motor cortex; rIFG: right inferior frontal gyrus; DLPFC: dorso lateral prefrontal cortex. Figure adapted from several previous Figures (Chambers et al., 2009; Haegelen et al., 2009; Neo, Thurlow, & McNaughton, 2011)

1.5 Simple inhibition - current models of simple stopping

The previous section reviewed the anatomy of the wide range of structures that are thought to be involved in the inhibition of behaviour, whether stopping of simple actions or of

inhibition of goals. Current models of simple stopping focus on a network connecting cortex with BG, which mediates inhibitory control of both action and cognition (Aron et al., 2007; Chambers et al., 2009; Eagle et al., 2008; Eagle & Robbins, 2003a; Schmidt et al., 2013). Before getting into the mechanisms of simple stopping, I will start with a brief description of the types of stopping and then review current models of action inhibition, i.e., simple stopping.

1.5.1 Types of stopping

Which neural circuit controls the behaviour of stopping depends on many factors, including stopping mechanisms and types of control. Most research has focused on reactive stopping. Reactive stopping involves control of cue-triggered stopping after the response process has been initiated. Such stopping requires the subject to stop completely in response to an external stimulus or stop signal. Reactive stopping may interfere with ongoing thought, action and feeling for decision-making or to prevent incorrect responses during lower interference (Aron, 2011). The results of reactive stopping could be non-selective because the hyper-direct pathway is involved (via the STN and has a broad effect on SNr/GPi), which leads to global suppression of the thalamo-cortical circuitry (Aron, 2011). Hence, the outcome of reactive stopping could be quick and inappropriate, or it may be expressed prematurely.

The kind of stopping that is prepared in advance is called proactive stopping (Aron, 2011; Obeso, Wilkinson, Rodríguez-Oroz, Obeso, & Jahanshahi, 2013). Proactive control could differ from reactive stopping because the response or motor output has to be put partially on hold until the decision is made. Proactive control subjects maintain the goal-relevant information prior to occurrence of events (Lavallee, Meemken, Herrmann, & Huster, 2014). The behavioural outcome of proactive stopping is that subjects slow down and if required to stop they may do it more quickly. The proactive control mechanism uses the indirect pathway so the outcome could be slow (Aron, 2011).

1.5.2 Mechanisms of simple motor stopping

The fronto-BG thalamic loop connects cortex (mainly frontal cortex) to the BG via three different pathways: direct, indirect and hyper-direct. These are the neural pathways to facilitate the initiation, execution and termination of the motor activity. The direct pathways involves CN, Put (which together form the STR), GPi and SNr. The indirect pathway in addition to structures in the direct pathway, involves GPe and STN. These two pathways have opposite effects on thalamic structures. Excitation of the direct pathway has net effects of exciting the thalamus and facilitates motor (or cognitive) programs in the cortex. In contrast, excitation of the indirect pathway has the net effect of inhibiting thalamic neurons, resulting in the suppression of competing motor programme. The hyperdirect pathway involves the STN, which receives excitatory projection from several cortical areas and sends excitatory projections to SNr/GPi (Jahanshahi et al., 2015).

In experimental studies, the cortico-BG-thalamo-cortical circuit has been divided into motor and non-motor BG circuits (Haegelen et al., 2009). Both BG and frontal cortex work together as a system and each area makes their own specific contributions. Different regions of frontal cortex represent actions and BG modulates this representation through distinct loops (DeLong, Kirby, Blitz, & Nusbaum, 2009). Aron (2011) explained that stopping or cancelling an action particularly involves the fronto-BG network in the right hemisphere, which includes preSMA, rIFG, DLPFC and the STN.

A wide variety of behavioural tests have been reported for the assessment of inhibitory control in clinical and experimental setups. Most commonly, it is studied using the stop signal task (SST) (Logan, Van Zandt, Verbruggen, & Wagenmakers, 1984). According to the 'race' model, initially proposed by Logan and Cowan (Logan, Cowan, & Davis, 1984), successful stopping depends on a hypothetical race between response activation and response inhibition processes (Fauth-Buhler et al., 2012). Verbruggen and Logan (2008a) described the SST paradigm as a "horse race" between "go" process (presentation of the go stimulus) and "stop"

process (presentation of the stop signal). Depending on whether the go or stop process 'wins', the response is executed or inhibited, respectively. Inhibiting the go response cannot be measured directly, so the stop signal reaction time (SSRT) is the key measure in this model. The SSRT cannot be directly observed, and is an estimate of the time at which the stopping process finished relative to the onset of the go signal, and the ability to stop (Eagle et al., 2008; Verbruggen & Logan, 2008a). In the SST, SSRT and stop signal delay (SSD) provide measures of reactive inhibition and proactive inhibition respectively. Inhibition functions are important as they show the ability to control responses. These functions can be affected by SSRT, go reaction time (GORT), and SSD (Verbruggen & Logan, 2009) see Figure 1.6.

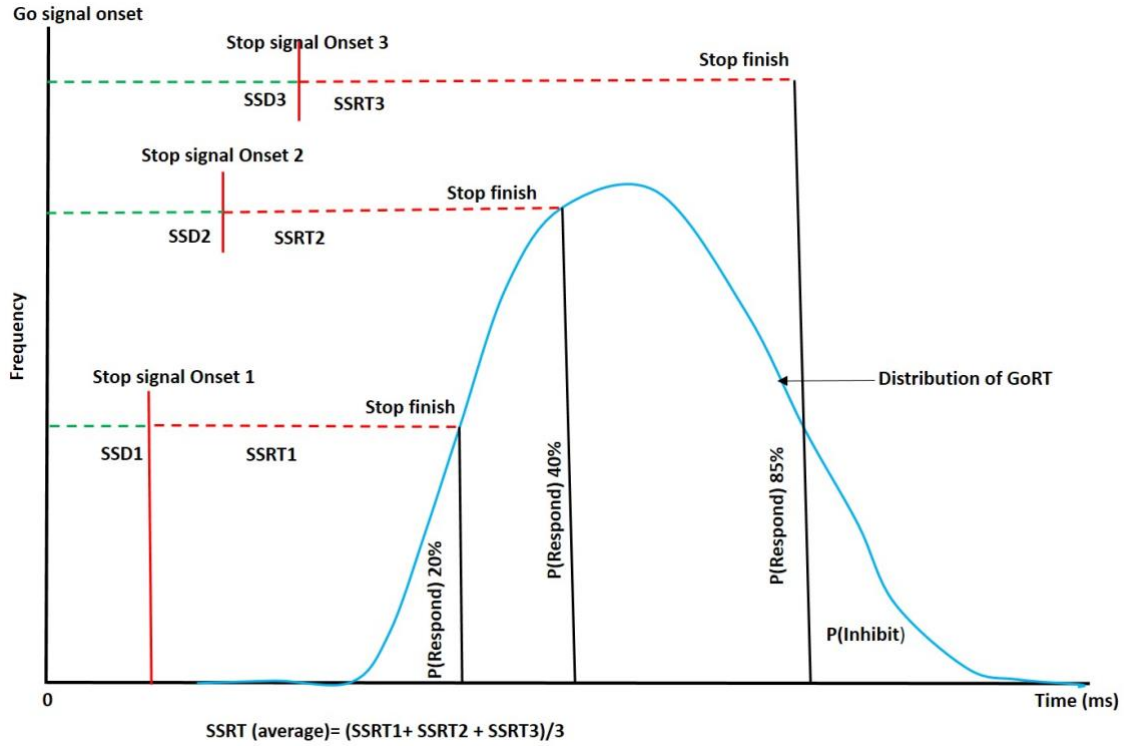

Figure 1.6 Graphic representation of the assumptions and predictions of the horse-race model.

Relationship between GO reaction time (GORT), stop signal delay (SSD-green dashed line) and stop signal reaction time (SSRT-red dashed line). P(Respond): probability of responding on the stop signal represented by area under the curve left and P(Inhibit): probability of inhibiting area under the curve right of the vertical lines. Figure adapted from C. H. Wang et al. (2013) and Verbruggen and Logan (2009)

As can be seen in Figure 1.7, a movement plan is initiated in the cortex (including dorsal premotor cortex, dPM, SMA, preSMA) which send excitatory signals to the STN; hyperdirect pathway and STR; direct and indirect pathways.

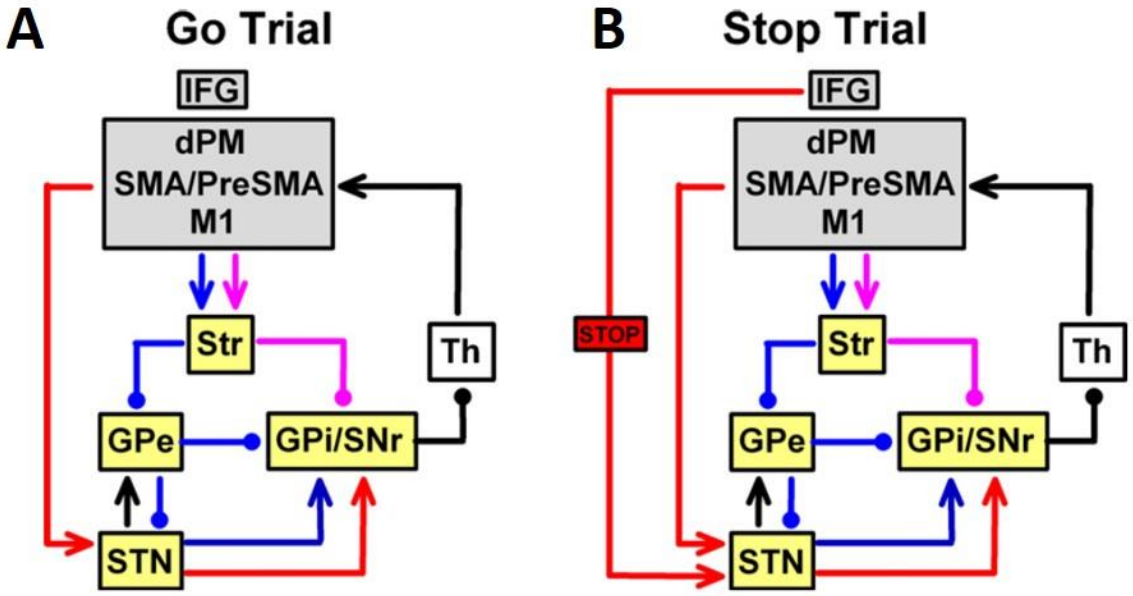

Figure 1.7 A fronto-basal ganglia model of response control in A. Go and B. Stop trials.

Arrows indicate excitatory (glutamatergic) connections, while circles indicate inhibitory (GABAergic) connections. Red, magenta and blue lines denote the hyperdirect, direct, and indirect pathways, respectively. Figure and legend copied with permission from Chambers et al. (2009).

The STR receives direct excitatory input mainly from cortical structures and sends monosynaptic projection to GPi/SNr through direct (arise from GABAergic striatal neurons) and polysynaptic projection to GPi/SNr through an indirect pathway involving GPe and STN (Nambu et al., 2002). On a Go trial (see Figure 1.7A) activation of the hyperdirect pathway, initially suppresses all motor programmes via *hyperdirect* pathway (exciting the GPi and SNr) Excitation of the GPi/SNr, inhibits the thalamus and suppresses excitatory projections to cortical motor areas. Following, this, the selected response is released via the *direct* pathway (fronto-strialtal). Lastly, the slow *indirect* pathway via the STR inhibits the GPe, down-regulating inhibitory connections between GPe-GPi/SNr and GPe-STN (Nambu et al., 2002). In this way, inhibition of GPe via the indirect pathway leads to increased activity in GPi/SNr,

suppressing thalamocortical projections and terminating the motor response at the appropriate time (Chambers et al., 2009). On a Stop trial, the sequence of events is identical until the stop-signal is processed. Then an additional hyperdirect projection from the IFG excites the STN, activating the GPi/ SNr and suppressing the thalamus. If this 'kill switch' is triggered in time, then response execution via the direct pathway can be cancelled (Chambers et al., 2009).

1.5.3 Summary

Simple stopping, then, appears to involve cortico-BG pathways with the primary locus of control depending on the speed with which stops must be achieved. On longer time scales, behaviour can be inhibited by preventing its initial production and by altering the processing of goals. Actions are usually more complex and could be made up of acts. Actions require higher levels of processing associated with different brain regions. These are selected in DLPFC, lOFC and implemented by associative circuits. The control of behaviour not only includes not only action or thought but also emotion and motivation. Motivation is the process that initiates, guides, and helps us reach our goals. A goal is what causes us to act. It determines the set of actions. Inhibitory control mediated by stopping a goal may be implemented in the brain by a variety of networks. These are selected by limbic areas such as prelimbic cortex, infralimbic cortex, ACC, mOFC and HPC. Thus, information can flow from limbic to cognitive to motor circuits to allow individuals to respond appropriately and the information flow depends on circuits and time available. The main current detailed theory of such goal-related inhibition invokes a "Behavioural Inhibition System", which I review in the next section.

1.6 Complex inhibition - the Behavioural Inhibition System (BIS)

1.6.1 Simple versus complex inhibition

Cognitive control is the process by which emotions, goals or plans influence behaviour that supports flexible, adaptive responses and complex goal-directed thought. Most studies of inhibitory control focus on motor stopping that involves frontal-BG circuits while similar circuits are also crucial for non-motor control (Kalivas & Volkow, 2005; Temel et al., 2005),

for instance emotion and motivational control. It is easy to conclude when motor inhibition has occurred, i.e. a motor response is withheld or withdrawn. By contrast, it is hard to find when behavioural inhibition has occurred. Behaviourally, they might look the same, but neurally they are different.

A goal has both cognitive and motivational properties (McNaughton, DeYoung, & Corr, 2016). People often use the word "goal" only in the positive sense where it achieves or obtains the desired result. But, from a more cybernetic perspective, a goal could be either positive (an attractor) or negative (a repeller). Presentation of a positive stimulus (or omission of a negative one) produces positive goals and is associated with positive motivation while the omission of a positive stimulus or loss generates aversive states and is associated with negative motivation.

1.6.2 Gray's Behavioural Inhibition System Theory

Jeffrey Alan Gray (Gray, 1982, 1987) hypothesized three separate systems that control goal-directed behaviour: the Behavioural Approach/Activation system (BAS); the Fight/Flight/Freeze system (FFFS); and the Behavioural Inhibition System (BIS). As can be seen in Figure 1.8, the delivery (+) or omission (−) of primary positive reinforcers (PosR), primary negative reinforcers (NegR), conditional stimuli (CS), innate stimuli (IS) or novel stimuli are the input events to the three separable systems. Such events affect behaviour, producing either approach (if such stimuli are associated with the delivery of PosR or omission of NegR) or avoidance (related to the delivery of NegR or omission of PosR). Approach and avoidance system operation is easy to understand if there is only one goal. The simple behavioural effects are produced when any one of the relatively pure approach or relatively pure avoidance tendencies predominate. A goal with a highly activated tendency will be a winner for control of the motor system. But selection could be complicated when incompatible simple approach and avoidance tendencies are concurrently activated, generating goal-conflict.

If there is no clear winner due to simultaneously activated, opposite tendencies, with nearly equal levels of activations between the different goals, the BIS will detect conflict.

When two goals are incompatible, e.g. an attractor and repeller that involves the same situation (and so generate both approach and avoidance) and compete for the behaviour, the BIS is engaged (Gray, 1982, 1987). The BIS has outputs that result in goal conflict resolution generated by increasing the weight of negative associations of each of the conflicting goals (McNaughton & Corr, 2004). The main behavioural output of the BIS during goal conflict is risk assessment. This includes not only inhibiting ongoing behaviour but also increased arousal and attention that are an adaptive process (Gray & McNaughton, 2000). The increase in attention helps to prepare for actions to reduce this aversive state.

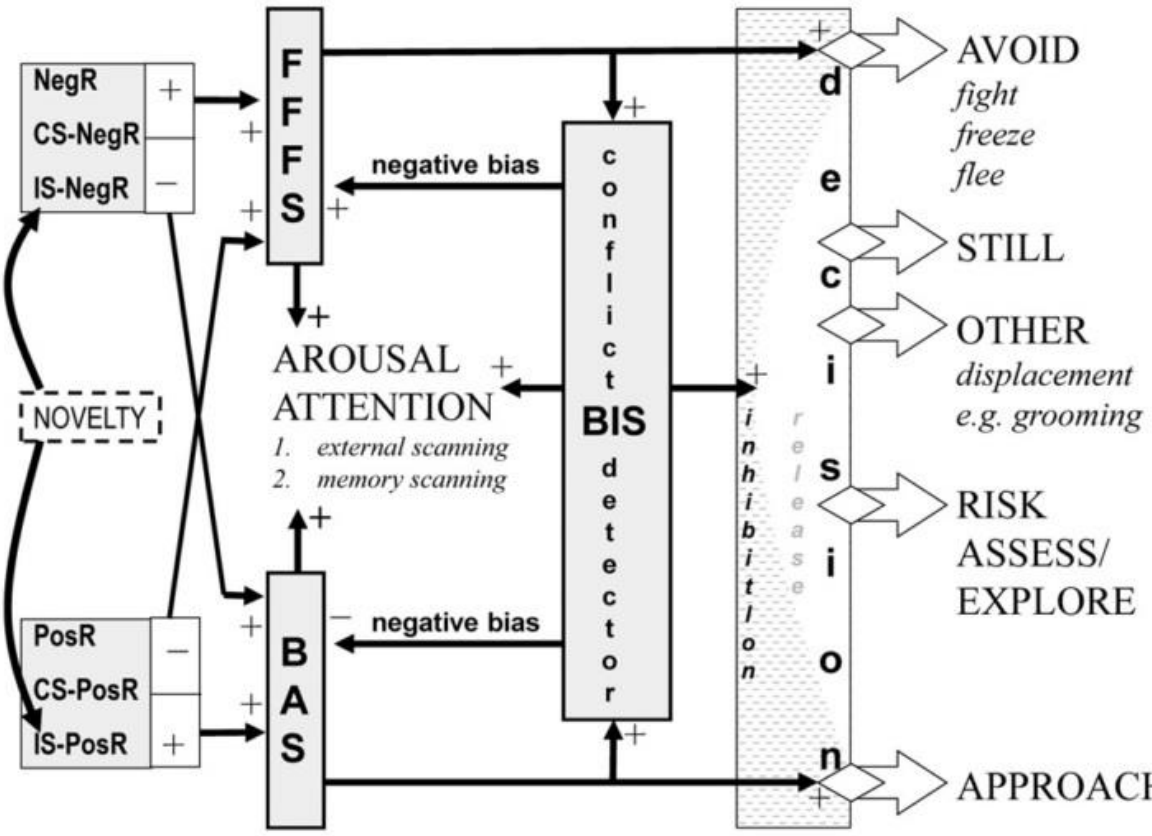

Figure 1.8 An updated model for the relationship of approach (BAS = behavioural approach/activation system), avoidance (FFFS = fight, freeze, flee), and conflict (BIS = behavioural inhibition systems)—an updated model.

The delivery (+) or omission (−) of primary positive reinforcers (PosR) or primary negative reinforcers (NegR) or conditional stimuli (CS) or innate stimuli (IS) are the input system that predict such primary events. BIS is activated when it detects approach-avoidance conflict—suppressing prepotent responses and eliciting risk assessment and displacement behaviours. See text for more details. The traits appear to operate in the shaded area. Figure copied with permission from McNaughton and Corr (2014).

1.6.3 Simple and complex inhibition – a number of possible networks

Several parallel cortico-BG circuits are present in the mammalian forebrain and implicated in the learning and control of actions. Sensorimotor circuits and associative circuits are among those widely studied in relation to action inhibition, while key roles of limbic circuit in control of goal inhibition have not been studied in detail. As discussed earlier in section 1.4, the fronto-BG model of action stopping involves a medial right frontal cortical network including rIFG, ACC and preSMA. Besides simple, fast action stopping, the neurobiological basis of goal stopping therefore could involve the limbic circuit and structures evaluation by the BIS (Gray & McNaughton, 2000).

Within the components of the limbic system noted earlier, the HPC system can be proposed to have a role in goal inhibition. The limbic circuit is one of three primary cortico-BG circuits. It principally includes cortical (such as PL, IL, mOFC and dACC) and subcortical areas (NAcc, vGP, mSTN, mSNr, CM) to form a loop (see Figure 1.2). In addition to the cortico-BG structures, the limbic circuit is extended to other limbic regions such as HPC and amygdala. We can find a reciprocal connection between CA1/subiculum areas of HPC and mPFC, mOFC (Cenquizca & Swanson, 2007; Ishikawa & Nakamura, 2003). The mOFC sends and receives dense projections with the anterior part of the EC, CA1 and subiculum (Insausti et al., 2017). OFC and ACC may receive input from HF through posterior cingulate and then projects into the downstream action circuit (see Figure 1.5). These pathways could be linked together as dorsal, and ventral STR circuitry parallels to each other controlling motor inhibition and goal inhibition respectively. Thus, we are interested in examining similar connections for

selective motor control that involves goals. See Figure 1.5 for proposed connections for goal inhibition.

1.6.4 Hippocampus as the main node in the BIS

The septum and HPC are strongly linked brain structures. The septal area mainly divides into medial and lateral septal and are connected to HPC. The HPC receives projection from medial septal nuclei and projects to the lateral septal nuclei. The effects of experimental lesions on the HF and the septal area have similar behavioural effects to anxiolytic drugs impairing the theta activity (McNaughton & Gray, 2000).

Gray and McNaughton (2000) proposed that the HPC is a comparator that resolves goal conflict. Information about any activated goal is transmitted to the HPC in the form of efference copies from where it is encoded in cortical and subcortical regions. Then the HPC compares the strength of the goals. For example, a goal with strong dominant tendency will overshadow the goal with less activated dominant tendency. In such a case, HPC will not detect conflict because there is an imbalance in the level of activation between the different goals. HPC only recognises and produces an output when two incompatible tendencies are concurrently activated between goals. Conflict between two or more goals can occur from concurrently activated approach-approach or avoidance-avoidance or approach-avoidance tendencies. Therefore, the HPC is the main node in the BIS for goal-conflicts resolution.

1.6.5 Hippocampal rhythmic slow activity

A particularly distinctive feature of hippocampal function is the theta rhythm in rodents: a 4-12 Hz, rhythmic, sinusoidal oscillatory activity. It is also referred to as rhythmic slow wave activity (RSA; hippocampal rhythmicity) (Bland, 1986; Buzsáki, 2002; Kramis et al., 1975) and can occur in cortical (Holsheimer, 1982; Jones & Wilson, 2005a) and subcortical structures (Jacobs, 2014; McNaughton, Ruan, & Woodnorth, 2006; Vertes et al., 2004) of the brain.

Gray and McNaughton (2000) studied the behavioural effects of the classical anxiolytic drugs and effects of experimental lesions in both hippocampal and septal regions. They

observed common behavioural effects of both experimental lesions and effects of anxiolytic drugs. They found anxiolytics affect septo-hippocampal system function by impairing the control of hippocampal RSA (Gray & McNaughton, 2000). Hippocampal RSA is thought to support cognitive operations in the brain such as working memory (Bird & Burgess, 2008; Duzel, Penny, & Burgess, 2010; Fujisawa & Buzsaki, 2011; Hyman, Zilli, Paley, & Hasselmo, 2010), spatial information processing (Burgess & O'Keefe, 2011), decision making, learning (Berke, Okatan, Skurski, & Eichenbaum, 2004; DeCoteau et al., 2007a; Tort et al., 2008) and timing (Emmons, Ruggiero, Kelley, Parker, & Narayanan, 2016; Gu, Kukreja, & Meck, 2018). Studies have correlated RSA with behavioural performance. Restoring RSA has been shown to restore initial learning, demonstrating brain rhythmicity can be important for mental processing (McNaughton et al., 2006). In addition, RSA plays a role in learning response inhibition to a conflicting stimulus (Gray & McNaughton, 2000; Sakimoto & Sakata, 2015). RSA has been linked to a general inhibition of systems not being used during motor behaviour or alert immobility (Sainsbury, 1998).

RSA is prominent during active waking, rapid eye movement (REM) sleep (Buzsáki, 2002) and increases with running speed (Ekstrom & Watrous, 2014). Tort et al. (2008) studied the LFP oscillatory activity recorded in dorsal HPC and dorsal STR when rats performed a navigation task in the T maze. They reported that, within the HPC, phase-amplitude coupling peaked during decision making while it was weak as the goal is approached.

Within large brain networks (in particular sensory, motor, and cognitive circuitry), synchronous activity at lower frequencies (delta and theta) is linked to a variety of cognitive functions. Jones and Wilson (2005b) investigated the interaction between HPC and mPFC during decision making in rats and found theta rhythmic activities coordinate HPC and mPFC interactions during a spatial working memory task. In a separate rodent study, LFPs between

HPC and mPFC exhibited increased theta coherence (5-10 Hz) during reward expectation (Benchenane et al., 2010). These studies suggest that HPC-mPFC theta coherence could be important for learning and reward prediction activity. Furthermore, oscillatory activity in the 4-8 Hz theta and 30–80 Hz gamma frequency bands has been implicated in a wide range of memory (working memory) and cognitive processes in human (Kahana, 2006).

RSA is thought to have a vital role in organizing the information in interconnected hippocampal circuits. Therefore, studying hippocampal rhythmicity and the neural circuitry involved could help us to understand the HPC and its interaction with other networks in more detail.

1.6.6 Neural circuitry involved in hippocampal rhythmicity

Much of the research data on hippocampal rhythmicity comes from recording from the rodent brain. Evidence of two types of hippocampal theta oscillations have been described in rats and rabbits (Brian, 1986). Type I theta or movement theta is recorded during voluntary movements such as running, swimming, jumping, exploratory sniffing and rearing, whereas type II theta appears when animals are immobile (Brian, 1986; Kramis, Vanderwolf, & Bland, 1975). Type I theta wave activity is usually at a frequency of 7-12 Hz and is not abolished by anticholinergic drugs (e.g. atropine) whereas type II theta wave activity usually occurs at 4-9 Hz but can reach to 10-12 Hz (Sainsbury, 1998) and is blocked by anticholinergic drugs (Brian, 1986; Kramis et al., 1975).

Within the hippocampus proper, theta is supposed to be generated from CA1 (stratum oriens) and dentate (stratum moleculare) regions, which are usually approximately 180° out of phase. Under urethane anaesthesia the two generators are separated by a short "null zone" where no theta is recorded (Brian, 1986). Theta generators that lie outside the HPC are cingulate cortex (Holsheimer, 1982; Leung & Borst, 1987) and EC (Michell & Ranck, 1980). More recently, other places such as the amygdala (Pare & Collins, 2000), mPFC (O'Neill, Gordon, & Sigurdsson, 2013) and OFC (van Wingerden, Vinck, Lankelma, & Pennartz, 2010)

have been reported as theta generators. Theta activity present in extrahippocampal structures may often be due to rhythmic impulse transmission to these structures based on the nature of extra hippocampal theta generation (Brian, 1986).

Recent work on the mechanisms of theta rhythm supports the belief that the septo-hippocampal system is responsible for theta generation (Goutagny, Jackson, & Williams, 2009). GABAergic neurons of the medial septum (MS) lead the hippocampal network during theta activity (Hangya, Borhegyi, Szilagyi, Freund, & Varga, 2009). Similarly, MS stimulation increased hippocampal theta oscillations (McNaughton et al., 2006; Vandecasteele et al., 2014). Taken together, HPC itself, the septum and EC are considered vital for theta generation *in vivo* (Buzsáki, 2002).

Figure 1.9 shows the hippocampal circuitry underlying theta oscillations. Two pathways (see Figure 1.9A) can generate theta oscillations (Pignatelli, Beyeler, & Leinekugel, 2012). First, rhythmic inhibitory inputs to CA1 basket cells arrive from the MS and provide rhythmic perisomatic inhibition of CA1 pyramidal cells. Second, EC provides rhythmic excitatory inputs at theta frequency through the perforant path to the granule cells of the DG and to the apical dendrites of CA1 and CA3 pyramidal cells.

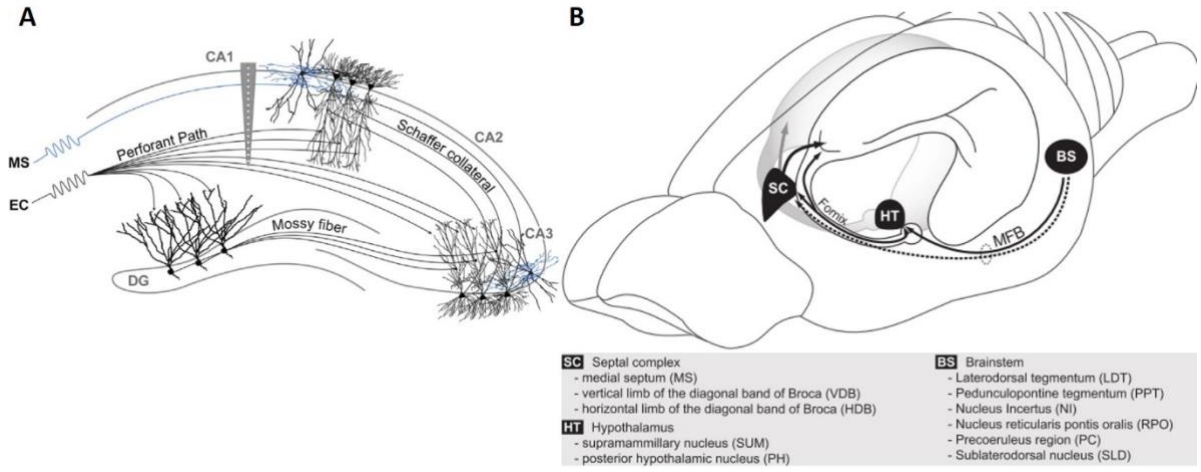

Figure 1.9 Neural circuitry involved in the generation of theta oscillations.

Hippocampal circuitry with excitatory (black) and inhibitory (blue) transmission. B. Direct (dotted line) and indirect pathways mediating the activation of the septal complex (SH); HT: hypothalamus; BS: brainstem. Figure copied with permission from Pignatelli et al. (2012)

Control of theta is complex because of interconnections among various hippocampal interneurons (Buzsáki, 2002). HPC theta activity is controlled by pacemaker cells located in the medial septal area, which themselves receive a frequency-setting input from structures in the midbrain, including the medial supramammillary nucleus (Kirk & McNaughton, 1991). Figure 1.9B shows control of the theta pacemaker operated by two pathways; first pathways projecting directly to septal complex (MS, vertical limb of the diagonal band of Broca, horizontal limb of the diagonal band of Broca) and second pathway mainly mediated by hypothalamus through supramammillary nuclei and posterior hypothalamic nuclei to MS. Both of them pass through the medial forebrain bundle (MFB) and the fornix (Pignatelli et al., 2012).

1.6.7 Summary

The concept of behavioural inhibition is ubiquitous in psychology. Many people use behavioural inhibition to refer to control over unwanted stimuli and responses/actions. However, behavioural inhibition could be a process of suppression/cancellation that is not merely motoric. As described in section 1.6.1, these types of inhibition could be distinguished as a simple motor inhibition and a more complex goal inhibition, respectively. Goal inhibition appears to access to motor circuits. For goal inhibition, subjects must have information on what behaviour to stop and use this information to determine how and when inhibition should be implemented. This likely involves the limbic system, particularly the HPC. Theta is a prominent feature of HPC function. Rhythmic activity in the theta range has been proposed to be important not only for communication between distant brain structures but also for inhibiting unwanted goals (goal inhibition).

1.7 Hypotheses of the current thesis

For all the experiments in this thesis, I used the stop signal task (SST) as the basic behavioural paradigm because many people would see it as involving behavioural inhibition in the sense of action stopping. However, it also imposes a goal conflict due to both going (approach) and stopping (avoidance) being present (McNaughton, 2014; McNaughton, Swart, Neo, Bates, & Glue, 2013). Goal conflict will activate the BIS (McNaughton & Corr, 2004) to inhibit inappropriate behavioural routines and provide conflict resolution. Human data provide evidence of EEG activation of the BIS that is separate from (and likely slower than) action stopping (Neo et al., 2011). The paradigm as a whole, therefore, provides examples of simple going, simple stopping, and (provided the rat brain is activated like the human brain) goal conflict processing.

The experiments described in this thesis focused mainly on the dynamic interaction between BG (both STR and STN), OFC and HPC for the control of behavioural inhibition. The present study was undertaken to determine how behavioural inhibition processed in the brain? Experiment 1, reported in Chapter 4, performed to examine how LFP oscillatory activity was modulated between STR, OFC and HPC during a simple task. The experiment determined whether the STR and its connections to cortical and hippocampal network were involved directly in the modulation of motor behaviour. Both STR and HPC have been implicated in response learning and memory of different sequences (DeCoteau et al., 2007b; Hasselmo & Eichenbaum, 2005; Packard & Knowlton, 2002). Rodent study navigating the T-maze found that BG (mainly striatal), and HPC LFP oscillations were modulated during performance of a task (DeCoteau et al., 2007a). However, it was not clear whether the STR and HPC system work independently or in coordination with frontal cortex during acquisition of the task. Therefore, I tested the following hypotheses:

H1: STR and HPC will interact with frontal cortex during acquisition of the task.

H2: Reward expectancy will increase theta coherence between OFC-HPC

Experiment 2, reported in Chapter 5, examined how oscillatory activity in the STN, OFC and HPC responds to the cancellation of an ongoing action as required in stop-signal tasks. It also examined how behavioural stopping was implemented in hippocampal-subthalamic circuits. Previous study showed increased cortico-subthalamic and cortico-hippocampus interaction during response inhibition, but again, not sure if the hippocampal-subthalamic interaction supports behavioural inhibition. Electrophysiological and behavioural studies confirmed STN as a major target for the production of action stopping. STN receives a hyper-direct projection from rIFG for rapid cancelation of action. rIFG in humans is thought to be a homologous region to OFC in rats, due to strong functional similarities (Birrell & Brown, 2000; Eagle et al., 2008). Furthermore, contextual information for performing a tasks is detected by both BG and HPC and such actions are executed through frontal cortex at the appropriate time (Leisman et al., 2014). Here, I predicted that:

H3: Correctly stopping an ongoing action will increase the beta band activity in the STN and also increase the coherence between OFC-STN.

H4: HPC-STN coherent activity will increase in the theta frequency band when the animal fails to stop an ongoing action.

The study presented in Chapter 6, investigated the interaction between HPC, OFC and STN to test the neural effects of goal-conflict. Previous studies suggest right frontal cortex, HPC and STN may all be activated during conflict processing. However, it is not clear if activation of these brain areas includes a goal-conflict component. Human studies on the SST suggests that goal-conflict processing is associated with 4-12 Hz activation in right frontal cortex (McNaughton et al., 2013; Neo et al., 2011; Shadli, Glue, McIntosh, & McNaughton, 2015). Similarly, previous findings on the role of theta oscillations (4-8 Hz) demonstrated that high conflict trials in human are related to greater theta coherence between medial frontal

cortex and STN (Zavala et al., 2016; Zavala et al., 2014). In addition, recent studies in rodents have reported theta phase coherence between frontal cortex and HPC in conflict situations (Jacinto, Cerqueira, & Sousa, 2016). Based on these previous studies, I hypothesized that:

H5: An increase in power at HPC, OFC and STN LFP in the low frequency band will occur if goal conflict is detected.

H6: Coherence between HPC-STN will increase during high conflict trials.

Chapter 2. General Methods

This Chapter contains a description of the general surgical and technical procedures, and the materials, used in this thesis. It also summarizes the common methods used to acquire all the experimental data reported in this thesis. Animal housing, handling, surgery, acquisition setup, histological procedures, LFPs and data processing were all common among the animals in different experiments. Details regarding the behavioural procedures, and statistical analysis that are unique to each experiment are described separately in each experimental Chapter. Histological methods are described in Chapter 3.

2.1 Subjects/permissions

A total of 52 male Long Evans rats were used in this project; they were obtained from the Hercus Taieri Resource Unit of the University of Otago and weighed 200-250 gm on arrival in the laboratory. Final data analysis was performed on ten animals that completed the SST. A first batch of 5 animals were used to provide analysis for the Go task. However, some of the first batch of animals did not produce good Stop data. So, a second batch of five animals was used for the Stop signal task. Out of 42 animals that were not used for SST, 15 animals were used for pilot surgeries (testing coordinates and optimization of the SST task), 10 animals died during or shortly after surgery due to anaesthetic complications with the injectable anaesthetic initially used, stroke and seizures. Another 17 animals not included in this thesis were used for pilot optogenetic experiments. Optogenetic stimulation of STN did not produce the desired LFP responses and induced unusual (potentially compulsive, trichotillomania-like) behaviour. Further testing was also prevented by ongoing problems with virus supply, where the appropriate constructs are failing to be expressed in vivo. We, therefore, decided that optogenetic could not be used by us in the context of the current experimental questions. All experiments were conducted in accordance with the New Zealand animal welfare legislation. Ethical approval was provided by the Animal Ethics Committee of the University of Otago

(Approval number: 15/15). The optogentic pilot part of this project was conducted under Environmental Protection Authority approval GMD03091.

After arriving in the laboratory, rats were housed together in a temperature controlled (20-22^{o} C) room, on a 12h/12h light-dark cycle with lights on at 6 a.m. The experiments were conducted during the light phase. The group cages used were standard ones with a white plastic base (34cm x 24cm x 26cm) and a fitting wire top with a flap door (17cm x 19cm). After surgery, rats were housed in single cages for the remainder of the study. The single cages were kept beside those of other animals to allow visual and auditory contact, and had a white plastic base (16cm x 25cm x 18cm) and a fitting wire top. Food and water were available *ad libitum* prior to and for 10 days after surgery. The rats were then food restricted (see section 2.4.1).

2.2 Electrode Array Construction

All electrode implants consisted of three electrode arrays with a total of 28 working channels: HPC-STN (12), BG (8), OFC (7), and reference (1) (see section 2.2.1 and 2.2.3) plus one earth electrode (6cm of 0.25mm silver wire; WPI Inc., Sarasota, USA), all of which were connected to a Mini Grid Array (MGA) 32-pin gold connector (SK-MGA6-32A-01, Ironwood Electronics, MN, USA; see Figure 2.1) before implantation. The reference electrode was soldered to a designated gold pin on the 32 male gold pin connector.

2.2.1 Reference Electrode and Earth electrode

The insulation of the stainless steel wire (A-M Systems Inc, USA; 0.008" Teflon coated ,0.005" bare) was scraped and wrapped around a stainless steel screw (Fine Science Tools, Canada) and secured using silver solder. During surgery, this screw was fixed to the skull area just behind lambda considering the area to be electrically neutral. However, due to conductivity, most of the locations on the head are electrically active therefore, it's hard to meet the criteria of the ideal reference. An earth electrode or ground was built with a section of bare silver wire with 0.005" thickness (AM Systems, USA). It was soldered to a designated gold pin and was positioned around the edge of the skull outside the implant during surgery.

2.2.2 Construction of electrodes for 28-channel recordings

The final construction methods for the arrays used were developed as part of this PhD project and so full details are given here. To assemble single electrodes in an array, a ~36cm long piece of insulated nichrome wires (0.001" diameter, California Fine Wire Company, USA) was cut. A 3cm section in the middle of the wire was exposed to heat gun (Robert Bosch GmbH, Germany) at 600°C for 30 seconds to burn off the insulation. The un-insulated part of the wire was then cut in the middle with scissors so that two 18 cm pieces of wire were created, each including a ~ 1.5cm part without insulation.

The uninsulated end of each electrode wire was then wrapped around a short piece of silver wire that was bent in a "J"-shape and the J crimped onto the wire and soldered to it using silver solder. The silver wire was soldered to a designated gold pin on the connector and the excess silver wire was cut off.

The free end of the electrode was then threaded through a designated hole in a previously constructed Aclar plastic sheet (~ 3cm x 1cm, Ted Pella Inc. Canada). For the HPC-STN, BG and OFC arrays, Aclar sheets with 12, 8 and 7 holes respectively were used. The holes in the plastic sheet were spaced differently to target the brain regions and were melted into the plastic with an insect pin that was attached to a Weller soldering iron (Cooper Tool PTY limited, Australia) held in a stereotaxic manipulator, which controlled hole depth and spacing and ensured that the holes were in a straight line. The first hole was marked with "1" and the last with "12", "8" or "7" for the HPC-STN, BG and OFC arrays, respectively.

The Aclar plastic sheets were attached to the outer platforms of a wooden frame with Blu-Tack (Bostik, New Zealand Limited) at an approximate angle of 40° so that threading was easier. The wooden frame that was used for the construction of the electrode array consisted of three wooden platforms (6.5cm x 4.5cm x 2cm) spaced apart approx. 4cm and, attached to a wooden plate (25cm x 8.5cm, see Figure 2.1A). The connector was held in place by another connector fixed firmly to the middle of the platform. Each electrode array under construction

was attached to the outer wooden platform via the plastic sheet to ensure that the sheets were held in place about 8 cm away from the edge of the gold pin connector.

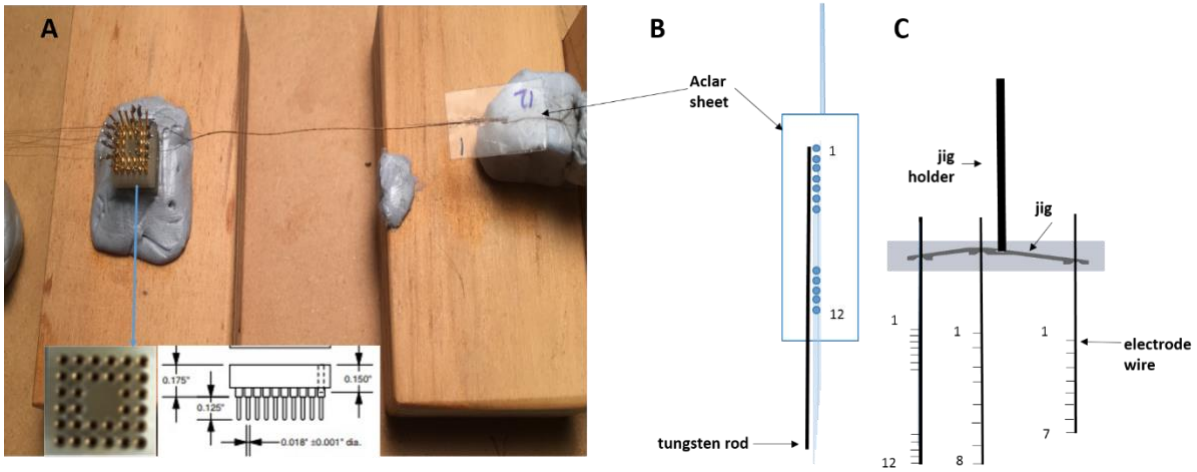

Figure 2.1 Procedure for 28 channel electrode construction.

A. Bottom view and specifications of MGA connector. MGA gold pin connector was placed on the middle platform connected to another gold pin connector that was fixed with Blu-Tack to hold it in place. Single electrodes were soldered to their designated gold pin and threaded through a marked plastic sheet that was fixed with Blu-Tack to one of the outer wooden platforms. B. Plastic sheets were marked with a "1"at the beginning and a "12" at the end to distinguish threaded through electrodes. After threading through all electrodes, the array set-up was fixed with glue and stabilised by gluing attaching to a Tungsten wire. Electrodes were cut through straight with a scalpel blade to remove the array from the Aclar sheet. C. The combined electrode array (three different microelectrode array) with its electrode tips was attached at right angles to the jig (see Appendix 2). Finally, it was supported with paperclip rod. This allowed for stabilisation of the electrode during implantation procedure into the brain.

After the wires were threaded through the plastic sheets, the free end was held in place by a piece of Blu-Tack. Once all electrodes were in place for both arrays, the plastic sheets were turned so that they would lie flat with the top (electrode "1") nearest to the gold pin connector and the bottom (electrode "12", "8" or "7") furthest from the gold pin connector, so that the electrodes entered the plastic sheet through the upper surface and exited through the

lower one. With the electrodes and the plastic sheet in this position, the sheets were then each rotated so that the wires were twisted together all at the same time.

To increase the strength of the electrode array a small piece (approx. 1.5cm) of 0.005" diameter Tungsten wire was glued onto it (see Figure 2.1B) using Loctite 454 Instant Adhesive Gel (Loctite Corporation, Ireland) and left to dry. Afterwards, more adhesive layers were applied (approx. 3 to 4 applications) to the tungsten and electrode wires and left to dry between each application. The array wires were then cut along the line of the holes (see Figure 2.1B and Figure 2.3 for real electrode array with electrode tips) and the array separated from the plastic sheet using a carbon steel scalpel blade (Swann-Morten, England). Each electrode array was then attached to a jig to hold them in the correct relative positions for stereotactic implantation. The jig was made up of polylactic acid or polyactide (PLA) which is a biodegradable and bioactive polyester made up of lactic acid building blocks (Flynt, 2017). It was then designed and printed with a 3D printer (Ultimaker 2 Plus, Mindkit NZ) (see Figure 2.2). The jig was then attached to a 0.5mm paperclip rod which was approx. 4cm long (see Figure 2.1C). For individual arrays, the jig was not used therefore the individual array was lowered and cemented separately. The purpose of manufacturing the jig was to implant three different arrays at once as well as to reduce the total time during the surgical procedure and to allow concurrent optogenetic injections and light guide implantation.

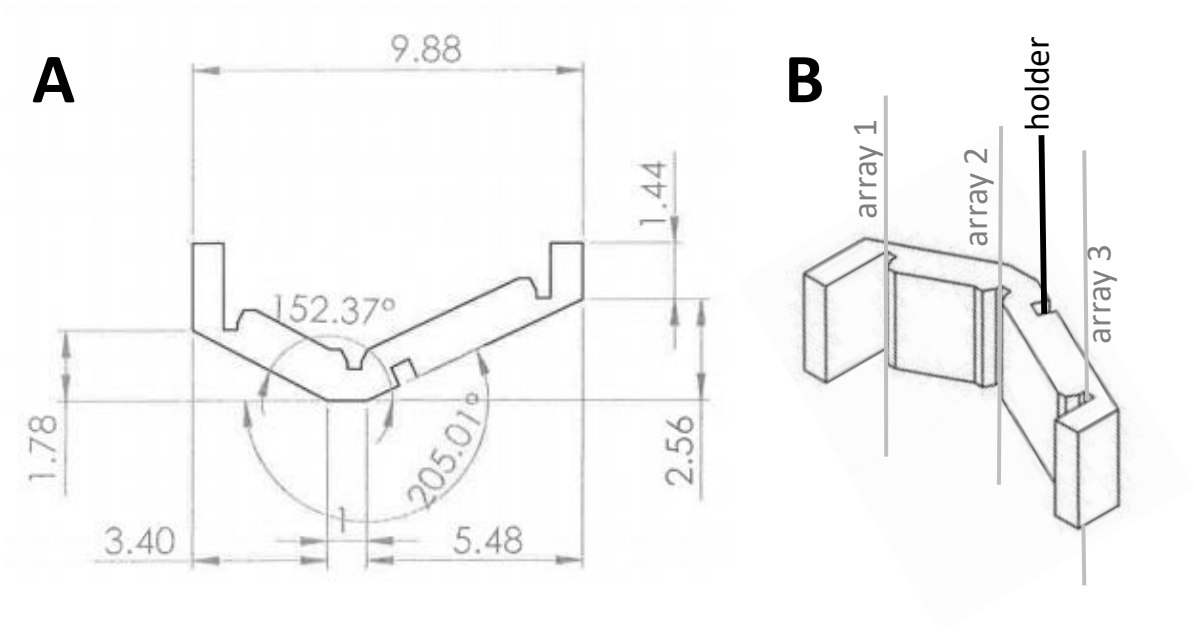

Figure 2.2 Jig for implanting the array.

A. Calculating length (mm) and angle based on the coordinates. B. Schematic diagram showing the final version of the jig with different arrays and holder.

Finally, the electrode arrays were tested for shorts between all possible electrode combinations and for the resistance of each individual tip in the array in 0.9 % physiological saline via a specially constructed connection box. Resistance for recordings for extracellular electrodes ranged from 0.2 to 0.6 MΩ. Then the positions of the individual electrode tips within the array were checked by passing a current through each individual electrode to produce a bubble. This was to ensure that electrodes had not been incorrectly threaded during construction. Prior to surgery, electrodes were disinfected by soaking in 70% ethanol.

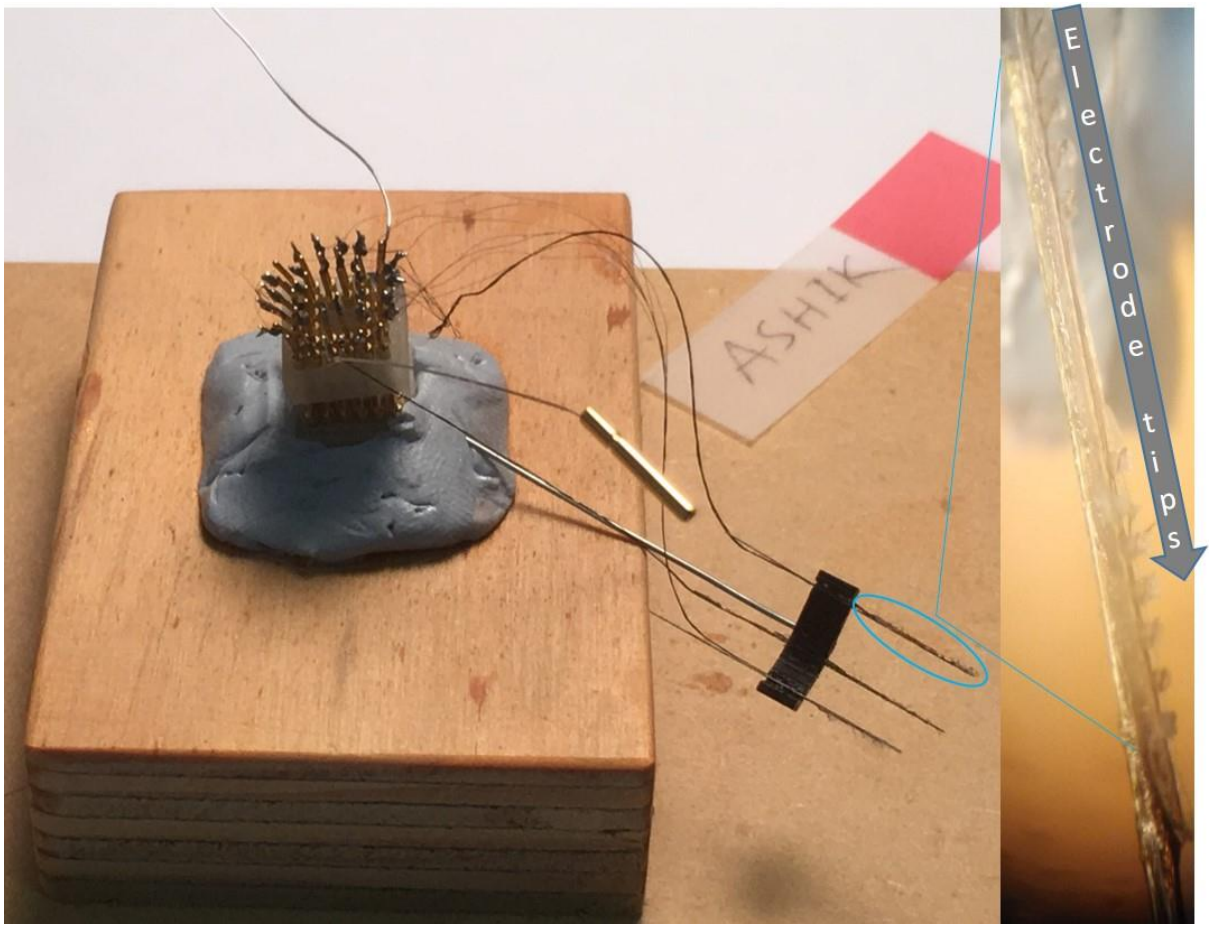

Figure 2.3 shows final multi electrode arrays with electrode tip for HPC-STN array.

2.3 Surgeries and Electrode Implantation

2.3.1 Surgery

All surgical instruments were sterilized in an autoclave (Mercer, Auckland, New Zealand) before use and were placed on a sterile field (stainless steel) during use. These included a scalpel handle (Fine Science Tools, Heidelberg, Germany), a pair of economy tweezers (angled tips: 0.4 x 0.5mm; WPI, Sarasota, Florida, USA), an ALM self-retaining retractor (Fine Science Tools, Heidelberg, Germany), a pair of Micro tweezers (tips serrated, angled; WPI, Sarasota, Florida, USA), a pair of Dumont forceps (tips 0.6 x 0.2mm; WPI, Sarasota, Florida, USA), a number of self-tapping stainless steel bone screws with pointed tips (Fine Science Tools, Heidelberg, Germany), a pair of Bonn Strabismus scissors (Fine Science Tools, Heidelberg, Germany), a 0.58mm E.S.T drill bit (Meisinger, Neuss, Germany), and a 1.4 mm E.S.T drill bit (Meisinger, Neuss, Germany). Sterilised Multisorb non-woven swabs

(5cm x 5cm; BSN medical, Mount Waverley, Australia) were also used during surgery to clean the skull. The surgical scalpel blades (Swann-Morton, Sheffield, England), 1 ml Tuberculin syringes (BD Pharmingen, Singapore), injection needles (26G ½ 0.45mm x 13mm; 25G 5/8 0.5mm x 16mm; 25G 1 0.5mm x 25mm), and 5 ml syringes (BD, Singapore) all came in sterile packs.

Prior to surgery, the rat was taken out of its group cage and placed into a single cage. Surgery was performed with injectable anaesthesia (Experiment 1, ketamine/dormitor) or gaseous anaesthesia (Experiment 2 isoflurane). Drugs, doses, administration route, supplier information and the reason for using them, are given in Table 2.1 and were consistent for all rats. For inhalation anesthesia, an isoflurane evaporator (E-Z Anesthesia, USA) was used. Rats were placed into the gas induction chamber and anaesthetized with isoflurane (5% in oxygen). After the animal was immobile isoflurane was reduced to 1.5-2% (see Table 2.2).

Table 2.1 List of drugs used for surgeries and their designated concentrations and dose rate.

WHEN	***USE***	***DRUG***	***ROUTE***	***DOSE mg/kg***	***Conc. mg/ml***	***Suppliers***
Before Surgery	**Analgesia/ Anaesthesia***	Ketamine	SC	75	100	Phoenix Pharma Distributors, NZ
		Dormitor (Medotomidine)	SC	0.5	1	Pfizer NZ Ltd.
	Local Anaesthetics	Marcaine	SC	2	5	AstraZeneca, Australia
	Local Anaesthetics	Lopaine (Lidocaine)	SC	4	20	Ethical Agents Ltd, NZ
	Anaesthetic Support	Atropine	SC	0.1	0.05	Phoenix Pharma Distributors, NZ

To Finish Surgery	**Hydration**	Saline	SC	10ml/ animal	--	--
	Anti-Inflammatory	Carprieve (Carprofen)	SC	5	5	Norbrook NZ Ltd.
	Antibiotic	Amphoprim	SC	30	60	Virbac Animal Health, Virbac New Zealand Ltd.
To Finish Surgery	**Anesthesia Reversal***	Antisedan	SC	2.5	5	Zoetis NZ Ltd.
After End of Testing	**Euthanasia**	Pentobarbitone	IP	300	300	Provet NZ Ltd., Christchurch, New Zealand

* Experiment 1. Later experiments used gaseous anesthetic.

Table 2.2 Amount of Isoflurane anesthesia in different surgical periods

Period	***Induction***	***Surgery start***	***During surgery***	***Surgery end***
Events	Gas induction chamber	Incision, drilling holes, screw	Electrode implantation	Cementing the implant
Isoflurane	5%	2%	1-1.5%	0.5%

After the rat was anesthetized, it was placed into a Kopf stereotaxic surgical frame (David Kopf Instruments, Tujunga, California, USA) with a heating pad and checked for any reflexes by pinching the toes. If the rat did not show any reflexes then the head was fixed using non-traumatic ear bars (855, David Kopf Instruments, Tujunga, California, USA). The snout was placed over a nose bar, taking care that the teeth were clear of the horizontal part of the bar, and the skull was flat. The eyes were covered with moisturising eye gel (Genteal gel -

Alcon laboratories Pty Ltd, Australia) to avoid any damage to the cornea due to drying. Marcaine (2mg/kg) and Lidocaine (4mg/kg) were injected under the scalp. The scalp was sterilised with Betadine (Faulding Pharmaceuticals, Australia). The head and body were covered with a glad "press n seal" wrap plastic sheet. A single midline incision (approximately 2.5 cm long) was made in the scalp. Superficial muscles were pushed to either side with a sterile swab (BSN medical, Mount Waverley, Australia) and the surface of the skull scraped clean. The sides of the incision were then kept separate with a self-retaining retractor (Fine Science Tools, Heidelberg, Germany). At the end of the surgery, Carprieve (5mg/kg) and prophylactic antibiotic treatment (Amphoprim, 30mg/kg, SC) were administered. The rat was monitored for respiration, heartbeat and pain during the surgery. Sterile 0.9% Saline (10ml) was also administered to maintain fluid balance and blood pressure during the surgery. After finishing the surgery, antisedan (2.5mg/kg, SC) was given in experiment 1. For experiments that used gas anesthesia, gas was turned down to 0.5 % during cementing.

2.3.2 Electrode Implantation

After the skull was exposed, holes for stainless steel screws and the electrodes were made with a dental drill attached to the stereotaxic frame. The coordinates were based on the stereotaxic atlas of Paxinos and Watson (Paxinos & Watson, 2007). OFC electrode coordinates: AP, +4.20mm; ML, +1.4 and DV, -7.00; BG electrode coordinates: AP, -0.60 mm; ML, +3.2 and DV, -8.6; HPC-STN electrode coordinates: AP, -3.72mm; ML, +2.2 and DV, -8.6) (see Figure 2.4). After drilling the holes, the isoflurane was decreased to 1%. The screws were implanted into the predrilled holes so that their tips just protruded below the skull. The reference electrode was fixed to the skull area just behind lambda.

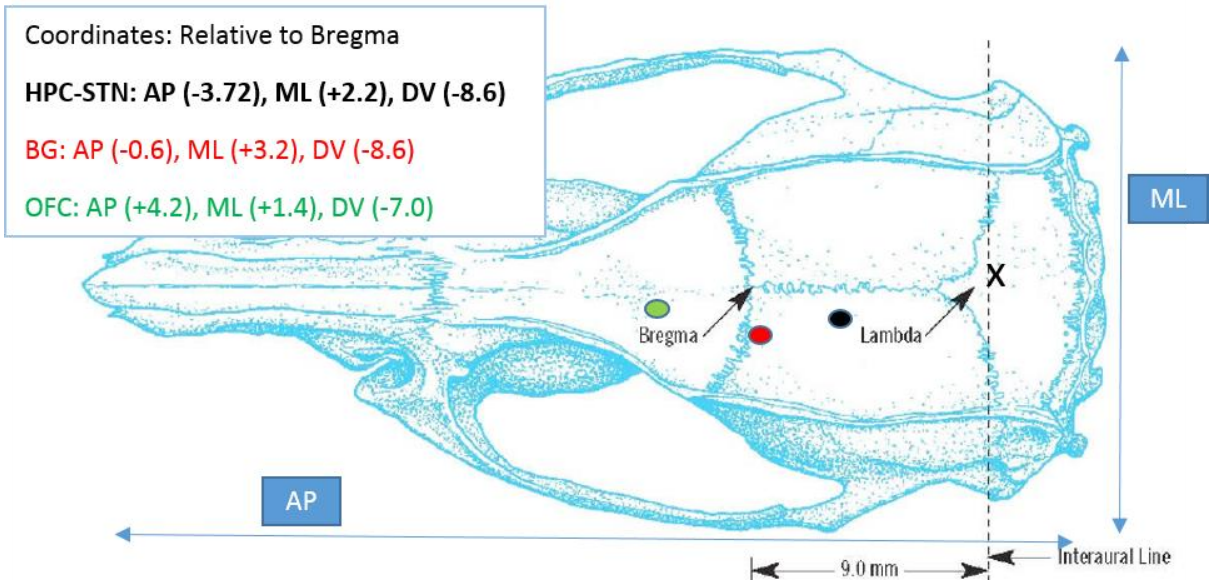

Figure 2.4 The location for unilateral stereotaxic electrode implantation into HPC-STN, BG and OFC. X; location of reference electrode. The recording sites mapped from Paxinos and Watson (2007).

The jig holding the electrode arrays with its stainless-steel rod was attached to a stereotaxic arm and brought in position directly above the designated coordinates and slowly lowered down into the brain. The HPC-STN array was used to judge the specific depths. All the electrodes were implanted in the left hemisphere. Then, the ground electrode (silver wire) was twisted around all skull screws. The male pin of the reference electrode was connected to the female pin in the MGA connector. Then the area surrounding the electrode arrays was cleaned and dried with a sterile swab. Dental cement (Lang Dental MFG. CO. Wheeling, IL, USA) was then applied and left to dry and harden. The MGA connector was cemented in with the female face of the connector towards the rear of the rat; and the headpiece was cemented up (except the female face of the connector) so that no wires were left on the surface and the structure looked smooth and sufficiently covered (see Figure 2.5).

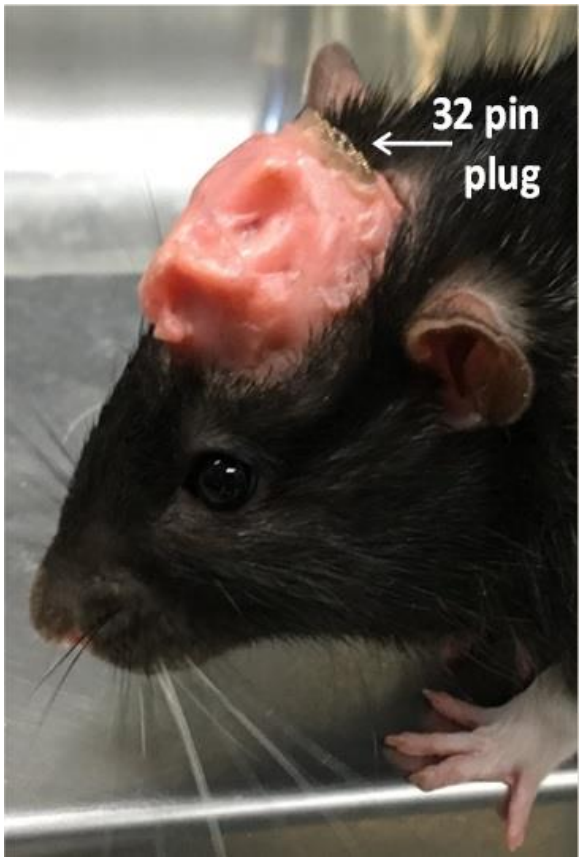

Figure 2.5 Rat with 32pin-3 array implant.

2.3.3 Recovery from Surgery

After surgery, the rats were kept under observation for several hours in a warm cage and allowed to recover for at least 10 days before electrophysiological recording and behavioural testing. They were monitored using standard University of Otago animal welfare score sheets (see appendix) every ~12 hours for the first 5 days after surgery (including through weekends) and checked more frequently if needed. During this time, they were provided with a mash that was made from pounded dry pellets and mixed to a paste with water and were provided with water in a separate dish. These were in addition to the normal supplies of food and normal water. The animals were given analgesics (Carprieve) as necessary (e.g. if showing signs of pain).

2.4 General Experimental Procedure

2.4.1 Food Restriction Scheme

Food restriction was started at least 10 days after surgery and prior to any manipulations. The rats were placed on deprivation gradually with free food for the first 8 hrs then 4 hrs, 2 hrs and 1 hr (each for two days). Final food restriction was ~15 g/day/animal of standard rat chow in addition to food obtained during execution of the tasks to ensure motivation to perform for food rewards. Animals on the restricted diet were weighed daily and the restriction eased if they reached <85% of their initial or projected body weight.

2.4.2 D-Maze Apparatus

For the behavioural test, a D-maze apparatus was developed as part of this PhD project. The D-maze box (see Figure 2.6) is a white plastic half-barrel; that is, a D-shaped half cylinder with a circle diameter of 82 cm. Each wall was 60 cm high. Five lights and sensors (one above the other, 15 cm and 10 cm above the base of the maze, respectively) were located in the curved wall and one light+sensor in the straight wall. Each light had a sensor below that detected when the rat approached the light. Rats responded by contacting the light (rather than the sensor) when it was on. A food tray was placed on the floor close to the straight wall at an equal distance (41 cm) from all the lights. 45mg food pellets (Chocolate flavor, Bio-serv Dustless Precision Pellets) could be delivered into this small food tray. The lights/sensors in the curved wall are identified below as 1, 2, 3, 4, 5 from left to right and the light/sensor in the straight wall as 0. Background illumination was provided by a ceiling light. The experiment was controlled and data were collected using programs written in Visual Basic 6, which controlled a LabJack U3-HV interface (LabJack Corporation,USA).

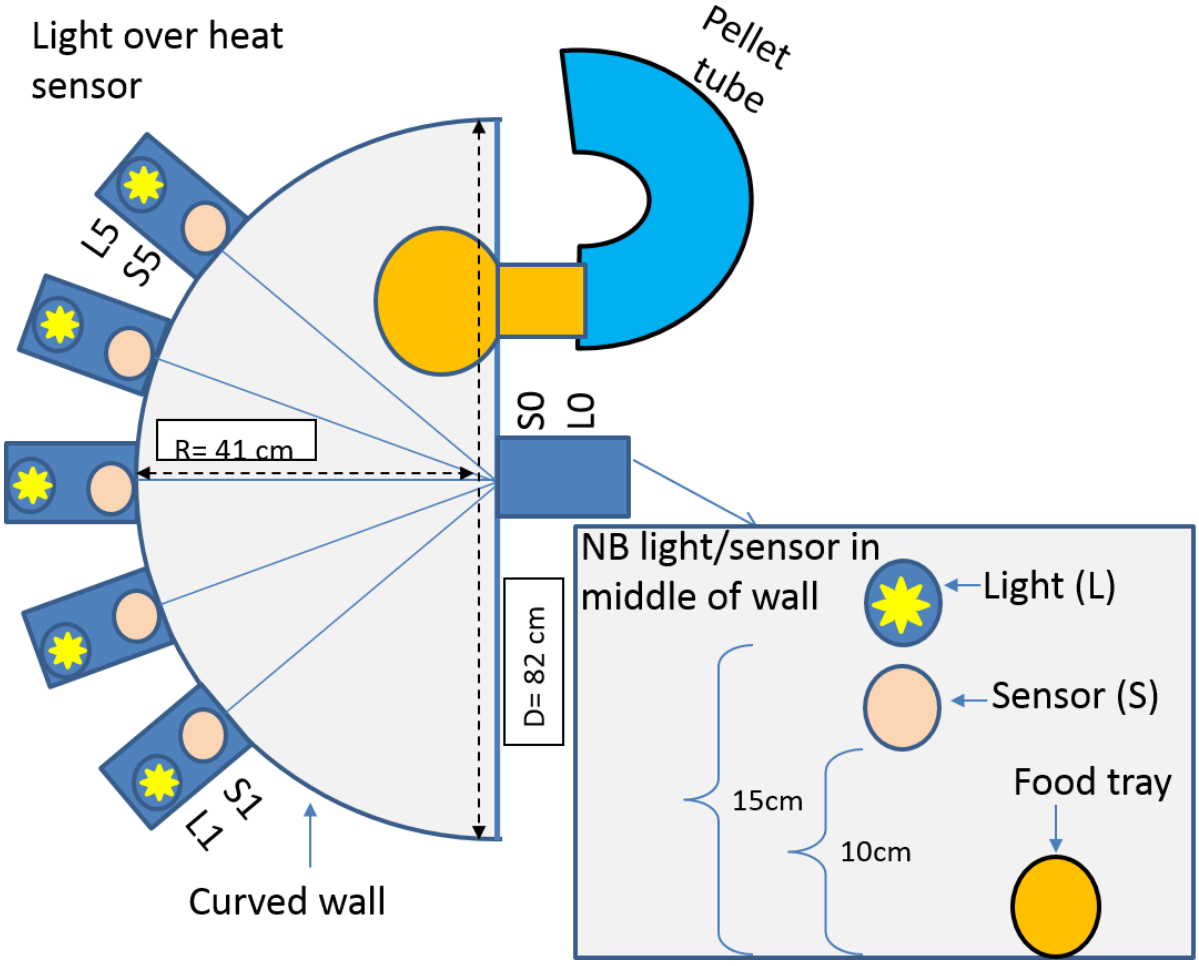

Figure 2.6 Schematic diagram of D-maze.

Two-dimensional view and main parts of D-maze; five lights over heat sensors on curved wall. The diameter of the D-maze is 82cm and all lights/sensors were an equal distance (41 cm) from the light/sensor in middle of wall. Inset: enlarge inner part of D-maze on straight wall consists of light, sensor (underneath the light) and a food tray. L1/S1; light1/sensor1, L5/S5; light5/sensor5, L0/S0; light0/sensor0.

2.4.3 Experimental Procedure

The D-maze apparatus was used for all behavioural testing. All the procedures were based on Eagle and Robbins (2003a).

2.4.3.1 Pre-training

Rats received 10-minute sessions with 80 food pellets that were scattered onto the floor of the D-Maze. This minimized neophobia and allowed rats to habituate to the apparatus. It was continued for at least 4 days or until all of the pellets were consumed.

2.4.3.2 Light 0 training: Sensor 0 (two sessions per day, 15 min each)

This training was designed to teach rats to make an association of Light 0 (L0) with food. Each rat received two 15-min sessions within a day. The aim was to train the rat to trigger Sensor 0 (S0) for food in the central food tray. At the beginning of the first trial, a pellet was delivered and L0 was switched ON. L0 remained on for 60s unless the rat triggered S0. If S0 was triggered while L0 was ON, L0 went OFF and food was delivered; and then there was a 1s intertrial interval before the start of the next trial. If the rat failed to trigger the sensor within the 60s limited hold (LH) period, the L0 was switched OFF and there was a timeout period (5s) before the beginning of the next trial. Rats were trained until they responded on at least 90% of trials for two consecutive days. Then, the rats proceeded to L1 training.

2.4.3.3 Light 1 Training: Sensor 1 (one session per day, 20 min each)

With this training, rats had to learn the association between Light 1 (L1) and food. A pellet was delivered to start the session. L1 was switched ON (L0 remained OFF). If the rat triggered S1, L1 was switched OFF and L0 was switched ON and the following events were as for L0 training. That is, triggering S0 delivered a pellet and started the next trial after a 1s delay. L1 had a limited hold of 60s with failure to trigger Sensor 1 delivering a 5s timeout period with both lights off before the beginning of next trial. Rats were trained until they responded on at least 70% of correct trials.

2.4.3.4 GO Training: Sensor 1 and then 5 (one session per day, 20 min each)

The purpose of Go training was to teach rats to make the Go response (respond to L1 to start the trial and then to Light 5 (L5) to complete it). The time taken by rats to move from S1 to S5 was taken as the Go reaction time (GRT). The animal had to respond to L5 within a LH time (see figure 2.7). The LH was set based on individual rat GRT performance to promote rapid training. The procedure for Go training was similar to L1 training except that when the rat triggered S1, L1 was switched OFF and L5 was switched ON. If the animal triggered S5 within the LH time then, L5 turned OFF and L0 was switched ON. Then the following events were as for L0 training. As can be seen in Figure 2.7, if the rat failed to trigger S5 within the

LH then the rat received a timeout period of 5s before the beginning of next trial. Rats were trained until they performed 70% of correct trials (and more than 40 trials total) at LH≤2.3s. L5 was presented for LH period (initially set at 60s and decreased in steps of 10s until a minimum of 2s) for the subsequent session if the rat completed more than 70% correct trials).

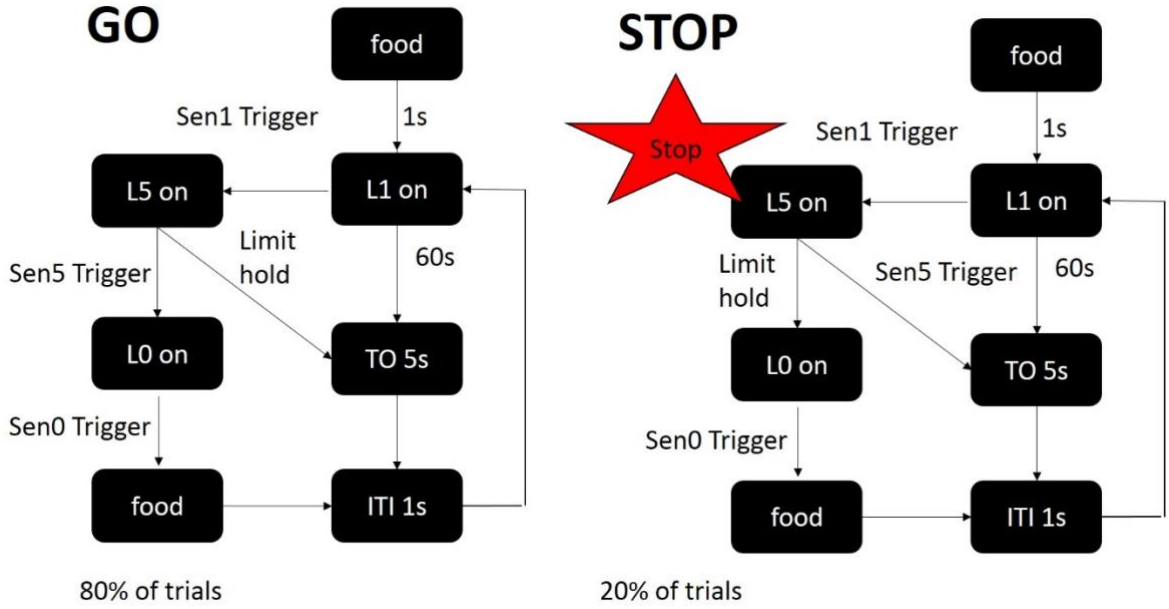

Figure 2.7 Flow chart showing contingencies for the Stop signal task.

Go trials were presented on 80% of the trials within the session to encourage the rats to go from L1 to L5. In stop trials (20% of the trials), a stop-signal tone (4500 Hz) was presented counterbalanced within blocks of trials to discourage the animals anticipating presentation of stop trials; and the rats were then required to stop completion of the Go response. TO; time out period, ITI; inter trial interval.

2.4.3.5 STOP Training

This was the final training stage of the Stop signal task. The rat had to learn to cancel or inhibit its ongoing Go response after the presentation of the Stop signal (a 4500 Hz, 40ms tone were presented randomly within the session to discourage the rats from anticipating presentation of the Stop trials). This training was as for Go training but with 20% of trials designated as Stop trials. After presentation of the Stop signal, if the rat did *not* trigger S5, trials were considered correct, S0 switched ON and a pellet was delivered. Triggering S5 after the Stop tone was considered incorrect and the rat received a time out period of 5s before the

beginning of the next trial. Occasionally, the rat responded on L5 before the onset of the tone (most often for later tone presentations), and these trials were reclassified as Go trials to maintain the overall proportion of valid Stop trials in each session at 20%. During initial training on the Stop/Go responses, the LH for Go trials (time in which rat had to respond) was set longer than the LH for Stop trials (in which the rat had to withhold the response). Both Go and Stop LHs for individual rats were then adjusted daily until they were at the same value. The time to respond during Go trials in which no Stop signal was present was calculated as Go reaction time (GoRT). On Go trials, the LH was set each day to mean GoRT (mRT)+200ms from the previous session for each particular rat (between 1s and 4s). Rats were trained until stable baseline performance was achieved (70% accuracy on both Go and Stop trials for three consecutive days).

Following initial Stop training, each rat received three baseline sessions, during which the Stop tone was presented with zero delay while L1 was ON, i.e., with no delay between the onset of the Go response and presentation of the Stop signal. The mRT and Stop signal delays (SSD) for each rat were calculated from a zero-delay session at the beginning of experimental set. SSDs were presented in the following order to reduce any ascending–descending order effects to a minimum. SSD = mRT-600ms, mRT-200ms, mRT-300ms, mRT-150ms, mRT-400ms, and mRT-500ms as in (Eagle & Robbins, 2003a). For each experimental set, the absolute value of SSD was changed between sessions but remained fixed within a session.

2.5 Local field potentials

Brain oscillations are characterized by rhythmic upward download fluctuations in time series (C. K. Young & Eggermont, 2009). LFP are summed electrical activity recorded extracellularly close to neuronal sources. LFP waveform are characterized by amplitude and frequency that depends upon the contributions of multiple sources/brain structures. As electric potential amplitudes are inversely proportional to distance of the recording electrodes from

sources, computed LFP are poorly explanatory of actual activity during an episode of interest (Buzsaki, Anastassiou, & Koch, 2012). But, with the advent of modern recording and analysis technologies, LFPs are extensively studied for their role in specific cognitive abilities (Thut, Miniussi, & Gross, 2012).

LFP can be recorded directly or indirectly; invasive methods are used for direct recording such as implantation of microelectrode arrays (MEAs), microdrive and tetrodes while EEG, magnetoencephalography (MEG), electrocorticography (ECoG) records indirectly and so non-invasively (Buzsaki et al., 2012; Ojemann, Ojemann, & Ramsey, 2013; Thut et al., 2012). Reference electrode position is key for the recording of the LFP because if it is too distant (with conventional monopolar recording) it could record signals from surrounding brain structures that add to the signal from the active electrode; while if it is local (as with conventional bipolar recording) the signal could be lost because both electrodes record it at the same amplitude (Sharott, 2014).

2.6 Behaviour and LFP Recording

Timing of events (sensor breaks, lights, food delivery) in the D-maze apparatus was controlled and recorded by a VB6 control program written by me. The behaviour of all the subjects was also video recorded. During the D-maze tests, animals were tracked using EthoVision XT (Noldus Information Technology, Wageningen, Netherlands). The electrical output from all array electrodes was recorded using Spike 2, Version 5 (CED, Cambridge, UK), which was synchronised with Ethovision via an LED in the camera's field of view. LFP signals were fed to a 32 channel Grass Model 15 Neurodata Amplifier system via the 32-pin plug connected to an FET system (see Figure 2.8). LFP were amplified (x 1000) and filtered (bandpass 1-300 Hz). The amplifier output was digitized and acquired by a CED Micro1401 data acquisition system through the Spike2 interface. LFP output was stored continuously at

256 Hz. “Level/Event+” channels were used to record events such as LED lights on and off, sensors triggered, stimulus lights on and off, and food delivered.

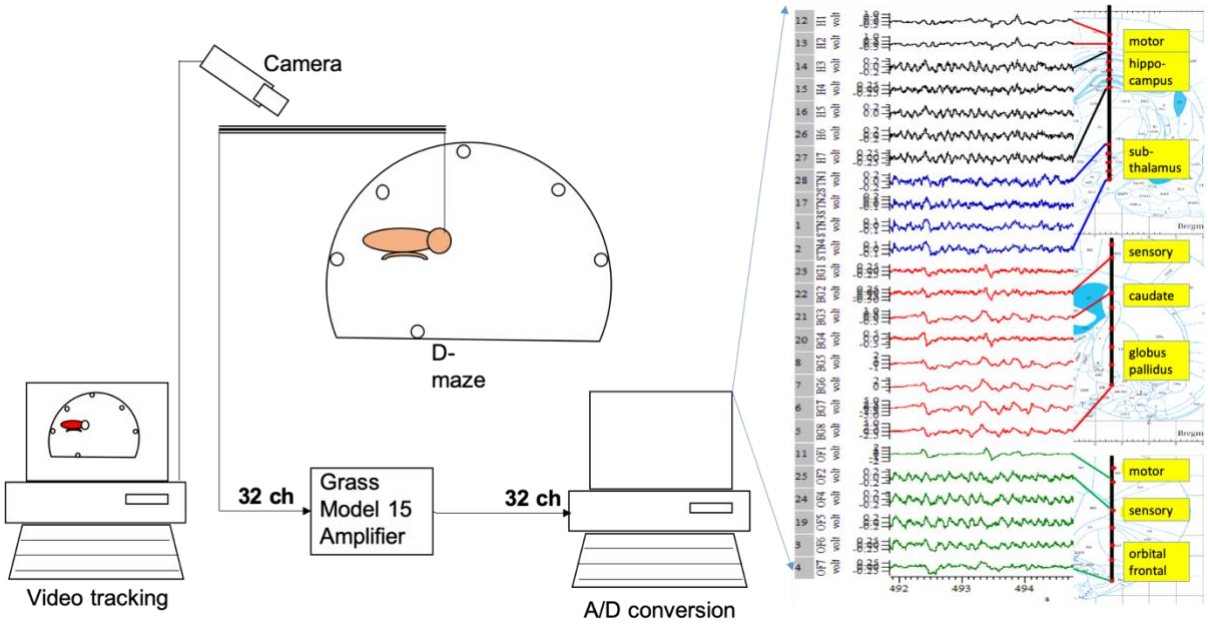

Figure 2.8 Experimental setup and LFP recordings

This diagram shows the combination of LFP recording and experimental setup for the SST in the D-maze with video tracking. 32 ch = 32 channels

2.7 Data processing and Electrophysiological Analysis

Behavioural output TXT files generated from Visual Basic 6 were first exported into Spike2 and the resultant datasets fed into custom-written analysis software (MATLAB R2015b, MathWorks). MatLab routines were designed and adapted by Dr Calvin Young. He also advised, supervised and provided training on how to conduct the analysis through a Spike2-MatLab-SPSS workflow. The acquisition, handling and processing of the datasets were done by me under his supervision and guidance.

LFPs were visualized using Spike2 that also showed simultaneous signal and event flag data. For data processing, the files were down sampled to 256 Hz using the in-built cubic spline interpolation in Spike2 (CED, UK) and exported to Matlab (Mathworks, USA).

The LFPs were further down sampled by a factor of 2 (to 128 Hz). Four seconds (-2 to +2s referenced to event markers) of LFPs were extracted for spectral analyses. Multitaper spectrograms were computed for display and simple power spectra were computed for ANOVA.

Multitaper spectrograms were computed with a time-bandwidth product of 5. All time-frequency analyses were done with a 2s moving window, stepping of each window was 0.05s with 90% overlap in the Chronux toolbox (http://www.chronux.org) using the function mtspectogramc (frequency range of 0 to 45 Hz with three tapers for spectral smoothing).

Simple power data for ANOVA were computed using Fast Fourier Transforms (FFTs) on 1s overlapping Hanning windows, with the start of the first window at 750ms before the event marker and start of the second window at 250ms before. The Hanning window is a cosine wave and so its power extraction is biased to its center, the resulting power spectra were assigned for analysis to the 500ms before and 500ms after the event. The use of the Hanning both improves the quality of the resultant FET and also doubles its frequency resolution relative to a 500ms square window. A LOG_{10} transform was then applied to normalize error variance before further statistical analysis. Based on the histological reconstruction, the electrodes centred in our regions of interest (STR, STN, OFC and HPC) were selected for all data analysis. Individual LFP data from each rat, and each session, were processed for coherence and power analysis.

2.8 Statistical Analysis

All statistical analyses were calculated using SPSS version 24 Statistics (IBM SPSS Version 24.0. Armonk, NY: IBM Corp, USA). Results are presented as mean ± SEM. In the current study, data analysis used a within-subjects repeated-measures ANOVA. The factors and levels for ANOVA to each experiment are described in detail in the respective Chapters.

Following repeated measures, *post hoc* analysis was used where appropriate using one way ANOVA or paired *t* tests were used for analyses of within-subject contrast. P values below 0.05 were considered statistically significant.

Chapter 3. Assessment of electrode positioning

3.1 Introduction

In this Chapter I describe the histology for the two final experiments for which the data in the thesis are reported. The final experiments involved two batches of animals: for the first batch (n=5) the individual electrode arrays were implanted separately at their relevant coordinates; and for the second batch (n=5) we designed and manufactured a jig (see method Chapter for description) and implanted all three electrode arrays together. Histological assessment of the positioning of the electrodes was carried out before analysis of the experimental data. In general, specific tissue damage could be seen as an indication for the position of an electrode in a specific area. Mostly, tissue showed a track mark going through the brain regions. Places where the final electrode tip of an array was located were identified through the characteristic form of damage in the tissue. Locations of other tips, further up the array, were derived from their distance from the bottom tip. Allocation of electrode placement to brain regions of interest was determined using a standard brain atlas (Paxinos & Watson, 2007).

3.2 Histological methods

After completion of *in-vivo* experiments, rats were deeply anaesthetised with sodium pentobarbitone intraperitoneally (300 mg/ml, i.p.) and perfused transcardially with cold (approx. 4°C) 250ml of 0.01M phosphate-buffered saline (PBS) and then 250 ml of 4% paraformaldehyde (PFA) and 0.01M PBS. Extracted brains were then kept in PFA/PBS solution for 24 h after which the brains were placed over to 30 % sucrose in PBS solution until they sank or for 7 days. The brains were placed on a microtome (Leica 1320, Germany), covered with a cryoprotecting gel (VWR Chemicals, Germany) and frozen with carbon dioxide. A freezing microtome using gaseous carbon dioxide was used to slice through the areas of interest producing 90 µm coronal sections. The sections were then wet mounted

directly to gelatin coated glass slides. For electrode positions, slices were stained with thionin and covered with a mounting medium (DPX, Merck, Germany), and at least 24 hours allowed for drying. The sectioned and mounted slices were then digitized using a digital macro camera (Dino-Lite, AD4013MTL, USA) and the photo files were used to reconstruct electrode placements according to the atlas of Paxinos and Watson (2007).

3.3 Results

3.3.1 Assessment of OFC electrode positioning

Histology confirmed the final position of the OFC electrode array. The OFC electrode array was positioned between bregma +3.0 up to bregma +4.2 mm (Figure 3.1). Figure 3.1A shows the anatomical illustration of the OFC with the final (lowest) positions of the electrode. Figure 3.1B shows an example of histological confirmation for the track of OFC array.

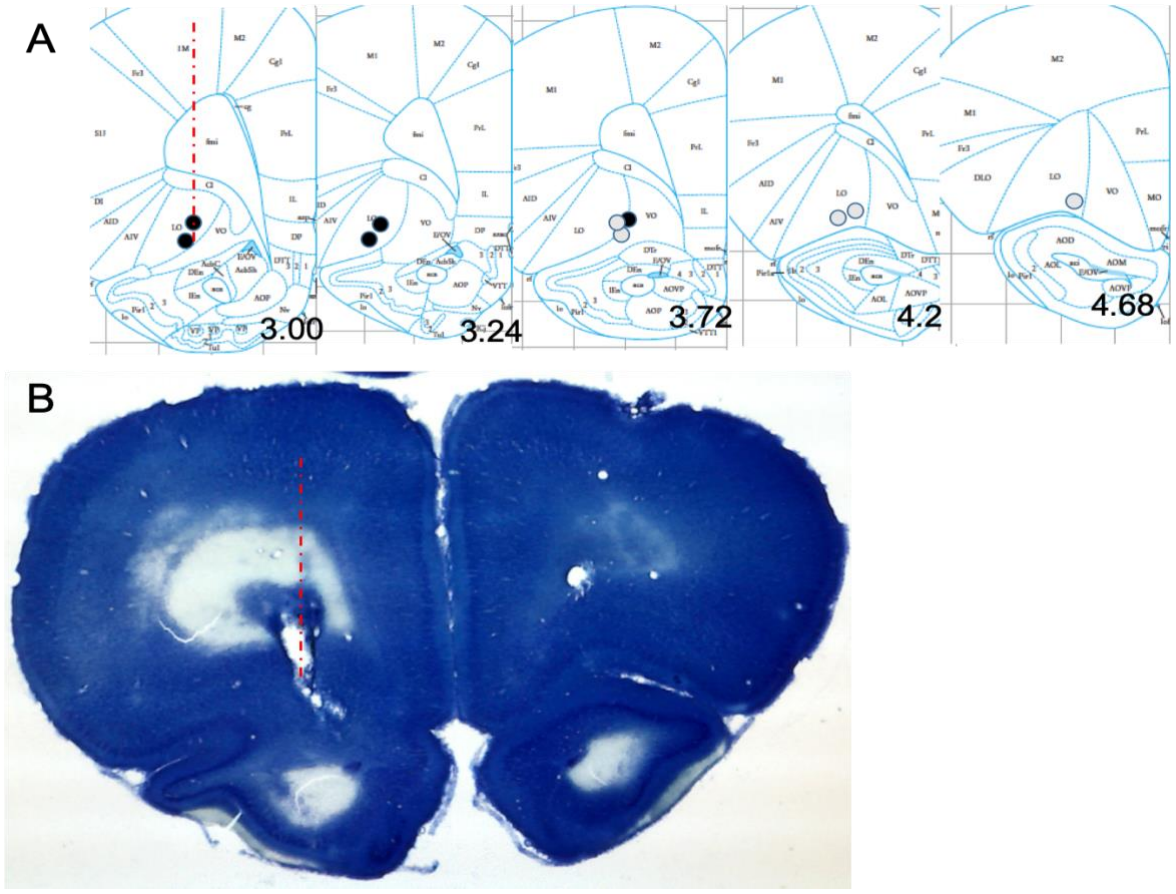

Figure 3.1 Histological placements of OFC electrodes.

A. shows the placement of electrodes in all animals (indicated by black dot: first batch and grey dot: second batch). OFC: 3.0 to 4.68 mm AP, but placements are shown collapsed on a single section. B. Shows representative thionin stained photomicrograph showing the electrode track (red broken lines) from the OFC array (+3.00 mm AP) on an implanted animal.

3.3.2 Assessment of striatum electrode positioning

When looking at the electrode positioning for the STR it was found that the AP position of the arrays varied between +0.12 to -0.6 mm from bregma. Histological assessment confirmed all electrodes were in the STR (Figure 3.2A). Figure 3.2B showed representative electrode trace from the STR on an implanted animal.

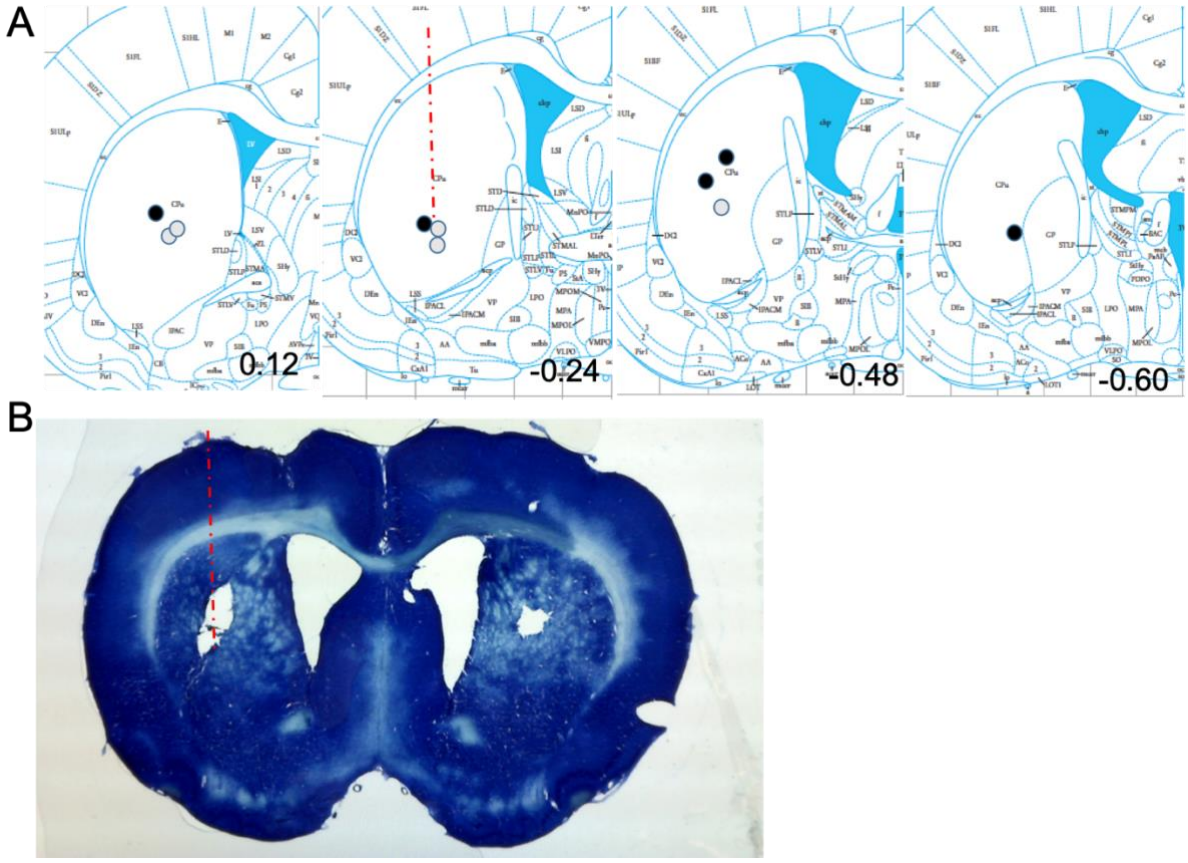

Figure 3.2 Histological placements of STR recording electrodes.

A. shows the placement of electrodes in all animals (indicated by black dot: first batch and grey dot: second batch). STR: 0.12 to -0.6 AP, but placements are shown on a single section. B. Shows representative thionin stained photomicrograph showing the electrode track (red broken lines) from the STR array (-0.24 mm AP) on an implanted animal.

3.3.3 Assessment of hippocampus-subthalamic electrode positioning

Histological investigation of the hippocampus-subthalamic electrode array found that electrodes ranged from -3.36 mm to -3.72 mm from bregma (Figure 3.3A). An example of histological confirmation showed the track of HPC-STN array.

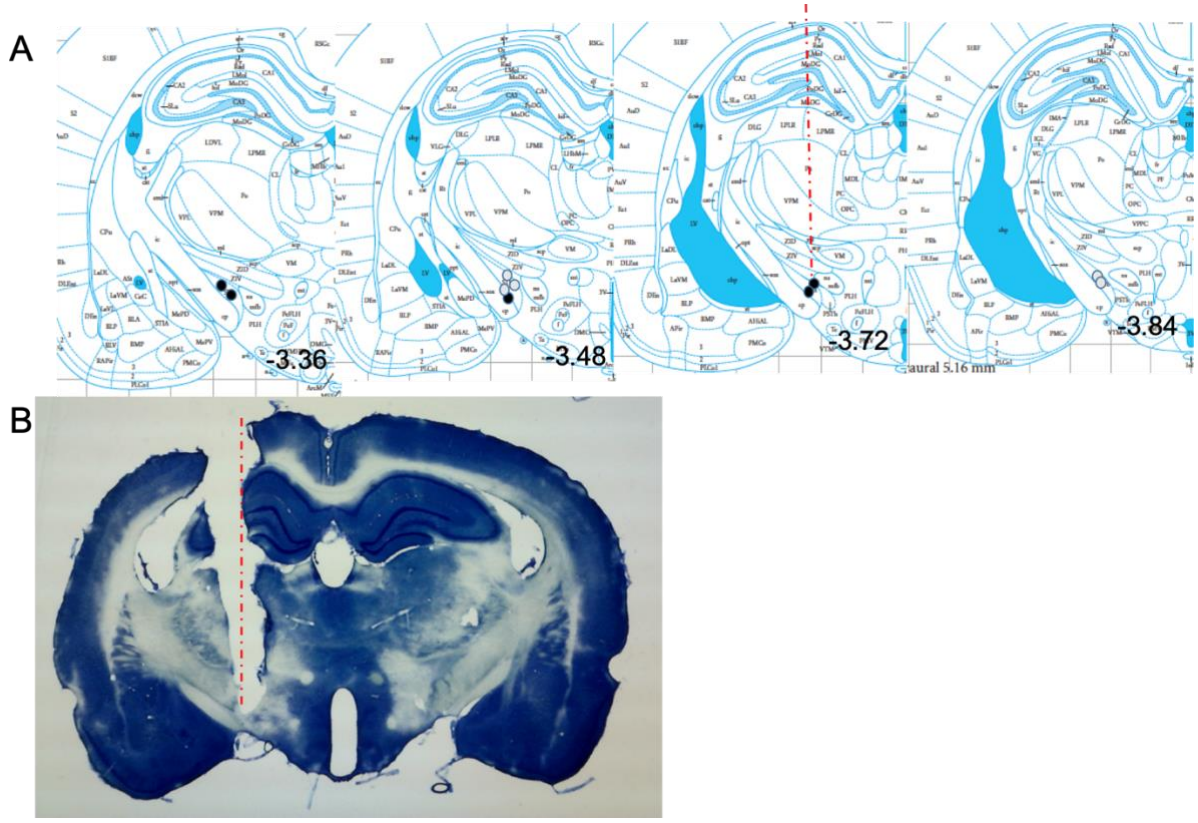

Figure 3.3 Histological placements of HPC-STN recording electrodes.

A. shows the placement of electrodes in all animals (indicated by black dot: first batch and grey dot: second batch). HPC: -3.36 to -3.84 AP, but placements are shown collapsed on a single section. B. shows representative thionin stained photomicrograph showing the electrode track (red broken lines) from the HPC-STN array (-3.72 mm AP) on an implanted animal.

3.4 Conclusion

The MEA electrodes were implanted in the left-brain hemisphere. Although, there were differences in electrode implantation methods, the targeted areas consistently exhibited a track mark going through into the targeted brain regions. In some rats there was some additional damage to other adjacent areas, but this was relatively minor.

Chapter 4. Electrophysiological investigation of striatal, orbitofrontal and hippocampal dynamic interactions during simple motor learning

4.1 Introduction

4.1.1 The role of the striatum and orbitofrontal cortex in simple motor learning

Motor learning involves both cortical (prefrontal, mainly motor) and subcortical (striatal) networks. As described in Chapter 1, the striatum is associated with the execution of the motor response, reward (Balleine, Delgado, & Hikosaka, 2007; Haber, 2003; Rothenhoefer et al., 2017), and also cognitive and motivational processing (Baldo et al., 2013; Tricomi & Lempert, 2015). Rat dorsal striatum consists of dorsomedial striatum (DMS) and dorsolateral striatum (DLS), which are homologous to caudate nucleus and putamen in humans respectively (Devan, Hong, & McDonald, 2011; Lanciego et al., 2012; Packard & Knowlton, 2002). DMS and DLS, together with nucleus accumbens are important for optimizing the individual response to stimulus-response contingencies (Graybiel & Grafton, 2015; Liljeholm & O'Doherty, 2012).

There is also evidence of dissociable functions among striatal sub-regions during motor learning, and motivational and cognitive tasks (Balleine et al., 2007; Devan et al., 2011; Graybiel & Grafton, 2015; Haber, 2003). For instance, rodent studies suggest that lesions in DLS differentially impair performance and recall (Jacobson, Gruenbaum, & Markus, 2012) implicating them in motor learning and memory (Packard & Knowlton, 2002). Conversely, goal-directed learning (Balleine et al., 2007; Devan et al., 2011; Hilario, Holloway, Jin, & Costa, 2012; Shan, Ge, Christie, & Balleine, 2014; Yin, Ostlund, Knowlton, & Balleine, 2005) and updating of stimulus-response-outcome contingencies (Devan et al., 2011; Yin et al., 2005) are associated strongly with DMS. Similarly, OFC is thought to contribute to reward-based learning and goal-directed behaviours (Tricomi & Lempert, 2015). During learning, OFC

particularly plays an important role in encoding information and updating the values of expected outcomes.

4.1.2 The role of the hippocampus in simple motor learning

In Chapter 1, I discussed the overall role of the HPC. Therefore, in this section I will focus on the hippocampal role only in learning, in particular early and late acquisition. Lesion studies in rats have shown that medial temporal lobe structures, such as the HPC play an important role in declarative learning and declarative memory (Jarrard, 1993) and lesions of the hippocampal network impair memory guided behaviour (Hasselmo & Eichenbaum, 2005; Hyman et al., 2010). The HPC appears to be important in early aspects of acquisition (Maviel, Durkin, Menzaghi, & Bontempi, 2004) and restoring hippocampal slow activity in rats restores initial learning in the Morris water maze (McNaughton et al., 2006).

In contrast, procedural learning involves acquiring and improving skills through practice. It includes both motor or perceptual and cognitive systems (Schmidtke, Manner, Kaufmann, & Schmolck, 2002). Previous studies have suggested that HPC is not involved during acquisition of the simple learning of e.g. running (Gould et al., 2002; Gray & McNaughton, 1983). Therefore, if HPC is not required during acquisition of simple motor learning, it would be interesting to see if, nonetheless, STR or OFC or both sends information to HPC during simple motor learning.

4.1.3 Interaction between striatum, orbitofrontal cortex and hippocampus in motor learning

Both the HPC and STR are functionally connected (Packard & Knowlton, 2002) and can be considered together as a learning and memory system (DeCoteau et al., 2007a). Human functional neuroimaging has shown motor memory consolidation involves a hippocampal-striatal network (Albouy et al., 2013). In particular, HPC competes with striatum during initial

learning and motor sequence memory consolidation to optimize subsequent behaviour (Albouy et al., 2008).

But STR and HPC are involved in learning and memory of different sorts. Research in human and animals has implicated the striatum in response learning and procedural memory (Bergstrom et al., 2018; Packard & Knowlton, 2002). HPC and striatum (particularly caudate nucleus) both have anatomical links with the OFC (Brown, Ross, Tobyne, & Stern, 2012). OFC can influence information processing in the HPC as it receives direct projections from HPC and sends projections to entorhinal cortex, the input structure of HPC (Cavada et al., 2000; Haber & Calzavara, 2009; Roberts et al., 2007).

In the present experiment we are particularly interested in the dynamics of frontal, striatal and hippocampal systems during GO task learning in rats. The task was cue based associative learning, a "GO-learning task" that is also the initial part of the stop signal task (see method section, Figure 2.7). We used multi-electrode arrays for *in vivo* electrophysiological recordings in rodents to examine the functional relationship among STR, OFC and HPC LFPs during two phases of learning, early and late.

Therefore, the first aim of our study was to examine changes in STR, OFC and HPC LFP oscillatory power and coherence over the course of learning. The second aim was to examine the functional relationship between STR and HPC in acquisition of simple motor type learning. We hypothesized in Chapter 1 that the STR sends information to HPC during initial learning of motor behaviour. Furthermore, OFC-HPC coherence might increase during expectancy of reward outcome.

4.2 Methods

The majority of the methods are explained in Chapter 2. Electrodes were implanted as an individual array. Some slight changes to the general procedures for this experiment are detailed below.

4.2.1 GO Task

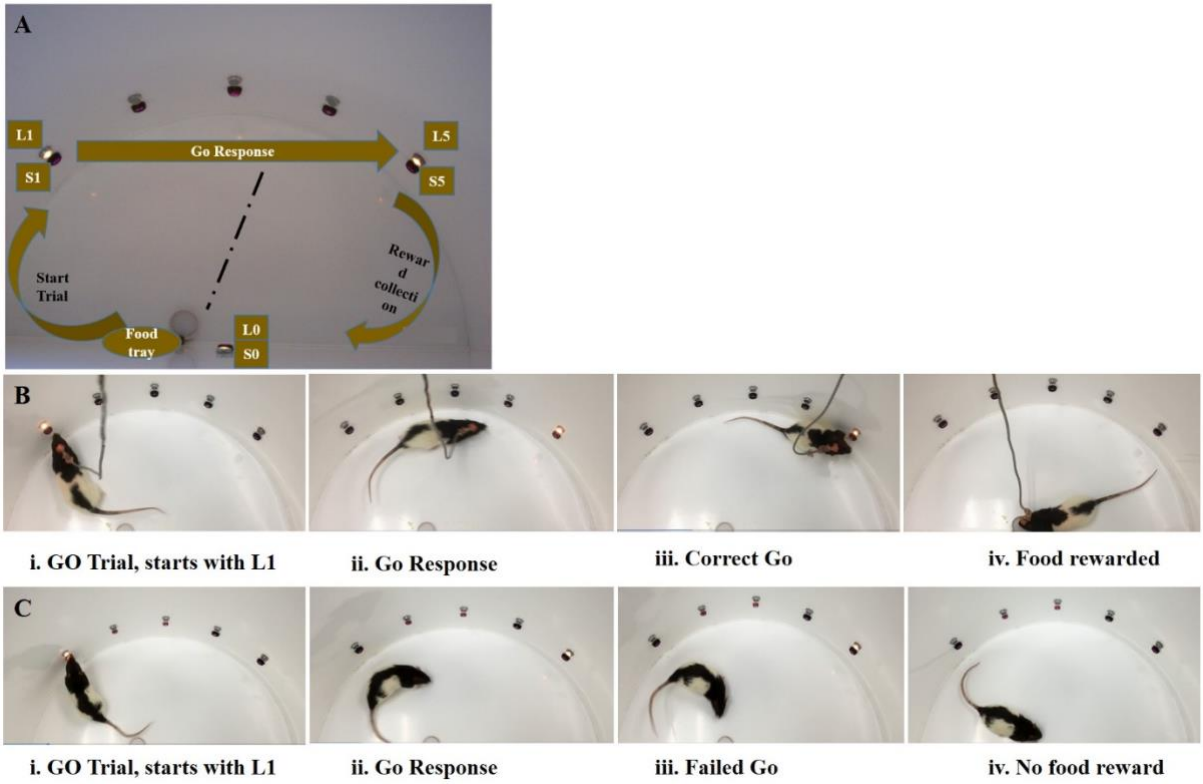

Figure 4.1 Photographic representation of animal performing Go Task.

A. Photograph of D-maze apparatus and diagrammatic representation of behavioural Go task. L1: Light1; L5: Light5; L0: Light0; S1: Sensor1; S5: Sensor5; S0: Sensor0. B. correct go trials. C. failed go trials. i, ii, ii, iv: successive steps in the trial.

Briefly, the purpose of GO training was to teach rats to make the go response (respond to L1 to start the trial and then to L5 to complete it). The time taken by rats to move from S1 to S5 was taken as the go reaction time (GoRT). The animal had to respond to L5 within a limited time - the limited hold (LH) time (see Figure 2.7). The LH was set based on individual rat GoRT performance to promote rapid training. The final stable LH was ranged between 1 and 1.9 s and were constant for each rat throughout the experiment. The procedure for Go training was similar to L1 training except when the rat triggered S1 (trial initiation), L1 was switched OFF and L5 was switched ON. If the animal triggered S5 (Go response) within the LH time then, L5 turned OFF and Light 0 was switched ON. Triggering sensor 0 (S0) then delivered food. Going from L1 to L5 was correct Go (CGo) and rewarded while failure to go

from L1 to L5 was considered failed Go (FGo) and animals were not rewarded. (See Figure 4.1).

4.2.2 Data processing

4.2.2.1 Behavioural data

The behavioural experiment was conducted until the animal had learned the task (8 days, D1-D8). Then experimental sessions were divided for analysis into two phases (blocks of 4 days): the early phase of learning; (D1-D4) and the late phase of training; (D5-D8). The average of early phase across animals (D1+D2+D3+D4/4) was compared to average of late period of trainings (D5+D6+D7+D8/4). Paired t-test between two sample for means was calculated. Go trial accuracy (%), mean go reaction time (MGRT), and variance of MGRT were measured as the performance indicator on the Go task in experiment 1 between early and late phase of training. MGRT was the mean of the time taken by the rats to trigger S5 after trial initiation. In addition, the total number of go trials was compared between the early and late phases of learning.

4.2.2.2 Event triggered power spectra – Go task

Power was measured before and after presentation of the Go stimulus during learning of the D-maze go task for early and late phases; and the late-early difference was also calculated. We analysed the power spectrum for frequencies between 1 and 45 Hz from LFPs simultaneously recorded from three brain areas. Average power of HPC, STR and OFC oscillations over four frequency ranges of interest was calculated at first response - trial initiation (trigger S1) and Go response (trigger S5) and reward delivery (trigger S0). Power 0.5s before and after triggering each sensor were then averaged separately for each band. Effects specific to learning were assessed as the difference in power between late and early phase within delta (1-4 Hz), theta (5-12 Hz), beta (14-23 Hz) and low gamma (25-35 Hz) frequency at the HPC, STR and OFC. These frequency ranges were chosen in correspondence with previous work (DeCoteau et al., 2007a; Lansink et al., 2016).

4.2.2.3 Event triggered coherence spectra – Go task

The 0.5s period before and after the key events (S1, S5 and S0 triggered) in the Go task was assigned a coherence spectrum between pairs of structures: HPC-STR, OFC-STR and HPC-OFC oscillations for the four frequency bands. Coherence spectra for delta, theta, beta and low gamma before and after triggering each sensor were then averaged separately.

4.2.3 Statistical analysis

All statistical procedures were as described in Chapter 2. The factors and levels for ANOVA to this experiment are described in detail here. ANOVA with a 2 x 3 x 4 x 3 factorial design [Phase (two levels: early / late) x Events (three levels: S1 / S5 / S0) x Frequency (four levels: delta / theta / beta / gamma) x Brain area (three levels: OFC / HPC / STR] was used to test the effects of learning. For coherence analysis, rather than brain area, the main factor of interest was pairs of brain areas, which were treated as a 'circuit' factor (three levels: HPC-STR / OFC-HPC / OFC-STR).

Given that the factor Events has three levels, the "quadratic" component in this case can be thought of as representing the difference between the S5 condition and a value obtained by averaging the two adjacent conditions (S1 and S0). Similar to trial type, brain area also has three levels, OFC, HPC and STR. The quadratic component can be thought of as representing the difference between HPC regions and a value obtained by averaging the OFC and STR levels. Furthermore, quadratic component of circuit can be thought of as representing the difference between OFC-HPC interaction and a value obtained by averaging the HPC-STR and OFC-STR levels.

4.3 Results

4.3.1 Behavioural Data

The key behavioural measures that characterize performance in the Go task are Go trial accuracy (%) and mean go reaction time (MGRT). MGRT is the average time taken by the rat to trigger S5 after trial initiation. MGRT differed across days of learning. As can be seen in

Figure 4.2A, at the beginning of learning, rats showed long MGRT, which decreased rapidly over the first 4 days as the animals learned the task. From the 4th day onwards the MGRT was short and stable. After the training, MGRT was significantly reduced (paired t test, early-late period), $t(4) = 8.51$, $p < 0.001$). Figure 4.2B summarize total number of go trials completed in the early and late period of learning. At the beginning of learning, the total number of go trials completed was low. Rats displayed more time moving around the D-maze. After the 4th day, the total number of trials completed was significantly high (See Figure 4.2B). A summary of the performance of the rats can be seen in Table 4.1.

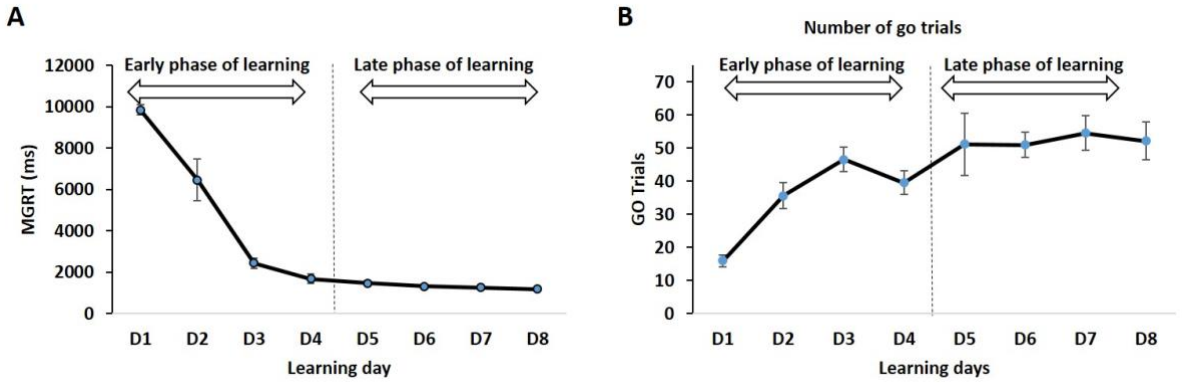

Figure 4.2 Early and late response on the Go trials.

A. Mean response time (MGRT; in milliseconds) on the go trials. We can see a clear change in MGRT before and after the task is learned. B. Total number of go trials completed on the task increased in the late period of learning. Error bars represent ±SEM. D1-D4 early and D5-D8 are late period of trainings for the averages of Table 4.1.

Table 4.1 Performance on the Go task. Data presented are average across rats across sessions.

Measures	**Early**		**Late**		***P***
	M	***SEM***	***M***	***SEM***	
Go trial accuracy (%)	71.9	5.5	87	2.4	*<0.01*
MGRT (ms)	4608.3	452.3	1319.2	76.9	*<0.001*
Go trial numbers	34.45	6.55	52.25	0.82	*<0.03*

Movement trajectory:

Figure 4.3 shows a schematic of movement patterns across learning stages for a single rat across learning sessions. The rat's trajectories are associated with response to the light stimulus for L1, L5 and L0. During the early period of learning in the Go task, after trial initiation (triggering S1) the rat tended to turn to the right (i.e. toward the food tray) and often did not trigger S5 (Figure 4.1Biii). After a few days the rat almost always triggered S5 and then S0 to collect the food (Figure 4.1Aiii, iv).

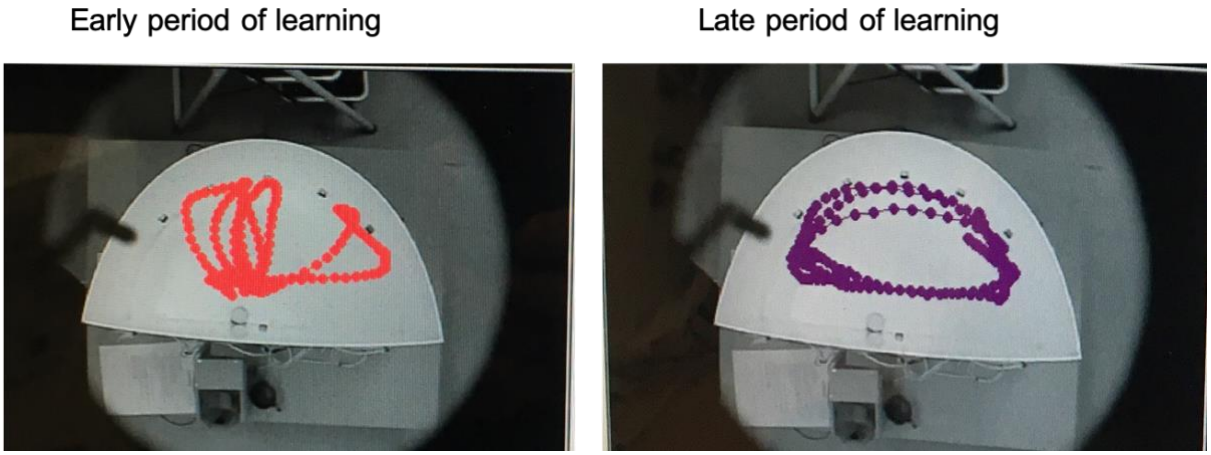

Figure 4.3 Pictorial representation of movement profiles across early and late period of learning sessions.

During early phase, rats tend to move towards food tray after triggering S1 rather going to L5. In contrast, at late phase animals move towards L5 to complete the task correctly and then moves to food tray to start next trial.

These behavioural results imply that the rat's behaviour changes due to the levels of learning achieved, but it does not actually suggest how brain areas (BG or OFC or HPC or all of them) and neural processing contribute to changes in each stage of learning. I therefore assessed the specific neural correlates of successful learning and adaption. For this purpose, I focused on analysing LFP oscillations in the STR, OFC and HPC during successive task events (triggering of S1, S5, S0), which is related to attention to the stimulus presented, monitoring and completion of the go task (running towards the S5), motivation and collection of reward.

4.3.2 Electrophysiological Analysis of task events (S1, S5 and S0)

4.3.2.1 Description: Power spectrograms for striatum, orbitofrontal cortex and hippocampus

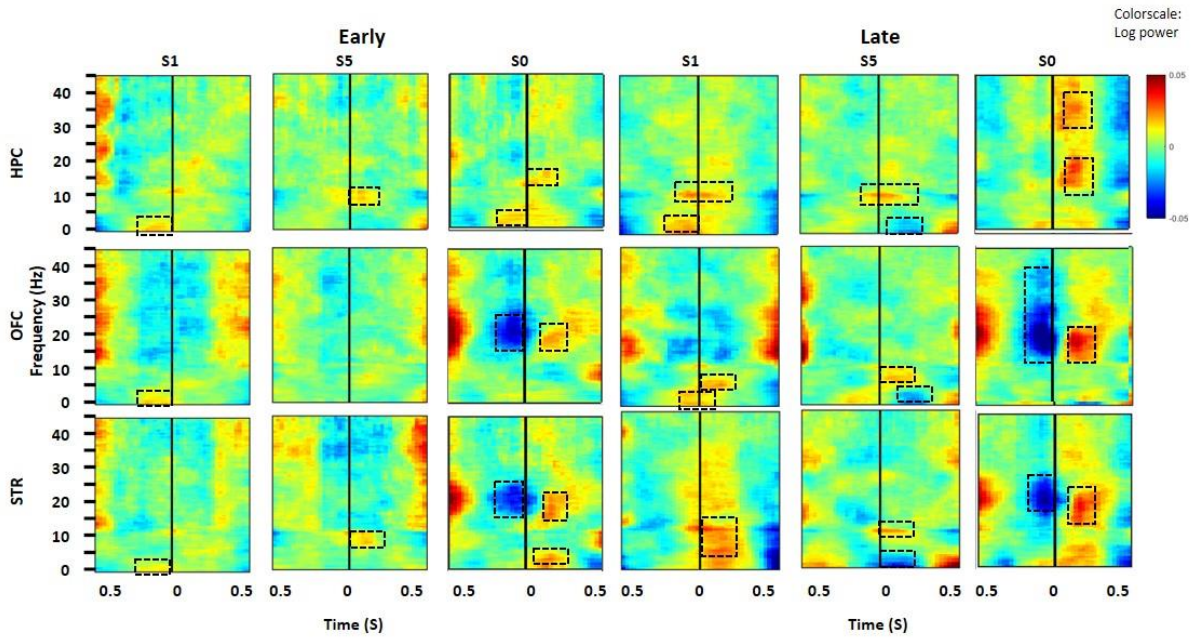

Figure 4.4 Average time frequency power spectra over all sessions across rats (n=5).

The HPC, OFC and STR power for successive task events at early and late period of training. Note power values were log transformed before averaging and plotting. Vertical solid line indicate time of sensor triggered (S1: sensor 1 triggered, trial initiation; S5: sensor 5 triggered, Go response; S0: sensor 0 triggered, reward delivery)

Figure 4.4 shows time frequency spectrograms for the three recording sites. LFP power in STR, OFC and HPC LFPs was modulated by task events (as the rat triggers S1, S5 and S0). The spectral content shows differences across different frequency bands. During early learning, delta (1-4 Hz) power was greater before the rat triggered S1 in all brain areas (left panels). In the late period, STR delta and theta power increased while power decreased in HPC after trial initiation (S1 triggered). A theta band (5-15) activity can be seen in HPC (top panel) and STR (bottom panel) after sensor triggered at early period of learning. Interestingly, delta power among all three areas decreased in late period after go response (S5 triggered). Within the theta band, power in all regions becomes greater after the task is learned (late period; top and bottom panel). On the other hand, OFC shows such increases in theta power for late learning only. In low gamma band (23-35 Hz), HPC power was greater after the food is delivered. Interestingly,

both early and late period of learning showed enhanced beta power across all structures following a reward delivery.

4.3.2.2 Analysis: STR, OFC and HPC LFP power are modulated with task events during early and late period of learning

Before sensor triggering: Figure 4.5 shows that the STR, OFC and HPC across four frequency bands exhibit different task-dependent power modulation during learning of the D-maze GO task before sensor triggering. The effects of learning (late-early differences) are displayed in the right panel. Results from repeated measures ANOVA yielded a significant three-way interaction (Events [quadratic] x Frequency [linear] x Brain area [linear], $F(1, 4) = 14.689$, $p = 0.019$). *Post hoc* tests were carried out to clarify the effects driving this interaction.

In the delta frequency, when the rat triggers S5 (second response on the Go task), the OFC power was greater than STR ($t(4) = 2.951$, $p = 0.042$). However, the lower power in HPC and STR at S5 was similar ($t(4) = 1.127$, $p = 0.323$).

In the theta band, both OFC and HPC power increase at trial initiation and reward expectation but did not differ from each other (Event [linear] x Brain area [linear], $F(1, 4) = 0.048$, $p = 0.837$). All other comparison were not significant. Similarly, in the beta band, we saw similar pattern to theta across all brain areas. The increase in HPC and STR power did not differ between events ($t(4) = -0.906$, $p = 0.416$). All the other comparisons are non-significant

Finally, within the low gamma band, HPC power increased across task events compared to OFC and STR (Brain area [quadratic] x Event [linear], $F(1, 4) = 35.047$, $p = 0.004$). However, we did not see significant difference between OFC and STR ((Brain area [linear] x Event [linear], $F(1, 4) = 0.053$, $p = 0.829$). Combined these results demonstrated that reward expectancy increases the theta power both in OFC and HPC. In addition, LFP activity was increased in STR immediately after the S5 was triggered.

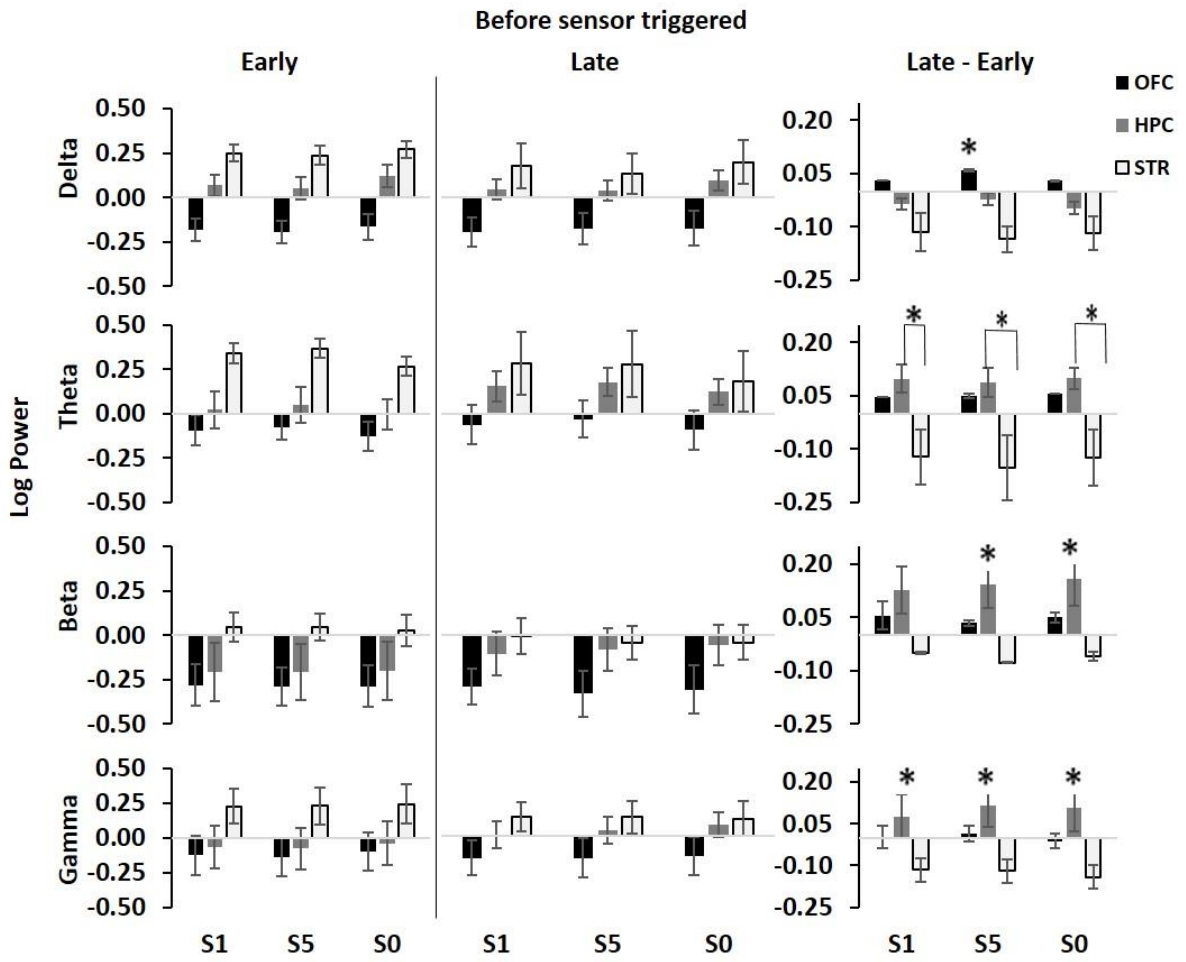

Figure 4.5 STR, OFC and HPC power at four frequency bands are differentially modulated during learning of D-maze GO task before sensor triggered.

Events labels; S1: sensor 1 triggered; S5: sensor 5 triggered; S0: sensor 0 triggered. ns: non-significant, * : significant

After sensor triggering: The effects of learning (late-early differences) after each of the sensor is triggered is displayed in the right panel of Figure 4.6. Results from repeated measures ANOVA yielded a significant three-way interaction (Events [linear] x Frequency [linear] x Brain area [quadratic], F (1, 4) = 11.545, $p = 0.027$). *Post hoc* tests were carried out to clarify the effects driving this interaction.

We observed significant effects at beta frequencies. OFC beta activity showed a linear increase in power across the 3 brain areas (Events [linear] x Brain area [linear], F (1, 4) = 12.707, $p = 0.023$). All other interactions are non-significant.

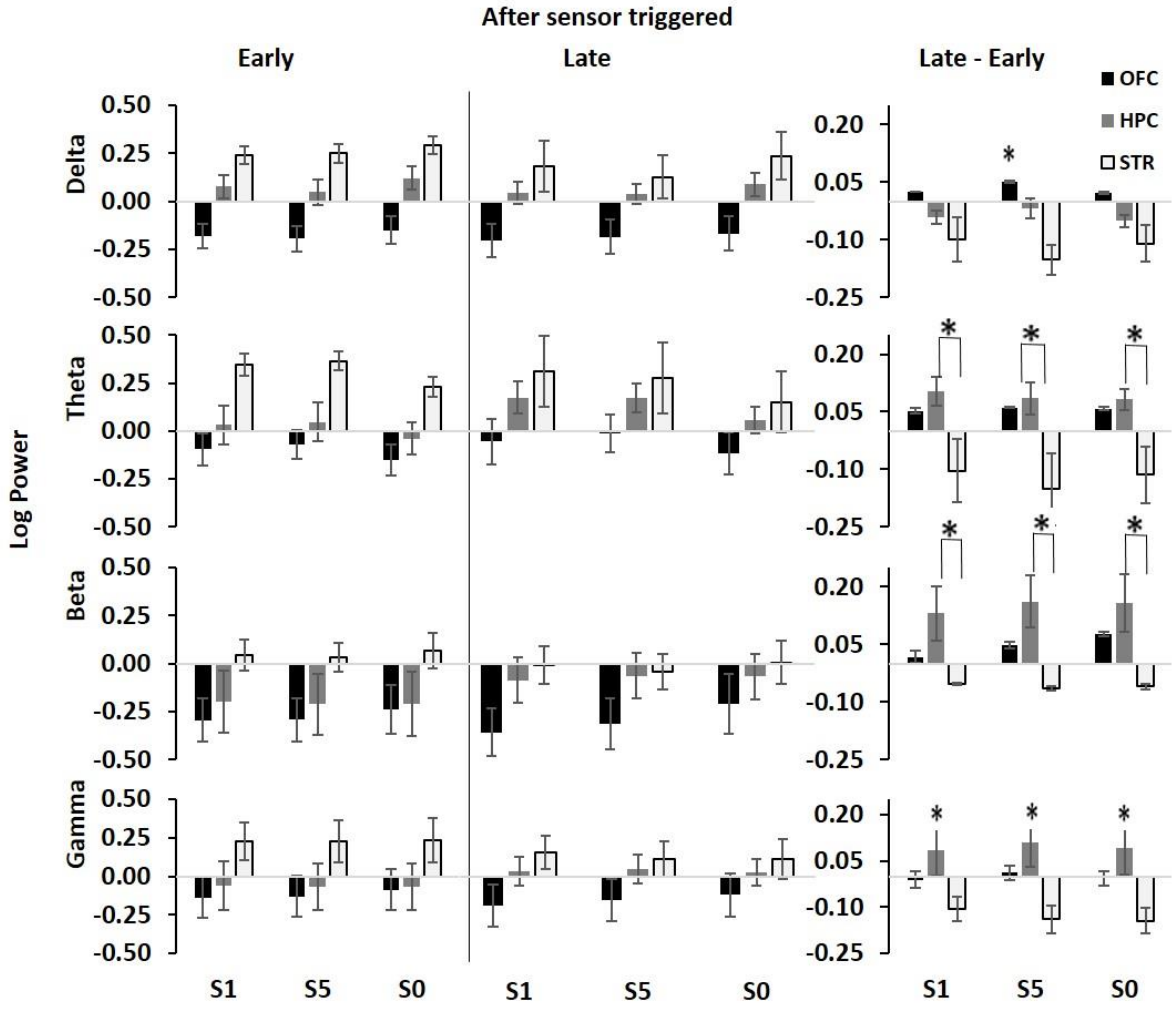

Figure 4.6 STR, OFC and HPC power at four frequency bands are differentially modulated during learning of D-maze GO task after sensor triggered.

Events labels; S1: sensor 1 triggered; S5: sensor 5 triggered; S0: sensor 0 triggered. ns: non-significant, * : significant

After-before sensor triggering: Figure 4.7 shows the change in power in relation to the sensor being triggered between brain areas after the animal learned the task (late-early differences, right panel). We observed borderline significant effects of learning (Events [quadratic] x Frequency [quadratic] x Brain area [quadratic], F (1, 4) = 7.630, p = 0.05). *Post hoc* testing showed in the delta frequency, HPC increased activity after triggering S5 as compared to OFC and STR ((Events [quadratic] x Brain area [quadratic], F (1, 4) = 35.230, p = 0.004). The quadratic component can be thought of as representing the difference between

HPC regions and a value obtained by averaging the OFC and STR levels. In the theta band, S1 triggering (trial initiation) increased power of all brain areas, however, we observed reduced HPC power compared to STR after triggering of S0 (t (4) = -5.966, p = 0.004). OFC power at beta frequency was found to be greater after reward delivery compared to HPC (t (4) = 2.815, p = 0.048) but not with STR (t (4) = 0.866, p = 0.435). The gamma band did not show significant differences among brain areas (Brain [linear], F (1, 4) =0.010, p = 0.991).

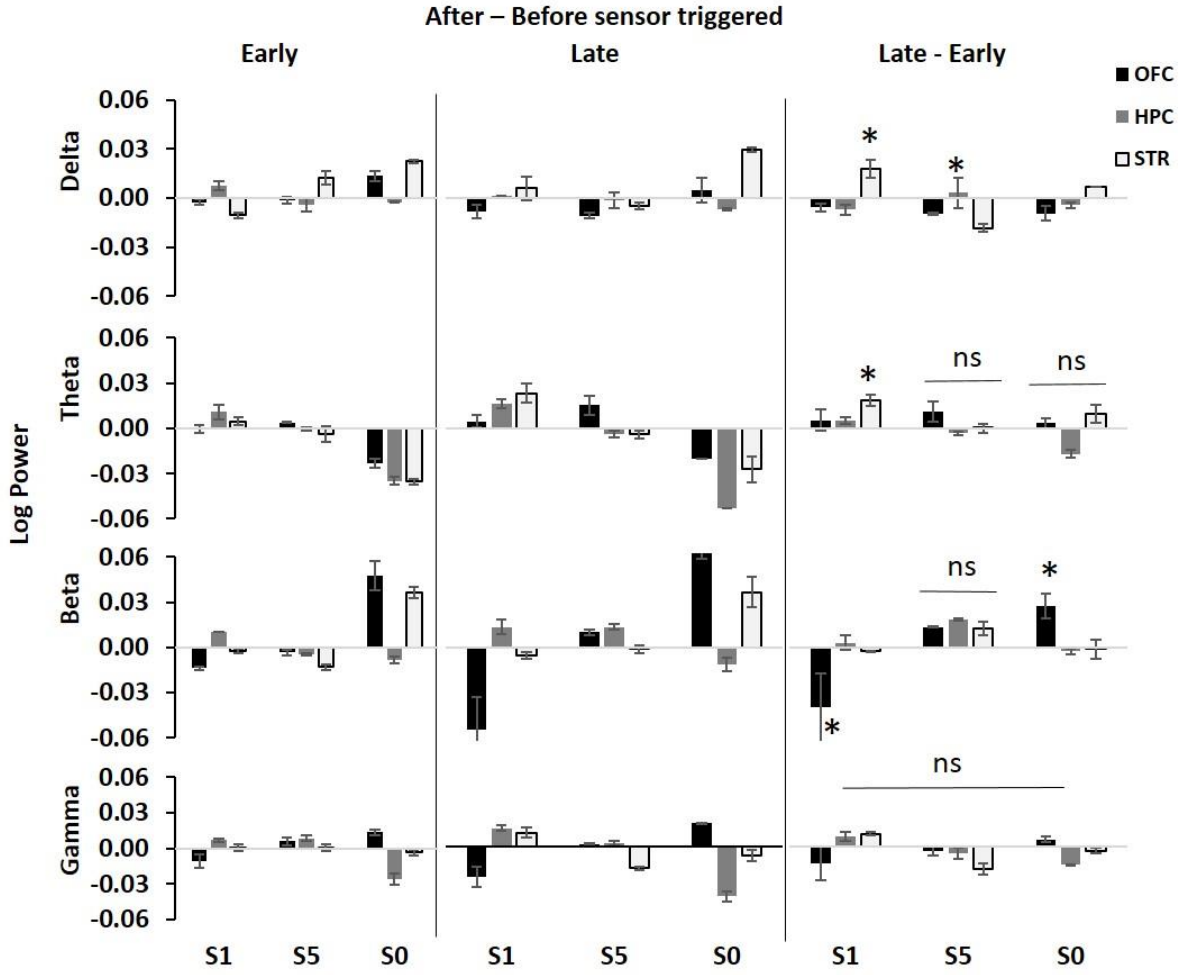

Figure 4.7 STR, OFC and HPC mean power at four frequency bands are differentially modulated during learning of GO task after-before sensor triggered.

Events labels; S1: sensor 1 triggered; S5: sensor 5 triggered; S0: sensor 0 triggered. ns: non-significant, * : significant

4.3.2.3 Description: Cohereogram between hippocampal-striatal, orbitofrontal-hippocampal and orbitofrontal-striatal during successive task events

Figure 4.8 shows cohereograms for pairs of structures (STR-HPC, OFC-HPC and OFC-STN) during task events. All pairs of brain structures show greater coherence in the theta band (5-12 Hz) during task performance in the D-maze. OFC-STR shows strong coherence in the beta band (23-35 Hz). Overall, coherence was greater in the early period compared to late.

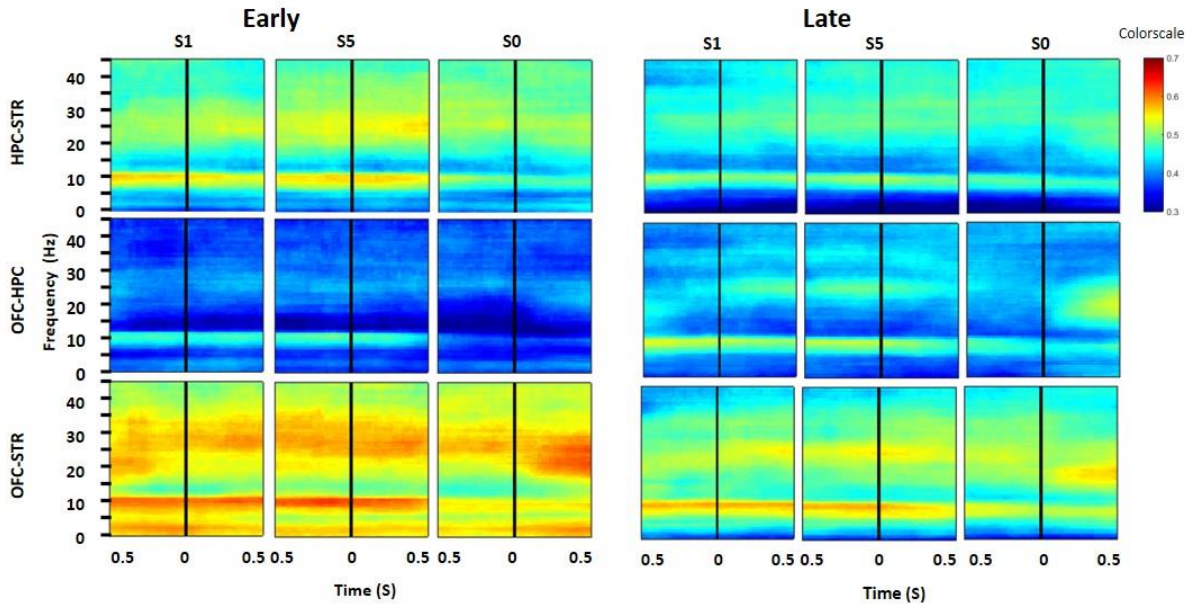

Figure 4.8 Coherogram average over all sessions across rats (n=5).

The coherence between HPC-STR, OFC-HPC and OFC-STR LFP oscillations during 0.5 s before and after sensor triggered for successive task events at early and late period of training. Vertical solid lines indicate time of sensor triggered (S1: sensor 1 triggered; S5: sensor 5 triggered; S0: sensor 0 triggered)

4.3.2.4 Analysis: STR, OFC and HPC shows task dependent patterns of coherence at four frequency bands, during learning of GO task

Before sensor triggering: Figure 4.9 shows the coherence between HPC-STR, OFC-HPC and OFC-STR before sensor triggered at four frequency bands. The effects of learning (late-early differences) displayed in the right panel shows significant interaction between factors (Event [linear] x Frequency [quadratic] x Phase [linear], F (1, 4) = 19.020, p = 0.012). *Post hoc* testing displayed quadratic effect of OFC-HPC. This suggest greater coherence between OFC-HPC compared to two pairs of STR (HPC-STR and OFC-STR) after the task is learned (Circuit [quadratic], F (1, 4) = 11.976, p = 0.026) (see right panels). However, we did

not find a change in coherence between HPC-STR and OFC-STR during task events (Circuit [linear], F (1, 4) = 0.497, p = 0.520). Additionally, interaction between event and circuits at delta and theta frequency was not significant (Events [linear] x circuit [linear], F (1, 4) = 0.789, p = 0.425) and (Events [linear] x circuit [linear], F (1, 4) = 1.361, p = 0.308) respectively.

Interestingly, in the beta band, interaction between factors was significant (Events [linear] x circuit [linear], F (1, 4) = 22.795, p = 0.009). *Post hoc* testing demonstrated increased coherence between HPC-STR after triggering S0 compared to HPC-OFC (t (0.464) = $p < 0.05$).

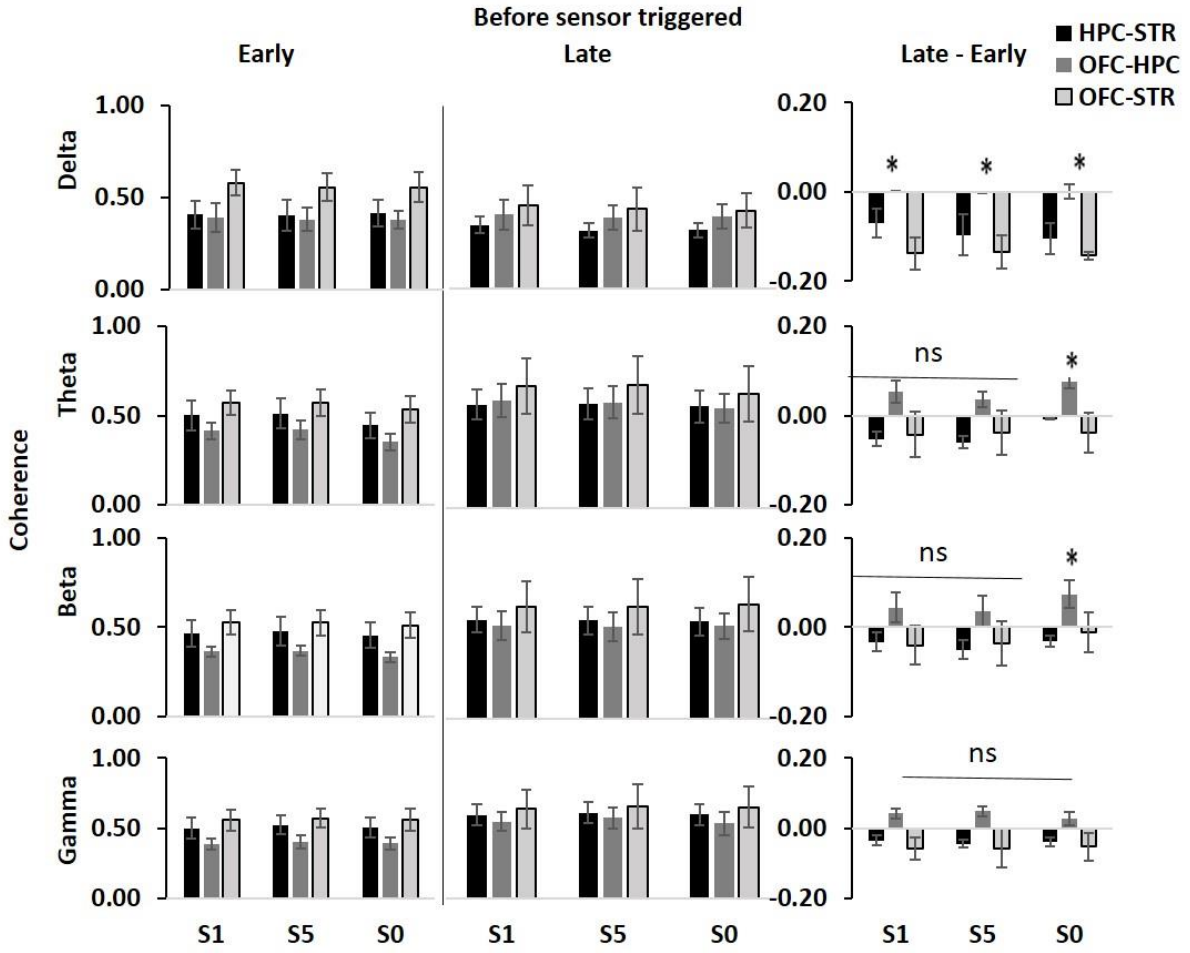

Figure 4.9 The mean coherence between HPC-STR, OFC-HPC and OFC-STR LFP oscillations before sensor triggered for successive task events at early and late period of training.

Events labels; S1: sensor 1 triggered; S5: sensor 5 triggered; S0: sensor 0 triggered. ns: non-significant, * : significant

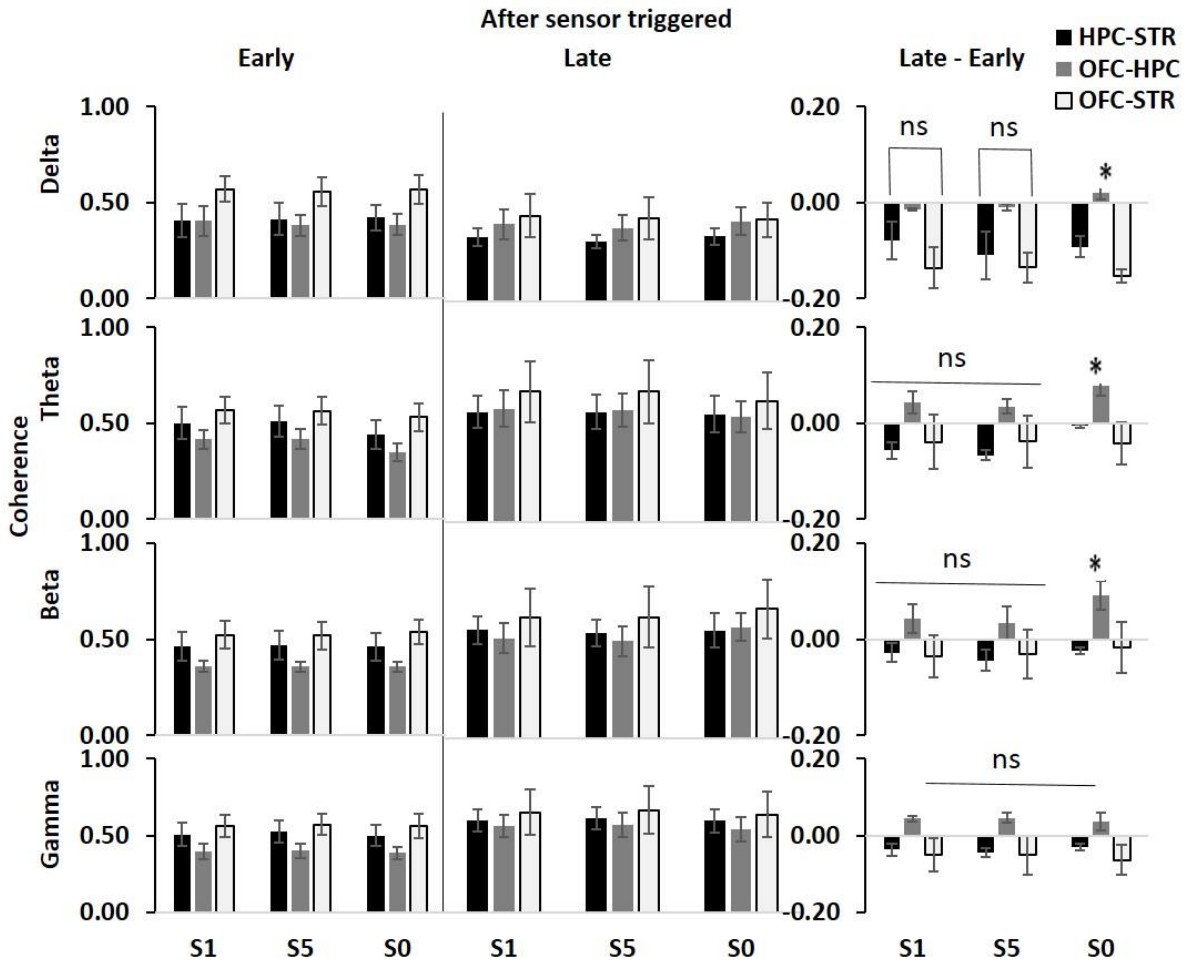

Figure 4.10 Distinct frequency bands exhibit different coherence variations in task events of after sensor triggered at early and late period of learning.

Events labels; S1: sensor 1 triggered; S5: sensor 5 triggered; S0: sensor 0 triggered. ns: non-significant, * : significant

After sensor triggering: Figure 4.10 shows the coherence between HPC-STR, OFC-HPC and OFC-STR after the sensor was triggered for each task events for four frequency bands. Overall, the effects of learning (late-early differences) shows similar coherence modulation as before. However, in contrast to before the stimulus was triggered, a significant interaction between factors (Circuit [linear] x Event [linear] x Frequency [cubic] x Phase [linear], F (1, 4) = 6.926, p = 0.05) was observed, whereby *post hoc* testing showed that after the animal learned the task, the OFC-HPC delta coherence was greater after triggering S0 (reward delivery) compared to triggering of S1 (trial initiation) and S5 (Go response).

In the theta and beta frequency bands, OFC-HPC coherence was greater after triggering S0 compared to triggering S1 (t (4) = 2.677, p = 0.05) and S5 (t (4) = -2.445, p = 0.05). In contrast, within the gamma band, the OFC-HPC interaction was not different among task events (Circuit [linear] x Event [linear], F (1, 4) = 0.644, p = 0.467). All other comparisons are not significant.

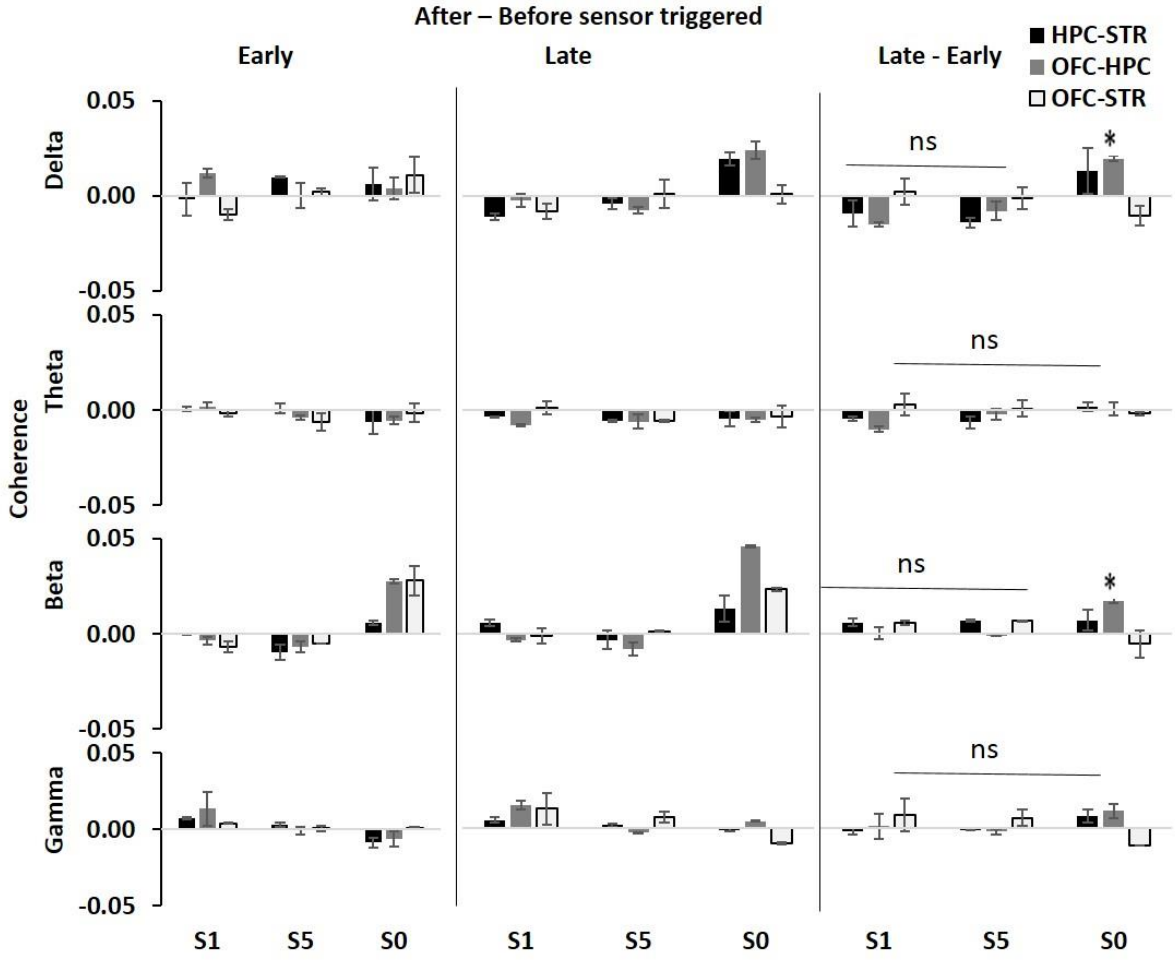

Figure 4.11 Mean coherence between HPC-STR, OFC-HPC and OFC-STR LFPs oscillations during 0.5s before and after sensor triggered for successive task events at early and late period of learning.

Events labels; S1: sensor 1 triggered; S5: sensor 5 triggered; S0: sensor 0 triggered, ns: non-significant, * : significant

After-Before sensor triggering: Figure 4.11 shows the coherence between pairs of structures (HPC-STR, OFC-HPC and OFC-STR) modulated after the task is learned. The effects of learning is shown by late-early differences at the right panel. A significant three-way

interaction was observed between factors (Event [linear] x Frequency [quadratic] x Phase [linear], F (1, 4) = 19.558, p = 0.011). *Post hoc* testing showed that the OFC-HPC coherence was found to be stronger than the average of HPC-STR and OFC-STR during reward collection at delta and beta frequency (Circuit [quadratic], F (1, 4) = 12.419, p = 0.024). In contrast, during trial initiation and Go response, coherence between pairs of STR (HPC-STR and OFC-STR) was stronger compared to OFC-HPC at beta. Furthermore, after the task is learned, gamma frequency did not show significant difference. (Circuit [linear], F (1, 4) = 0.499, p = 0.519).

4.4 Discussion

This study used a novel D-maze apparatus, which in contrast to a classical operant chamber had sensors to detect responding. When animals responded to the light stimulus by approaching it, the sensor was triggered. In this simple motor learning task, implanted rats were trained on a D-maze that required cue-based associative learning. Briefly, this task consisted of chain of processes i.e. first approach to L1 to trigger S1 then run towards L5 to trigger S5 and finally approach towards L0 to trigger S0 and get the reward. Therefore, the animal learned to collect rewards by approaching the light stimuli and triggering the sensors.

Oscillatory neuronal activity has been implicated in cognitive functions (Buzsáki & Watson, 2012), sequential motor learning (Day & Nick, 2013; van der Meer & Redish, 2009; van Wijk, Beek, & Daffertshofer, 2012), reward expectancy (Lansink et al., 2016; van der Meer & Redish, 2009), predicative processing (Yordanova, Kolev, & Kirov, 2012), working memory (Duzel et al., 2010) and attention (Cannon et al., 2014). The goal of the present study was to compare OFC, HPC, and STR when rats completed light stimulus-response association task. It was also the initial training step required for the stop signal task. Therefore, the first aim of our study was to examine the dynamic interactions between STR, OFC and HPC LFP activity during GO task learning. We demonstrated that during goal-directed behaviour, learning dependent coherence relationships between HPC-STR, OFC-HPC and OFC-STR was found.

4.4.1 Behaviour

After the animal learned the go task in the novel D-maze apparatus, they maintained a high level of accuracy. Latencies to respond in Go trials after the animal learned the task were short 1319.2 ms compared to early period 4608.3 ms. Also, rats learned the task faster. In addition, we found that rats can be exposed to novel apparatus and are able to learn and retain stimulus response outcome contingencies. These findings support the notion that rats can rapidly acquire visual learning in a novel behavioural apparatus (Furtak et al., 2009).

4.4.2 Striatal, orbitofrontal and hippocampus LFPs oscillations have different task-dependent coherence and power patterns

We directly compared the delta, theta, beta and gamma band LFP rhythms in three structures under similar behavioural conditions (triggering of S1, S5, S0) before and after sensor triggering in both the early (dynamic) and late (asymptotic) period of learning. We investigated LFP modulations in HPC, OFC and STR as the rat performed the maze task. Before and after the sensors triggered during early and late period of learning show similar patterns at four frequency bands. However, effects of learning in the GO task were clearly seen (as shown by the after-before and late-early difference). The key findings from the study are briefly summarized in this section. The detailed discussion is given in Chapter 7.

Delta: STR and OFC have been extensively studied in reward, motivation and acquisition of action-outcome associative learning (Balleine et al., 2007; Dayan & Balleine, 2002; Yin et al., 2005). OFC is thought to predict expected outcomes by integrating the history of stimulus-reward association and outcome of the task (Nogueira et al., 2017; Riceberg & Shapiro, 2012). The current results showed that before the rat triggers S5, OFC power increases. This is consistent with the literature that suggests neurons responding to task events become active before task-related motor behaviour (Balleine et al., 2007). The OFC-HPC delta coherence was greater before triggering S0 compared to triggering of S1 (trial initiation) and S5 (Go response). The HPC and OFC both have the excitatory innervation to the striatal

neurons in NAcc (Sesack & Grace, 2010). Reward expectancy signals may be coded by striatal neurons and affect the cortico-limbic system (Lansink et al., 2016). Furthermore, motivational information may be provided to CA1 through HPC DA signals generated through the ventral tegmental area (Zahm, 2000). This observation is similar to earlier studies that suggest stimulus-triggered reward expectancy increases HPC synchronisation with OFC by which the HPC may get access to systems modulating motivated behaviours (Lansink et al., 2016).

Theta: During early learning, we found OFC and STR power increased in the theta band when the rat initiated the task by approaching to S1. In the theta band, both OFC and HPC power increased at trial initiation and reward expectation but did not differ from each other. After the task is learned, in the theta band, S1 triggering (trial initiation) increased the power of STR. We observed greater coherence between OFC-STR and HPC-STR during reward expectancy. This may be because STR receives motivational and reinforcement learning signals from functionally connected limbic areas (Ross, Sherrill, & Stern, 2011; Shiflett & Balleine, 2010). As explained earlier, reinforced behaviour releases DA and it is likely that greater coherence between OFC-STR and HPC-STR drive to ongoing behaviour. Additionally, during an associative learning task OFC communicates with striatum and is important for reward value representation (van Wingerden et al., 2010). Furthermore, these results suggest that OFC theta may facilitate information between reward and motivation related brain areas during learning (van Wingerden, van der Meij, Kalenscher, Maris, & Pennartz, 2014; van Wingerden et al., 2010).

Beta: OFC and STR power at beta frequency was greater after Go response and reward delivery compared to early learning of Go task. LFP oscillations in the beta band are linked to sensory and motor processing (Feingold, Gibson, DePasquale, & Graybiel, 2015). OFC beta power shows increased in trend towards reward collection during learning. Additionally, our results also demonstrated increased beta coherence between HPC-STR after triggering trial

initiation. Increase in beta power results are in line with a study that found learning related increase in beta power (Howe, Atallah, McCool, Gibson, & Graybiel, 2011).

Gamma: Within the low gamma band, we saw increased STR power during movement initiation. Similar finding was reported in a study (van der Meer & Redish, 2009) but in contrast, the current study did not found significant increased gamma power in STR following reward delivery as shown by the study.

The effects of learning in the GO task (as shown by the after-before and late-early differences) showed as increased coherence between STR pairs (HPC-STR and OFC-STR) during trial initiation and Go response. STR exhibits coherence with OFC and contributes to simple learning of motor behaviour and reward processing. Additionally, this results supports as expected, theta rhythm important during initiation of movement. This result is in line with study suggesting theta rhythm supports coordination of movements and is important with the encoding and behaviour control (Kaplan et al., 2012).

In conclusion, our data suggest that during the early period of Go learning task, HPC-STR, HPC-OFC and OFC-STR show greater coherence in the delta band in the context of different behavioural states. After the task is learned, coherence decreases during trial initiation and the Go response. The reason could be that, once the going task is learned, STR is involved to maintain the motor behaviour (Albouy et al., 2013) but information become less dependent on hippocampal processing. In this study, we observed power fluctuations in OFC and STR at both low and high frequency in learning stages. OFC connectivity with HPC and STR support the notion that both low and high frequency could provide mechanism for coordination of distributed system as the goal directed behaviours are learned and performed (DeCoteau et al., 2007a; Howe et al., 2011; Nacher, Ledberg, Deco, & Romo, 2013; van Wingerden et al., 2010). These results support our hypothesis that STR and HPC interact with frontal cortex structures for associative learning. Additionally, greater coherence between theta OFC-STR and HPC-

STR during reward expectancy proves our second hypothesis. As expected, we saw dynamic changes of frontal, BG and hippocampal systems during “GO task learning” in rats. In the next Chapter, we will examine how oscillatory activity in the same networks respond to cancelling of an on-going action as required in the SST.

Chapter 5. Involvement of subthalamic, orbitofrontal and hippocampal oscillations in the Stop signal task

5.1 Introduction

5.1.1 Role of subthalamic nucleus, orbitofrontal cortex and hippocampus in response inhibition

In Chapter 1, I provided detailed evidence on the role of the STN, OFC and HPC in response inhibition to support flexible behaviour. In this Chapter I will briefly summarize the importance of these brain areas in response inhibition. The STN is activated by stopping or pausing as shown in neuroimaging in human primates (Aron & Poldrack, 2006), non-human primates (Isoda & Hikosaka, 2008) and rodents (Schmidt et al., 2013). Recently, studies have shown that unexpected events (Wessel & Aron, 2017) or surprising events (Fife et al., 2017; Wessel et al., 2016) or even conflict (Zavala, Zaghloul, & Brown, 2015) also recruit the STN for pausing or stopping. Another structure that may be important for inhibiting unwanted consequences is OFC. Dysfunction in the OFC has been linked to inhibitory control disorders (Dillon & Pizzagalli, 2007; Eagle & Baunez, 2010; Leventhal et al., 2012). It acts as an important area for suppression of behaviour (Bryden & Roesch, 2015; Mansouri, Buckley, & Tanaka, 2014). Most importantly, lesions of OFC and STN significantly reduce stop accuracy independent of stop signal delay (SSD) i.e. percent correct stopping (Eagle et al., 2008). Similarly, lesions of the ventral HPC result in inhibitory control deficits (Abela, Dougherty, Fagen, Hill, & Chudasama, 2013). Furthermore, there is a well-established role of the HPC in active inhibition of a behavioural response (McNaughton & Gray, 2000). The individual role of STN, OFC and HPC in response control has been tested separately however, it is not clear whether behavioural inhibition is mediated by shared or distinct neural pathways.

5.1.2 Cortico-subthalamic and Cortico-hippocampal interaction for behavioural inhibition

Research on both animals and humans has shown interaction between two brain areas, the STN and OFC, might be important for response inhibition in the SST (Aron et al., 2007; Band & van Boxtel, 1999; Eagle et al., 2008). Additionally, electrophysiological recordings suggest that HPC and frontal cortex are involved in learning inhibition of more complex behavioural responses (Lee & Byeon, 2014). Interestingly, lesion studies in rats provide evidence that functional interaction between HPC and frontal cortex is important for inhibitory control of behaviour (Chudasama, Doobay, & Liu, 2012).

There are currently no studies of non-human, including rats, that record brain oscillations concurrently from the STN, OFC and HPC engaged in voluntary behaviours as well as goal directed behaviours. So, in this experiment, I used the SST as one of the simplest forms of inhibition where we have control of Go timing and does not include confounding motivational states such as panic and fear and involves activation of parallel control circuits. I simultaneously recorded LFP from the STN, OFC and HPC in rats performing a SST, to examine the presence of rhythmic slow activity in STN, OFC and HPC during motor stopping.

Therefore, the experiments in this Chapter had two objectives. The first objective is to examine how oscillatory activity in the STN, OFC and HPC responds to the cancellation of an on-going actions as required in SST. The second is to examine how behavioural inhibition is implemented in the hippocampal-subthalamic circuit. The hypotheses for this study are described in detail in Chapter 1 (see section 1.7). Briefly, we predicted that inhibition of an ongoing action might increase beta power in STN and OFC and also coherence between OFC-STN. We also predicted hippocampal-subthalamic synchrosation would increase during failure of stopping.

5.2 Materials and Methods

5.2.1 Stop Signal Task

The SST task was based from the SST task for rats of Eagle and Robbins (2003a). All the details of the experimental procedure and training are described in Chapters 2 and 4, except the addition of a Stop signal. Briefly, in this task, the rat had to cancel or inhibit its ongoing Go response after the presentation of the Stop signal (4500 Hz, 40 ms tones were presented randomly within the session to discourage rats from anticipating presentation of the Stop trials) i.e. to refrain from triggering the S5 (Go response). This task was as for the Go task of Chapter 4 but with 20% of trials designated as Stop trials. After presentation of the Stop signal, if the rat did not trigger S5, trials were considered correct and a pellet was delivered. Triggering S5 after the Stop tone was considered incorrect and the rat received a time out period of 5 s before the beginning of the next trial. Figure 5.1 shows a rat performing the SST.

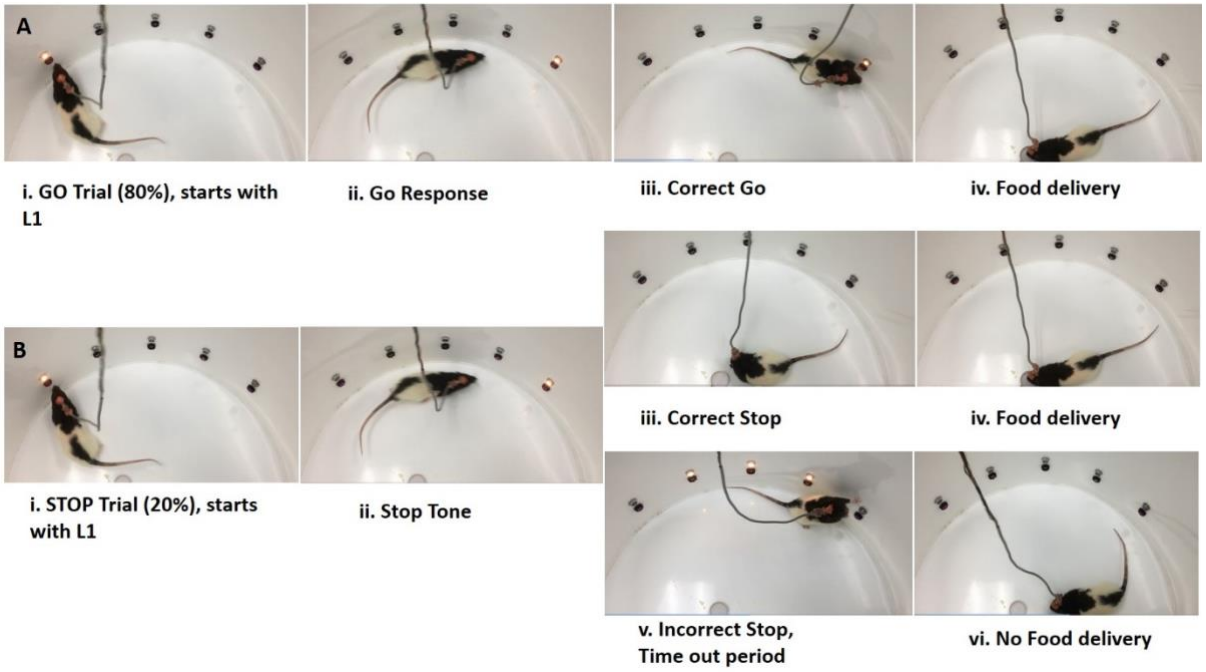

Figure 5.1 Rat performing Stop signal task.

A. The rat approaches the left light to start the trial (i) turning on the far-right light (ii). It normally then moves to the light (ii) to receive food (iv). B. Twenty percent of the time the light goes off, and a tone sounds, to signal "Stop" and the rat must suppress its response (ii) to receive food. Incorrect responding on Go or Stop trials (B. v) generates a 'time out' delay and (vi) no food is rewarded.

5.2.2 Electrophysiological Analysis

LFP was recorded and analysed as detailed in Chapter 2. To assess the differences in induced power between correct Go (CGo) and correct Stop (CSt) trials, the following approach was used. First, for Stop trials, the 0.5 s period before and after the sensor was triggered was assigned a power spectrum.

For every Go trial preceding a Stop trial, the same procedure was repeated for the 0.5 s period at which the tone was presented in the matching Stop trial. If the trial preceding a Stop trial was also a Stop trial, the Go trial following this Stop trial was used instead. LFP power was then log transformed to normalize error variance, and then averaged across trials. The mean power for Go and Stop at each frequency was calculated by averaging the power spectrum across trials.

5.2.3 Stop Signal Reaction Time (SSRT) Estimation

SSRT is the estimated time taken to Stop a response from the point at when a Stop-tone is presented, to the point at which inhibition is completed. SSRTs in this task were estimated using the protocol described in Eagle et al. (2008). The reaction times on Go trials (on which no Stop signal occurred) were rank ordered. The nth reaction time from the ranked list for a particular delay session was selected, (where n was obtained by multiplying the number of reaction times in the distribution by the probability of responding on Stop trials in the same session). This is an estimate of the time at which the stopping process finished, relative to the onset of the Go signal. To estimate SSRT (the time at which stopping finished relative to the Stop signal), we subtracted SSD from this value. This was done for each subject for each delay and then averaged.

Let us take an example of a session with 20 trials. Among the 20 trials, 16 are Go trials (from which GO reaction time; GoRT can be measured) and four are Stop trials. Let us assume that, among four stops, one is correct and three are incorrect then the probability of correctly stopping = 0.25. Therefore, the probability of responding [i.e., failing to Stop] on Stop trials =

0.75. Let us suppose that the Stop signal was presented at 680 ms after the onset of the Go stimulus, and the following GoRTs were obtained.

Rank	**1**	**2**	**3**	**4**	**5**	**6**	**7**	**8**	**9**	**10**	**11**	**12**	**13**	**14**	**15**	**16**
GoRT	1000	1063	1063	1125	1125	1125	1125	1125	1125	1125	1125	**1125**	1125	1125	1125	1187

To find the value of the nth reaction time:

n = number of GoRTs x probability of responding on Stop trials = 16 x 0.75 = 12

12th reaction time in GoRT distribution = 1125 ms

Assuming that the Stop process finished 1125 ms after the onset of the Go stimulus

SSRT = Stop time – Stop signal delay = 1125- 680 = 445 ms.

5.2.4 Statistical analysis

All statistical procedures were as described in Chapter 2. The factors and levels for ANOVA for this experiment are described in detail here. ANOVA with a 2 x 3 x 4 x 3 factorial design [Time (two levels: before / after) x Trial types (three levels: CGo ⁄ CSt / FSt) x Frequency (four levels: delta / theta / beta / gamma) x Brain area (three levels: OFC / HPC / STN] was used to test the effects of stopping. For coherence analysis, rather than brain area, the main factor of interest was pairs of brain areas, which were treated as a 'circuit' factor (three levels: HPC-STN / OFC-HPC / OFC-STN).

Given that trial type has three levels, the "quadratic" component in this case can be thought of as representing the difference between the correct stopping condition and a value obtained by averaging the two adjacent conditions (correct going and failed stopping). Similar to trial type, brain area also has three levels, OFC, HPC and STN. The quadratic component can be thought of as representing the difference between HPC regions and a value obtained by averaging the OFC and STN levels. Furthermore, the quadratic component of circuit can be thought of as representing the difference between OFC-HPC and a value obtained by averaging the HPC-STN and OFC-STN levels.

5.3 Results

5.3.1 Behavioural data

The key behavioural measures that characterize performance in the SST are the inhibition function, SSRT and the RT distribution for the responses on Go trials. A summary of the performance of rats can be seen in Table 5.1.

Table 5.1 Performance on the Stop Signal Task in Experiment 2

Measures	***Mean***	***SEM***
Stop trial accuracy (%)	65.85	5.91
Go Trial accuracy (%)	73.84	2.19
mRT(ms)	1309.34	23.93
SSRT (ms)	285.07	40.09

Note. mRT= mean reaction time on Go trials. SEM: standard error mean; SSRT = estimated Stop Signal Reaction Time (see text).

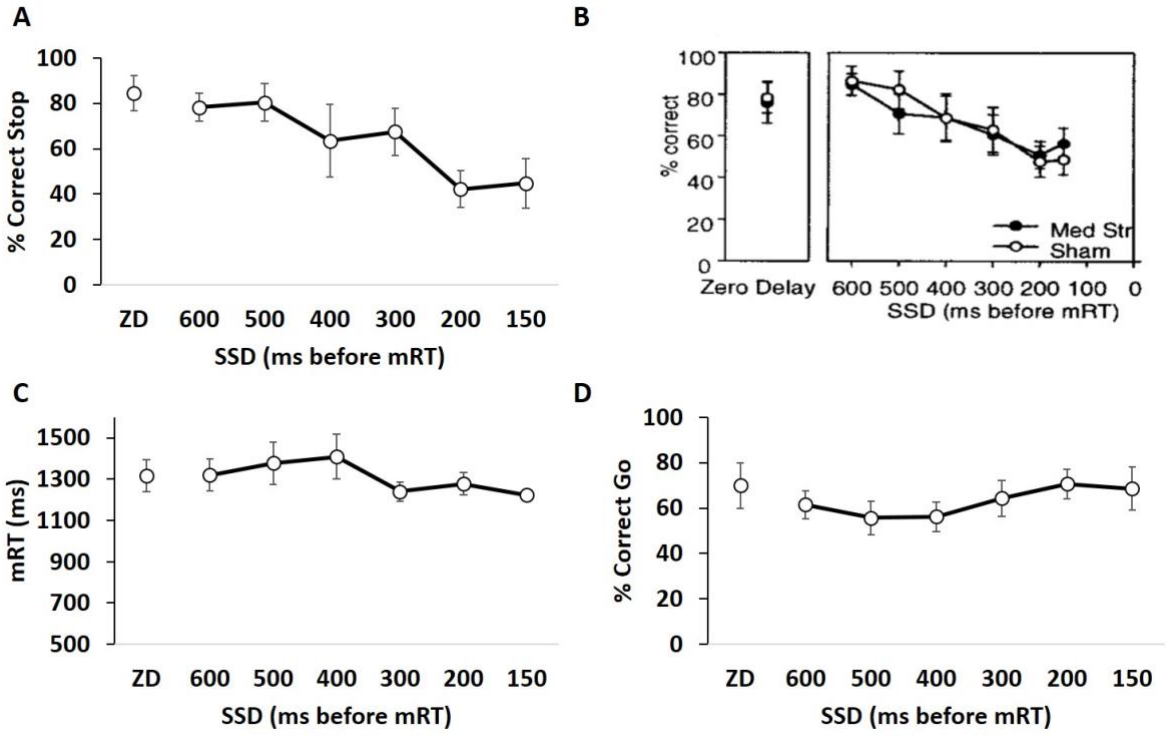

Figure 5.2 Behavioural measures across SSDs

A. Inhibition function (correct stopping versus SSD) in the current experiment, B. comparison function from Eagle et al (2008), C. Mean response time (in millisecond) on the Go trials (mRT) D. Response on Go trials. Error bars represent± SEM. ZD: Zero delay; SSD: Stop signal delay as set for the whole session.

The inhibition function plots the proportion of responding on Stop trials (i.e., trials in which the animal fails to Stop the ongoing movement) as a function of the SSD (Eagle et al., 2008). Our results show a similar inhibition function to that described by Eagle (2008), compare Figure 5.2A and 5.2B. The inhibition function has been considered a race between a Go process (that initiates movement) and a Stop process (that inhibits the response) (Logan et al., 1984). If the Stop process finishes before the Go-related activity is fully processed, the movement is cancelled. Conversely, if the Go process finishes before the Stop process, the movement is generated. Figure 5.2A shows the Stop accuracy on the Stop trials. When the Stop signal was presented close to initiation of the Go response rats performed more correct Stop trials. Similarly, performance was reduced when the Stop signal was presented closer to termination of the Go response.

Stop signal reaction time was calculated for each of the SSDs. The SSRTs obtained for each SSD are then averaged to compute a single SSRT estimate (Pani et al., 2014). Overall, estimated SSRT was 285.07 ms.

5.3.2 Neurophysiological data

5.3.2.1 Description: Power spectrum between correct Go, correct Stop and failed Stop trials

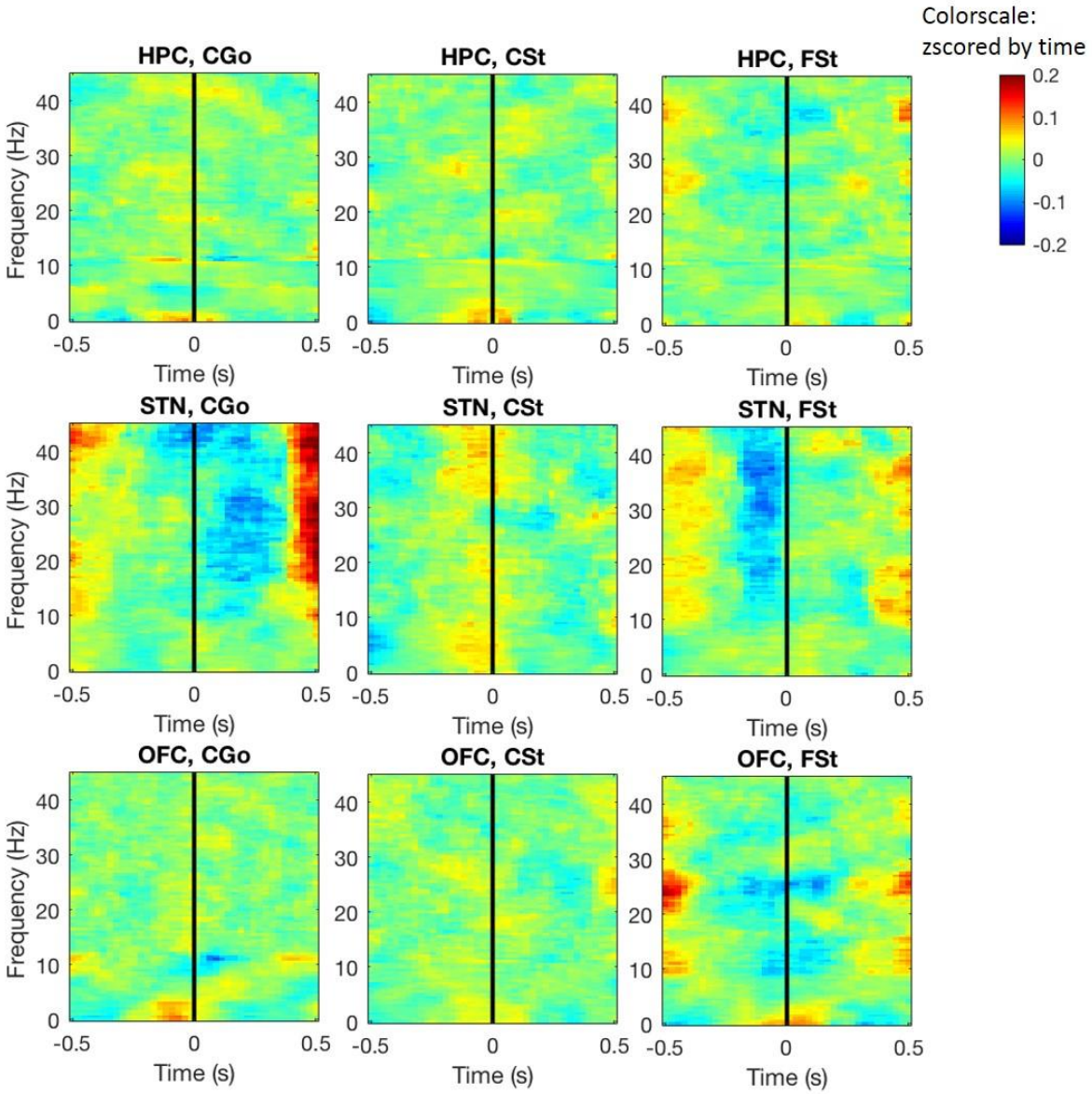

Figure 5.3 Average time-frequency plot showing LFP activity of correct Go trials (left panels) and matching correct Stop (center panels) and failed Stop (right panels).

Vertical black line indicates time of event marker triggered (Go: sensor 5 triggered and Stop: stop tone triggered). CGo: correct Go; correct Stop; FSt: failed Stop. Note power values were log transformed before averaging and plotting.

Figure 5.3 shows the time frequency plot of the recorded LFPs from STN, OFC, and HPC during CGo, CSt and FSt trials. The spectral content of these data shows regional differences localized to four distinct frequency bands, delta, theta, beta and low gamma. Before

the Stop signal appeared, activity was similar between correct Stop trials (center plot) and preceding correct Go trials (left plot) in HPC and OFC.

Key observations from the spectrograms are as follows. With correct going, HPC and OFC power was reduced only at 5-15 Hz while STN power decreased in three frequency bands; 5-15, 20-30 and 30-40 Hz. With successful stopping, STN power decreased just after the Stop tone at 20-30 Hz. Additionally, failed stopping showed increased HPC power at 30-40 Hz while STN power at 30-40 Hz and 15-30 Hz. Whereas OFC power increased at 1-4 Hz and decreased both at 5-15 and 15-30 Hz. For detailed analysis we focused on delta (1-4), theta (5-15), beta (20-30) and gamma (30-40 Hz) bands.

5.3.2.2 Analysis: Mean power between STN, OFC and HPC for four frequency bands during SST task

Figure 5.4 shows the mean power of STN, OFC and HPC during CSt, CGo and FSt for the four different frequency bands. The periods before and after event marker triggering show similar pattern however, the power patterns for delta and beta appeared to be stronger than for theta and gamma (see Figure 5.4, left and middle panel; Time [linear] x Trial type [linear] x Brain area [linear], x Frequency band [linear], F (1, 4) = 5.292, $p = 0.05$). *Post hoc* tests were carried out to clarify the effects causing this interaction. Interestingly, the event triggered effects (after-before, right panel) show clear differences for the four bands. The delta frequency range (1-4 Hz) shows an increasing trend in OFC after correct stopping. However, HPC and STN did not show such trend across the behavioural states.

Theta was larger for correct stopping versus correct going and failed going (Trial type [quadratic] x brain area [quadratic], F (1, 4) = 7.650, $p = 0.05$). Theta activity simultaneously increased during Stop failure in STN and OFC. The main effect of brain areas (Brain area [quadratic], F (1, 4) = 57.162, $p = 0.002$) indicates lower HPC power while both OFC and STN shows greater power during successful going. Additionally, OFC theta power was greater for correct inhibition compared to stop failure.

Similarly, in the beta band, correct stopping differed from failed stopping and correct going. During correct stopping, we observed relative increased beta power in STN. HPC power was greater than OFC during Stop failure (Trial type [quadratic] x brain area [quadratic], F (1, 4) = 6.816, p = 0.05). As can be seen in the last panel, overall, gamma (30-40 Hz) power increased in HPC and STN compared to OFC during Stop failure (Trial type [quadratic] x brain area [quadratic], F (1, 4) = 10.005, p = 0.034). Overall, the present results show that theta power OFC and STN theta power was greater at correct going while STN beta power was relatively increased due to stop signal (both correct and failed stopping).

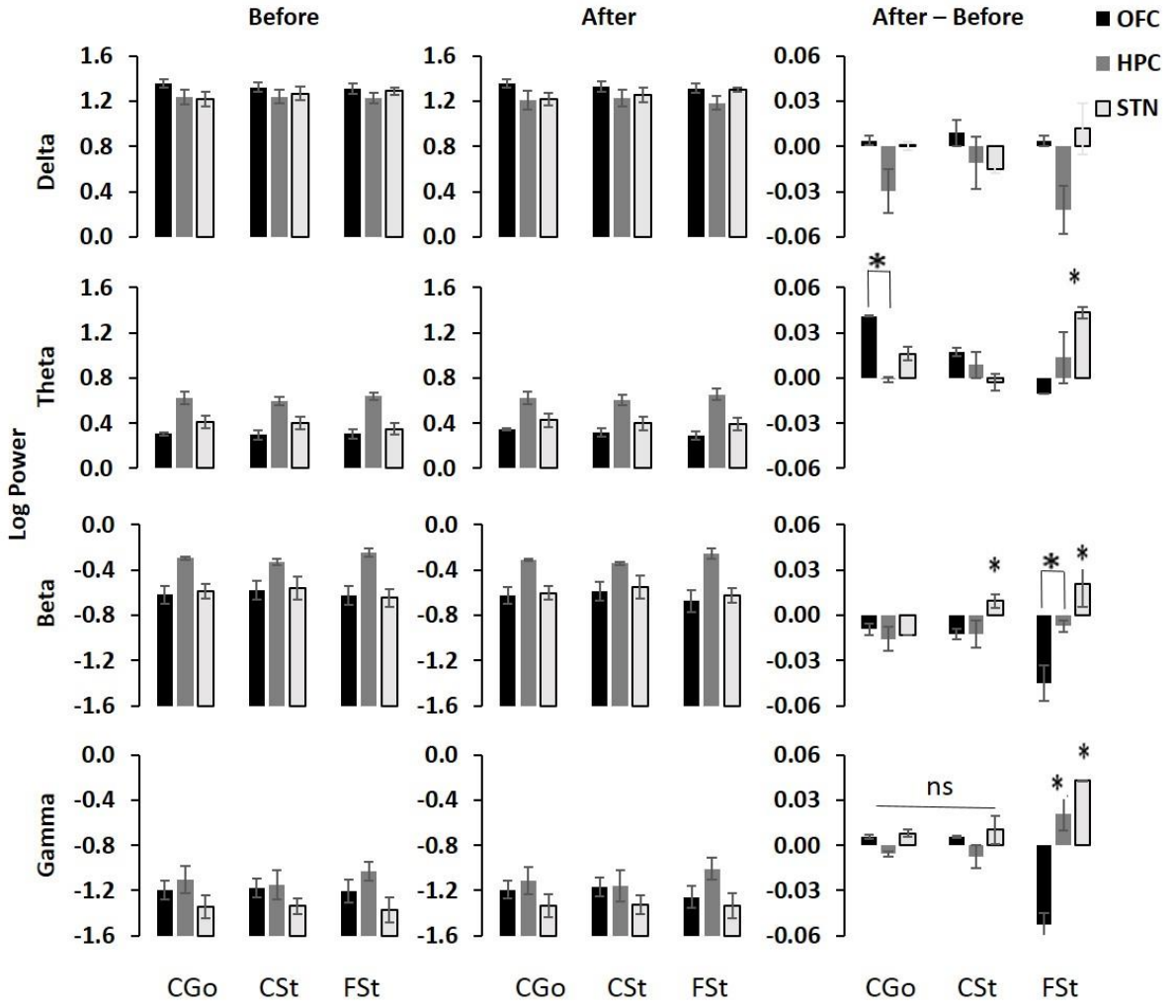

Figure 5.4 Mean power during Stop-signal task performance comparing correct Go, correct Stop, and fail stop before (left panels) and after (middle panels) event marker triggered. The right panels shows the difference between them.

5.3.2.3 Description: Comparison between correct Stop and correct Go trials

To examine the reactive control of movement, we compared LFP activity in correct Stop trials with that in the preceding correct Go trial closest in time to the correct Stop trial. Figure 5.5 shows the contrast between correct Stop and correct Go trials (right plot). Stop-Go power difference in HPC shows increase in theta and beta activity while OFC shows increase activity only at theta after the onset of stop signal. However, STN shows an increase in beta and gamma activity after the Stop signal (middle, right panel).

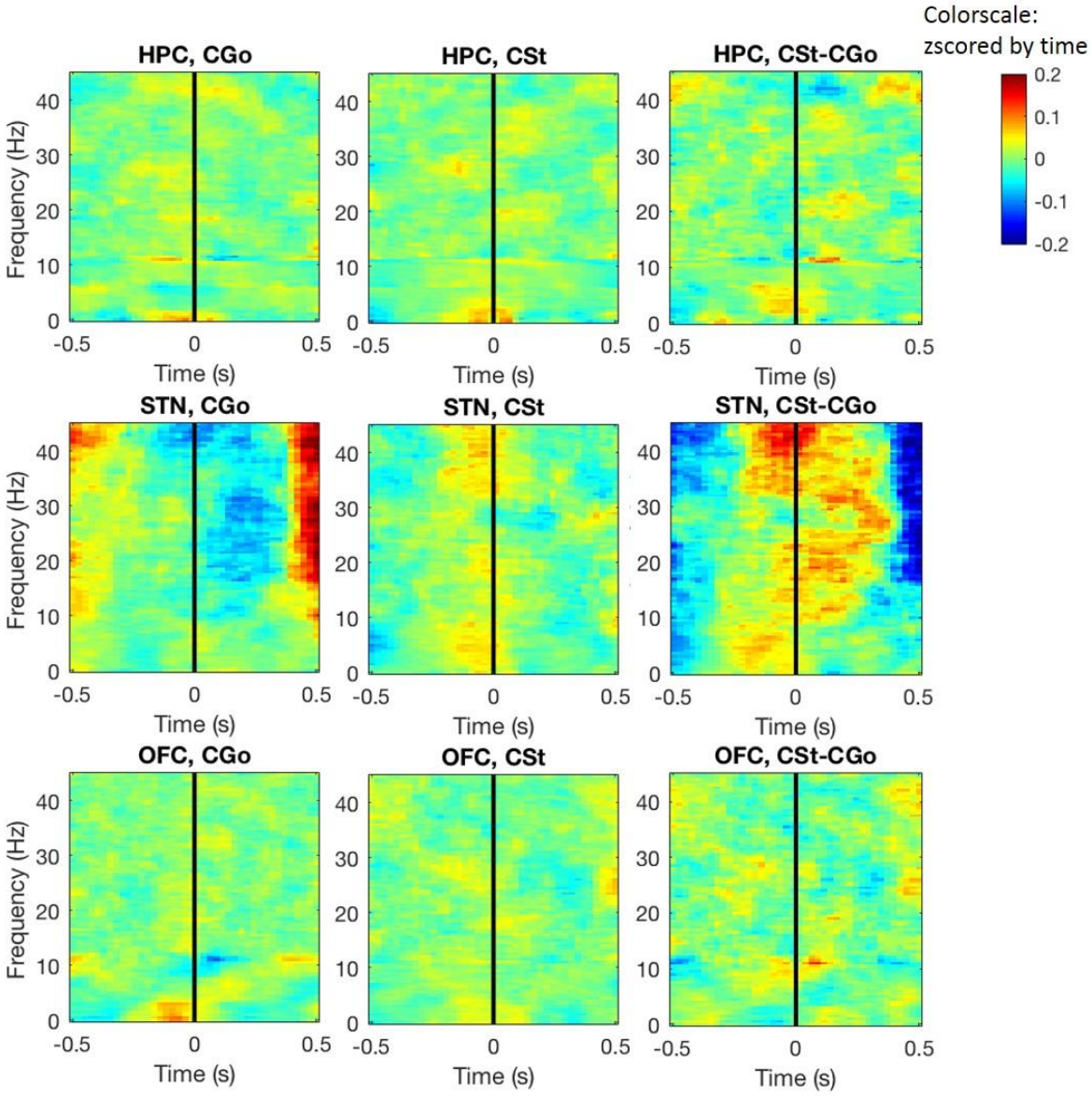

Figure 5.5 Average time-frequency plot showing LFP activity of correct Go trials (left panels) and latency-matched correct Stop (center panels) and their differences (right panels).

Vertical black line indicates time of event marker triggered (Go: sensor 5 triggered and Stop: stop tone triggered). CGo: correct Go; correct Stop; FSt: failed Stop

5.3.2.4 Description: Comparison between correct Stop and failed Stop trials

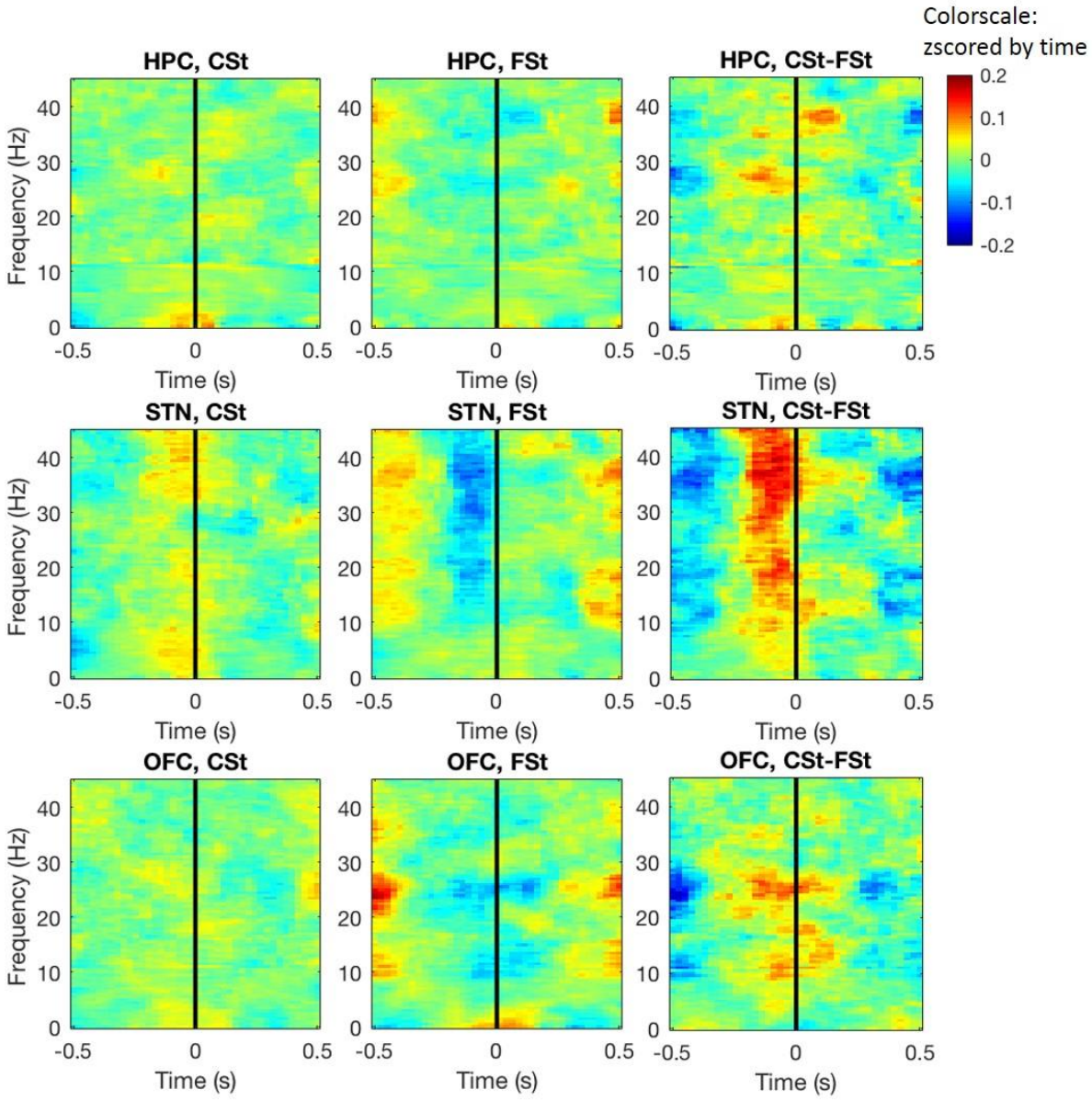

Figure 5.6 Average time-frequency plot showing LFP activity of correct Stop trials (left panels) and failed Stop (center panels) and their differences (right panels).

Vertical black line indicate time for stop tone triggered. CGo: correct Go; correct Stop; FSt: failed Stop

We also examined the effectiveness of reactive control by comparing correct Stop trials with failed Stop trials. We expected different patterns in failed Stop trials. In failed Stop trials, the Stop process is started but fails to suppress the movement. Figure 5.6 shows the contrast between correct Stop and failed Stop trials (right panel). The Correct Stop-failed Stop

difference was increased for beta and gamma power before the stop tone triggered at STN while OFC power increased for theta and gamma. But, HPC showed increased power only in the gamma band.

5.3.2.5 Description: Comparison between failed Stop and correct Go trials

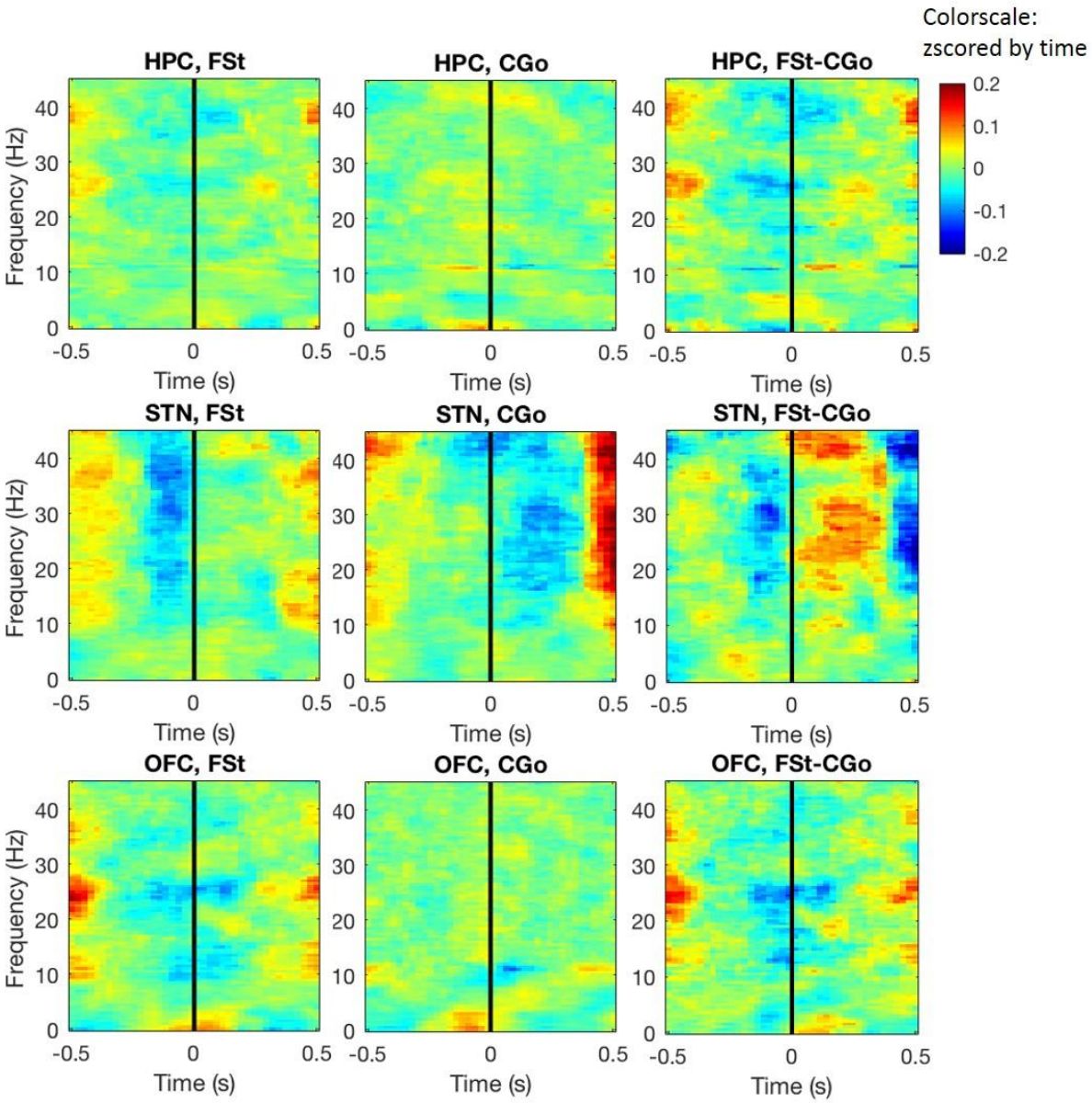

Figure 5.7 Average time-frequency plot showing LFP activity of failed Stop trials (left panels) and latency-matched correct Go (center panels) and their differences (right panels).

Vertical black line indicates time of event marker triggered (Go: sensor 5 triggered and Stop: stop tone triggered).

CGo: correct Go; correct Stop; FSt: failed Stop

We compared failed Stop trials (i.e., trials too fast to be inhibited) with preceding correct Go trial closest in time to the failed Stop trial. Comparing the time-frequency map, failed Stop-Go difference (right panel) showed a clear HPC theta and beta activity while OFC activity was seen at delta and beta band (Figure 5.7). In case of STN, increased beta and gamma activity was observed after the stop signal

5.3.2.6 Analysis: Stop-Go power differences (i.e. changes due to Stop signal) in correct and incorrect stopping for four frequency bands during SST task

To test the effect of stopping, Stop-Go differences in each brain area were calculated. Figure 5.8 shows the power changes due to the Stop signal. Results from a repeated measures ANOVA showed a significant three-way interaction between brain areas in four frequency bands during the behavioural states (Trial type [quadratic] x Frequency band [linear] x Brain area [quadratic], F (1, 4) = 6.960, $p = 0.05$). *Post hoc* test were carried out to dissociate three way interaction effects at each frequency.

Figure 5.8A shows Stop signal effects at the delta band. HPC power was greater than OFC and STN due to Stop signal (Brain [quadratic], F (1, 4) = 23.797, $p = 0.008$). The OFC and STN power (CSt-CGo) was not significantly different (t (4) = 0.062, $p = 0.059$).

In the theta frequency (Figure 5.8B), OFC power was increased due to Stop signal (CSt-FSt) in correct stopping than failed stopping. However, there was no significant difference due to Stop signal between CSt-CGo and FSt-CGo for HPC (t (4) = -0.521) = p> 0.05.).

The effects of stopping as seen in CSt-CGo and FSt-CGo revealed increased STN beta power which is close to significantly different compared to OFC (t (4) = -2.284), $p = 0.084$) but not with HPC (t (4) = -2.013, $p = 0.114$)(Figure 5.8C). Similarly, we also observed increased beta power in OFC due to stopping (CSt-FSt).

In the gamma range, unsuccessful stopping (FSt-CGo) shows increased gamma power in STN and HPC compared to correct stopping (CSt-CGo) (t (4) = -2.569, $p = 0.05$) but not in OFC (t (4) = 1.829, $p = 0.141$)(Figure 5.8D).

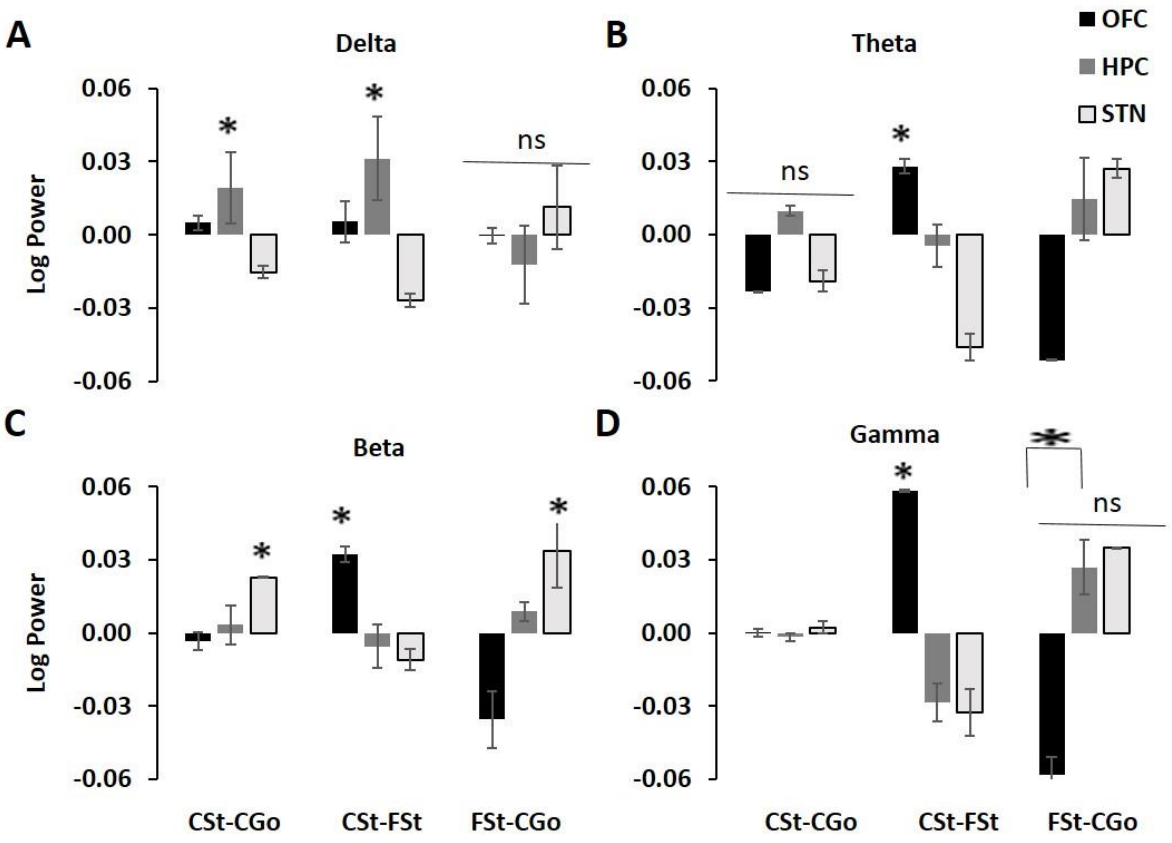

Figure 5.8 Changes in mean power during Stop signal task performance, comparing correct Stop-correct Go (CSt-CGo), correct Stop-failed Go (CSt-FGo) and failed Go-correct Go (FGo-CGo) at four frequency bands.

5.3.2.7 Description: Coherence spectrum between correct Go, correct Stop and failed Stop trials

Figure 5.9 shows cohereograms of the recorded LFPs from pairs of structures (HPC-OFC, HPC-STN and OFC-STN) during CGo, CSt and FSt. With CGo (left panel), HPC-OFC coherence was observed at 5-15 Hz and 20-30 Hz before rat triggers S5; with HPC-STN coherence interaction appears at 5-15 Hz and 20-30 Hz after S5 triggered while OFC-STN show strong coherence at 1- 4 Hz before triggering of S5 and bled shortly after. Additionally, strong coherence appears in OFC-STN at 5-15 Hz after the triggering of the S5.

With CSt (center panel), HPC-OFC interaction occurs at 5-15 Hz and 20-30 after the stop tone; HPC-STN interaction at 5-15 Hz and 30-40 Hz; OFC-STN was most prominent after the stop tone at 5-15 Hz and 15-25 Hz and

With FSt (right panel), HPC-OFC coherence was greater at 5-15 Hz before and after fail to stop while coherence appears at 20-30 Hz before the stop tone; Again, HPC-STN interaction is seen at 5-15 Hz before and after the stop failure. The OFC-STN interaction was strong both at 1-4 Hz and 5-15Hz.

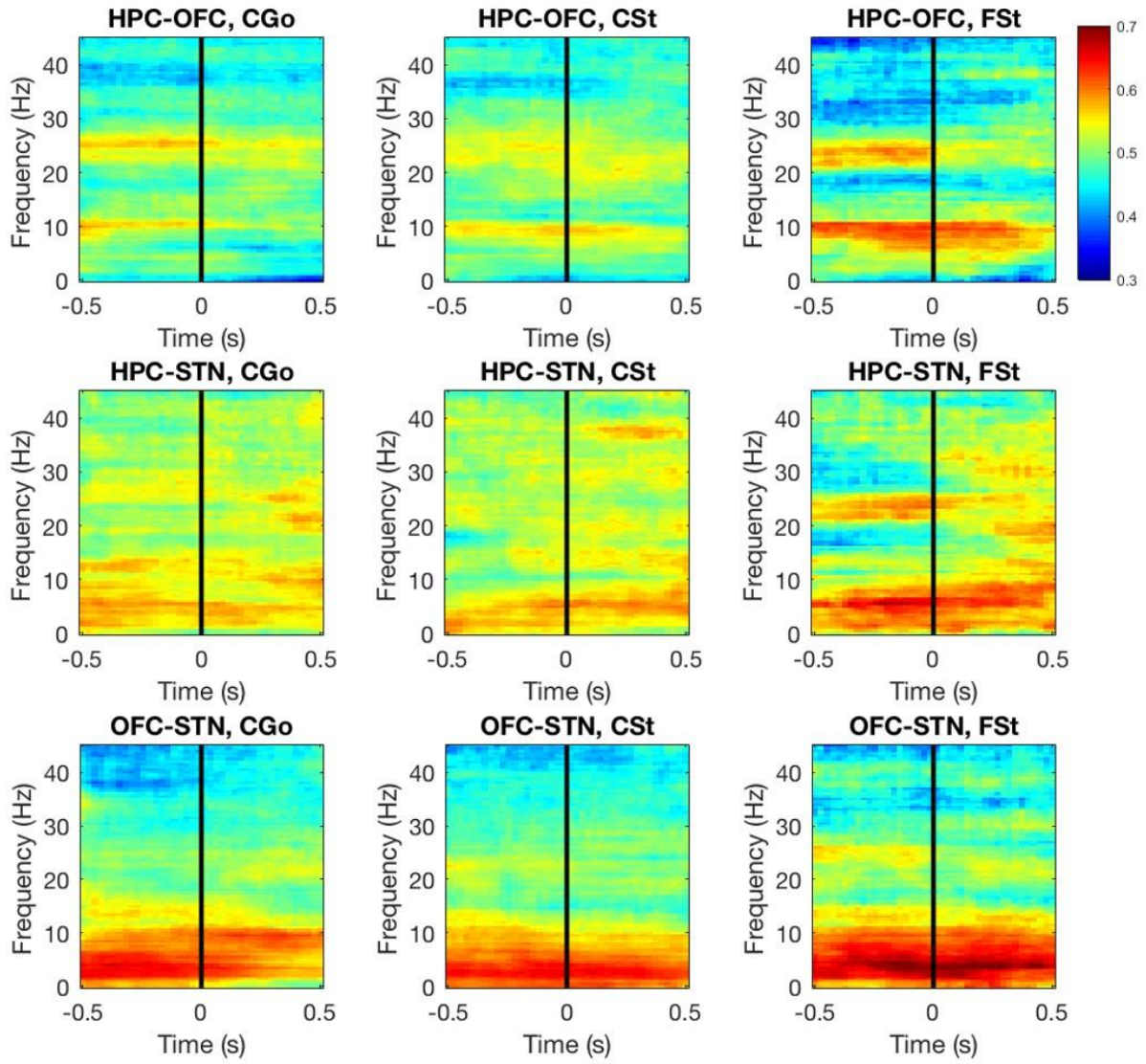

Figure 5.9 Time-frequency plot showing coherence between brain areas during correct Go, correct Stop and failed Stop. CGo; correct Go, CSt; correct Stop and FSt; failed Stop.

5.3.2.8 Analysis: Mean coherence between HPC-OFC, HPC-STN and OFC-STN for four frequency bands during SST task

Figure 5.10 shows the mean coherence between the pairs of structures (HPC-STN, OFC-HPC and OFC-STN) at four different frequency bands. The coherence between circuits was significantly different among frequency bands for different trial types (Time [linear] x

Trial type [linear] x Circuit [linear] x Frequency band [linear], F (1, 4) = 13.816, p = 0.021). *Post hoc* tests were carried out to clarify the effects driving this interaction.

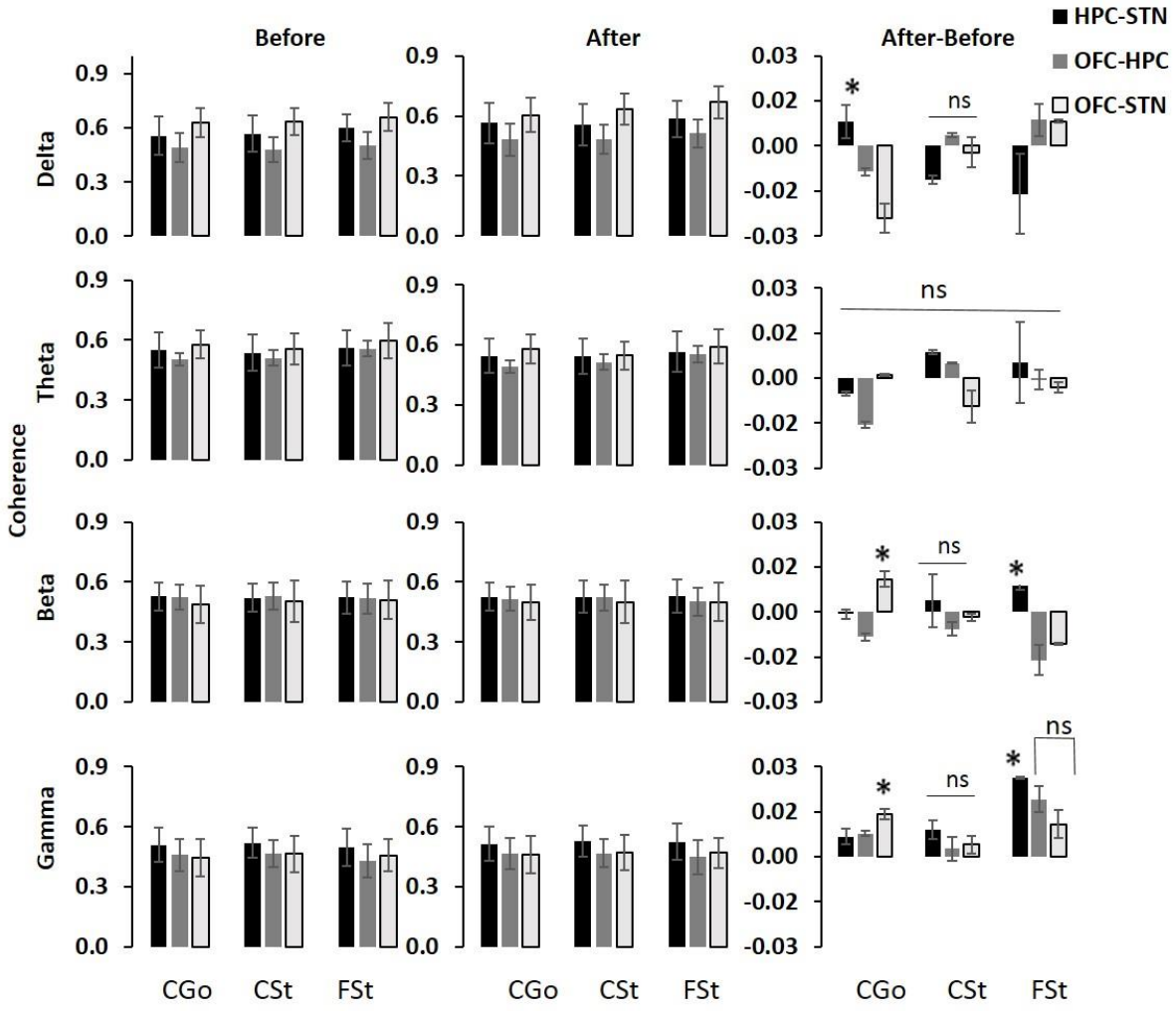

Figure 5.10 Mean coherence during Stop-signal task performance comparing correct GO (CGo), correct Stop (CSt) and Stop failure (FSt) before, after and difference (after-before).

The right panel shows the sensor triggered coherence (after-before sensor triggered) patterns between three pairs of structures at four different frequency bands. In the delta frequency, HPC-STN coherence increased with correct going compared to OFC-HPC (t (4) = 2.799, p = 0.049) but not with and OFC-STN (t (4) = 1.336, p = 0.252). We did not find other significant differences among brain structures for stopping. In the theta frequency, coherence did not change significantly between circuits and trial types (Trial type [linear] x Circuit

[linear], F (1, 4) = 0.176, p = 0.697). Similarly, in the beta range, coherence interaction between brain circuits and trial types was significant (Trial type [linear] x Circuit [linear], F (1, 4) = 10.118, p = 0.034). This suggest that coherence between HPC-STN is greater at Stop failure (t (4) = 5.919, p = 0.004) but not during correct stopping (t (4) = 1.107, p = 0.331). Interestingly, the gamma profile, demonstrated that failure to Stop increased the HPC-STN coherence significance (t (4) = 2.535, p = 0.044) compared to correct going but not with correct stopping (t (4) = -0.248, p = 0.816). Overall, the results suggest that delta coherence in HPC-STN is stronger during correct going while stop failure show increased gamma HPC-STN interaction.

5.3.2.9 Analysis: Stop-Go coherence differences (i.e. changes due to Stop signal) for correct and incorrect stopping for four different bands

Here, we are interested in Stop-Go coherence differences for correct and failed stopping. Figure 5.11 shows the coherence differences between stoppings due to Stop signal. The coherence between circuits was significantly different among frequency bands for Stop-Go (Circuit [linear] x Stop-Go [linear] x Frequency Band [linear], F (1, 4) = 12.945, p = 0.023. *Post hoc* tests were carried out to clarify the effects for this interaction.

Figure 5.11A, the OFC-STN shows greater delta coherence compared to HPC-STN at CSt-CGo (t (2.622) = p =0.04) but not for FSt-CGo due to the Stop signal (t (2.338) = p =0.05). In the theta frequency (Figure 5.11B), two pairs of HPC (HPC-STN and OFC-HPC) coherence was increased due to Stop signal (CSt-CGo) but are not significantly different to FSt-CGo (t (0.464) = p > 0.05). CSt-FSt revealed increased beta coherence between OFC-STN and OFC-HPC. In addition, HPC-STN beta coherence decrease during CSt-FSt compared to OFC-HPC (t (-2.723) = p =0.05) (Figure 5.11C). In the gamma range, we observed increased HPC-STN coherence due to Stop failure (FSt- CGo) relative to OFC-HPC (Figure 5.11D). All others are non-significant. Overall, this suggest that oscillatory activity in STN was coherent with OFC correct stopping increases delta coherence. In addition, during stop failure coherence between HPC-STN structures are greater at theta, beta and gamma.

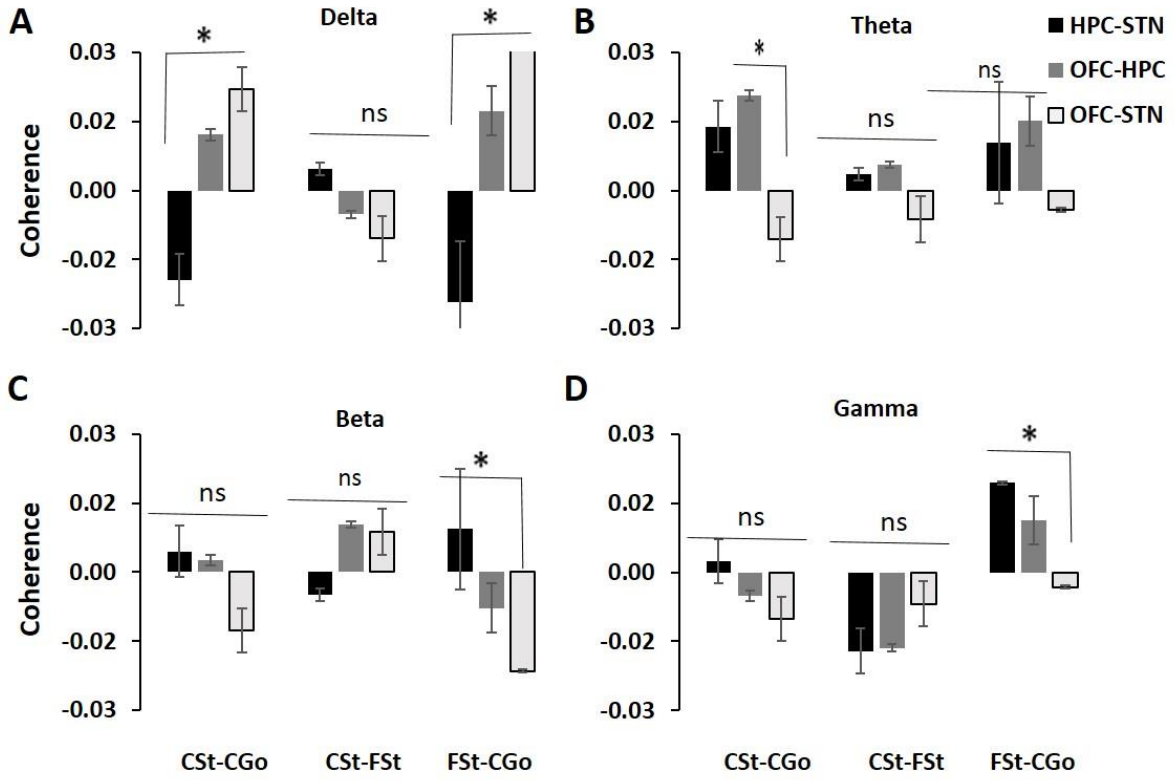

Figure 5.11 Changes in mean coherence during Stop signal task performance, comparing correct Stop-correct Go (CSt-CGo), correct Stop-failed Go (CSt-FGo) and failed Go- correct Go (FGo-CGo) at four frequency bands.

5.4 Discussion

The goal of the present study was to evaluate how oscillatory activity in the STN, OFC and HPC responds to cancellation of on-going actions as required in SST. Rats performed an SST that requires monitoring, working memory, attention and associations between stimuli. We are primarily interested in changes due to the Stop signal. Therefore, we compared correct Stop and correct Go to analyse the effect of the Stop signal, while largely cancelling out the effects of other processes. We found that the Stop signal differentially modulates delta, theta, beta and gamma band activity. Key findings and brief discussion from the experiments are summarized below. The detailed discussion is given in general discussion.

Delta: Increased delta power was observed in HPC compared to OFC and STN due to Stop signal. We found that correct stopping increases delta coherence for both pairs of OFC

circuits (OFC-STN and OFC-HPC) and decreases HPC-STN delta coherence. The current results show that oscillatory activity in STN was significantly coherent with OFC and HPC during cancellation of actions. Earlier studies have shown similar findings and suggest that increased delta coherence may be important for response inhibition (Ekstrom & Watrous, 2014; Harper, Malone, Bachman, & Bernat, 2016).

Theta: Theta coherence was greater during failed stopping between HPC-STN. Interestingly, HPC-OFC theta coherence was increased due to stop signal both at correct and failed stopping. OFC theta power was greater in correct stopping than failed stopping. OFC could be involved in correct stoppings that are most relevant to estimated reward. The HPC and OFC are reciprocally connected (J. J. Young & Shapiro, 2011) and appears to interact to selectively stop the action at theta frequency.

Beta: Stopping an ongoing action increased beta power in STN and also increased beta coherence between OFC-STN. The increase in OFC-STN coherence could be because in rodents there is projection from the OFC to the STN (Cavada et al., 2000; Haegelen et al., 2009) and may have use this direct pathway to inhibit ongoing action. This is consistent with observations that STN and OFC beta power has been observed to decrease during movement preparation and initiation (Leventhal et al., 2012; Schmidt et al., 2013). Increased beta activity may affect other brain regions that are involved in movement control such as STR (Berke et al., 2004) and frontal cortex (Brown 2007).

Gamma: We also observed increased gamma power during correct stopping in STN. This suggests that STN gamma activity not only increases during movement but also during movement inhibition (Fischer et al., 2017). HPC-STN coherence was also increased in the gamma range when the animal failed to Stop the ongoing action. In addition, we also observed decreased gamma activity in HPC for correct stopping while there was an increase in activity following a Stop failure.

In conclusion, the findings suggest that successful inhibition increases theta power in OFC and beta power in STN. In addition, delta and beta coherence between OFC-STN increases during correct stopping compared to stop failure. Additionally, HPC and STN could synchronise to each other at theta frequency only after stop failure during simple action inhibition. Here I described the dynamic interaction between subthalamic, orbitofrontal and hippocampal oscillations for simple stopping; in the next Chapter I will investigate how the same brain areas interact with each other under goal-conflict.

Chapter 6. Dynamic interaction between hippocampus, orbitofrontal cortex and subthalamic nucleus during goal-conflict in the Stop Signal Task

6.1 Introduction

6.1.1 The Role of the HPC, OFC and BG during conflict

In Chapter 5, I discussed the interaction between STN, OFC and HPC during stopping of the simple ongoing motor response. In this Chapter I will only focus on the importance of these regions in relation to the goal conflict that can occur during such stopping. Resolving goal conflict is a key cognitive skill. Daily decisions must be made in changing circumstances and are particularly complex when we have choices between items of similar value. A range of systems are activated by and implicated in conflict processing: cortical – e.g. mPFC (Cavanagh et al., 2011), dLPFC (Boschin, Brkic, Simons, & Buckley, 2017), ACC (Boschin et al., 2017; Botvinick, Cohen, & Carter, 2004), and OFC (Luks, Simpson, Dale, & Hough, 2007; Mansouri et al., 2014; Marx et al., 2012); archicortical – e.g. HPC (McNaughton & Corr, 2014; Neo et al., 2011); and subcortical – e.g. STN (Zavala et al., 2016; Zavala et al., 2014).

Recent studies of conflict generating situations and STN have mostly been in deep brain stimulation implanted Parkinson's diseases patients. When two or more responses are simultaneously activated, STN is thought to be crucial in suppressing the pre-potent response; implicating the STN in a role of "holding your horses" during high conflict decisions (Cavanagh et al., 2011; Zavala et al., 2015). In addition, previous human studies showed increased theta activity (5-13 Hz) during conflicting decisions in a moral task (Fumagalli et al., 2011), high conflict scenarios in a Stroop task (Brittain et al., 2012), and conflict monitoring in the flanker task (Zavala 2013). However, surprisingly there is no rodent study that examines the contributions of HPC theta and STN together to conflict.

6.1.2 Is goal conflict a separate process from simple behavioural inhibition?

As discussed earlier in Chapter 5, the neural mechanisms of simple action stopping are commonly studied using the SST (Logan, Cowan, et al., 1984), which is relatively uncontaminated by additional processes in comparison to other tasks such as GO/NO-GO, and the Wisconsin card sorting task.

According to BIS theory (explained in detail in section 1.6), the activation of goals linked to stopping and going could generate goal-conflict-related behavioural inhibition system processing. The probability of stopping correctly is high when the SSD is short, presented early or shortly after initiation of the Go signal. In contrast, the probability of stopping is low when the SSD is long, presented late or close to termination of the Go task. Therefore, stop signals presented early or late should have low goal-conflict because Stop and Go activation predominate respectively. Conversely, goal-conflict should be maximal at intermediate SSDs when Go and Stop activation are approximately equal (as indexed by correct stopping occurring on about 50% of trials).

Earlier studies have found that goal-conflict resolution mediated by the BIS is functionally dependent on hippocampal rhythmic slow activity in the 4-12 Hz range (McNaughton & Gray, 2000). Similarly, in rodents, hippocampal theta (5-12 Hz) activity occurs during risk assessment with exploratory behaviour (in the elevated plus maze) in approach-avoidance conflict (Jacinto et al., 2016). In addition, previous human data on the SST suggests that goal-conflict processing is associated with 4-12 Hz activation, albeit in right frontal cortex (McNaughton et al., 2013; Neo et al., 2011; Shadli et al., 2015).

Surprisingly, no earlier study has examined the LFPs recorded from HPC, OFC and STN during goal conflict. In this experiment, I will assess the detailed relations of activation of frontal cortex, limbic system and STN to behaviour in relation to varying conflict load and, in particular, analyse how these areas talk to each other and exhibit independence or

coordination during decision making under goal-conflict. I measured power and coherence of low frequency rhythms (5-12 Hz) in HPC, OFC and STN during goal-conflict. An increase in power in HPC, OFC and STN LFPs in low frequency bands at intermediate SSDs (50% correct stopping) was predicted, if goal conflict was detected. Similarly, we expected increased coherence between HPC-STN during high conflict trials (Neo et al., 2011).

6.2 Methods

6.2.1 Data processing

6.2.1.1 Separating low, intermediate and high delay stop trials
We sorted 34 sessions from 5 rats by *percent correct stopping* on stop trials and divided them into three groups; 75% correct stopping (66-97%), 50% correct stopping (40-58%) and 25% (14-38%) correct stopping for each individual rat to give low (25%), intermediate (50%) and high (75%) percent correct stopping (PCS) groups.

6.2.1.2 Spectral power and coherence post-processing – Stop and Go trials
LFP was recorded and analyzed as detailed in Chapter 2 and 5.

6.2.2 Data Analysis

All other statistical procedures were as described in Chapter 2. The factors and levels for ANOVA to this experiment are described in detail here. ANOVA with a 2x3x3x8 factorial design [Trial Type (two levels: correct Stop / correct Go) x PCS (three levels: low/intermediate/high) x Brain area (three levels: OFC / HPC / STN) x Frequencies (eight levels: 5, 6, 7, 8, 9, 10, 11, 12 Hz] was used to test the effects of conflict. The 8 levels of the frequency factors are determined by the frequency resolution of the FFT, which is equal to the inverse of continuous sampling time (s). I used 1s epochs, which gives a 1 Hz frequency resolution and so 8 steps in the range 5-12 Hz. For coherence analysis, rather than brain area, the main factor of interest was pairs of brain areas, which were treated as a 'circuit' factor (three levels: HPC-STN / OFC-HPC / OFC-STN).

The difference in power between Stop and Go trials (Stop-Go) in the 0.5 s duration of the Stop signal can be used to test the effects of goal-conflict. The intermediate trials represented maximum conflict with the two other PCS levels representing less conflict. Given that PCS has three levels, the "quadratic" component in this case can be thought of as representing the difference between the intermediate (conflicting) condition and a value obtained by averaging the two adjacent conditions. The quadratic components for "brain areas" and "circuit" were as described in Chapter 2.

6.3 Results

6.3.1 Mean power of OFC, HPC and STN theta LFPs at three correct stopping values (25%, 50% and 75%) during SST

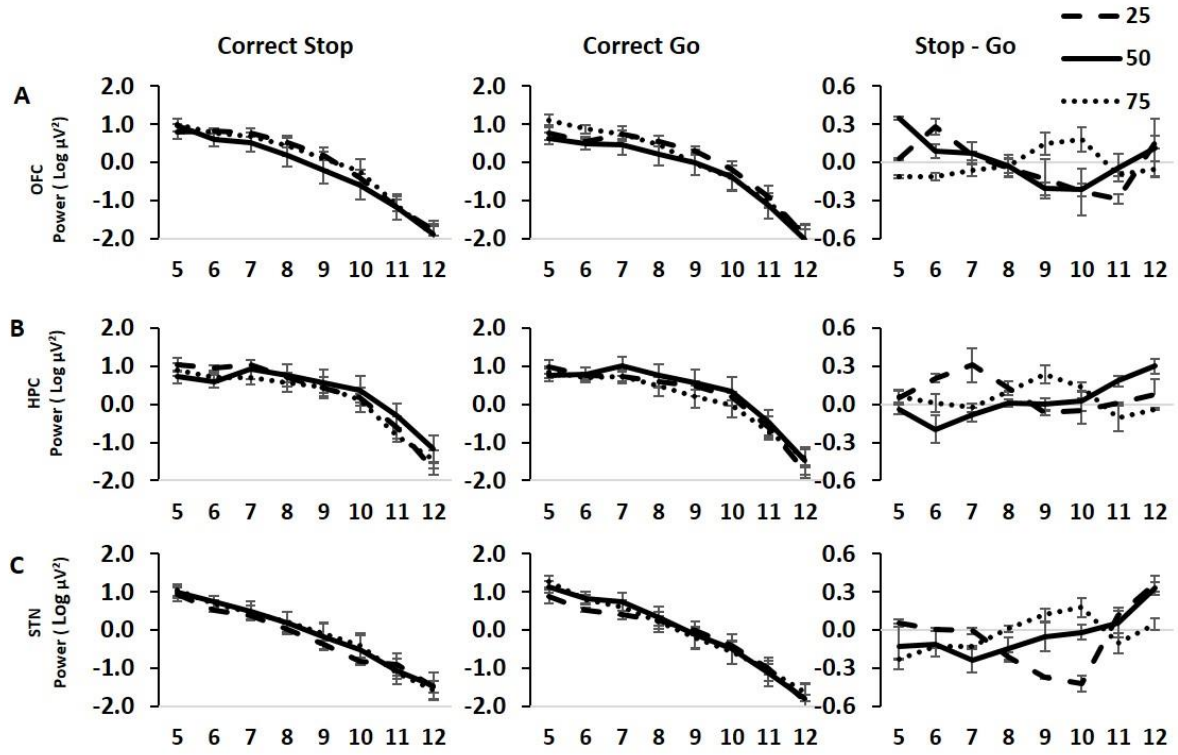

Figure 6.1 mean theta power during correct Stop, correct Go and Stop-Go differences.

75% Correct Stopping (66-97%, dotted line), 50% Correct Stopping (40-58%, solid line) and 25% Correct Stopping (14-38%, dashed line). (A) OFC (B) HPC and (C) STN

Figure 6.1, shows the three PCS during correct Stop and correct Go across OFC, HPC and STN. All three areas showed similar overall power patterns i.e. greater power at lower frequencies and smaller power at higher frequencies for both Stop and Go trials. However, the Stop-Go power difference (right panel) shows clear differences among the three types of PCS. With intermediate correct stopping OFC, HPC and STN power appeared greater at high theta frequencies (11-12 Hz). We then carried out a focused analysis on the quadratic effect of percent correct stopping to determine conflict-specific effects.

6.3.2 Quadratic and linear effects of percent correct stopping on power

In this analysis, Go trial activity was subtracted from Stop trial. The conflict effect was then calculated as the difference in spectral power between the intermediate and the average of the low and high PCS trials (quadratic component of PCS). Figure 6.2A shows the variation of the quadratic component in the 5-12 Hz frequency range across OFC, HPC and STN. At OFC, the conflict effect was greatest at the lowest frequency (5 Hz) and was negligible at the highest frequencies. In contrast both HPC and STN show a positive conflict effect only at higher theta frequencies (11-12 Hz). The linear frequency trend shown in Figure 6.2A was significantly more positive in HPC compared to the average of the other two areas (Brain area [quadratic] x Frequency [linear] x Stop-Go [linear] x PCS [quadratic], $F(1, 4) = 7.286$, $p = 0.05$). The apparent difference in this linear trend between OFC and STN did not approach significance (Brain area [linear] x Frequency [linear] x Stop-Go [linear] x PCS [quadratic], $F(1, 4) = 1.367$, $p = 0.307$). This suggest that goal-conflict effects was similar between OFC and STN.

We also calculated the linear contrast across PCS to assess proportionate variation with the three levels of PCS trials (see figure 6.2B). In this case, the linear contrast reflects the difference between high and low PCS trials, with no contribution from intermediate ones. As shown in Figure 6.2B there is a curvilinear frequency effect that involves a decrease in power in the region of 6 Hz and an increase at 9-10 Hz (Frequency [order 4] x Stop-Go [linear] x PCS

[linear], F (1, 4) = 7.449, p < 0.05). The brain areas did not show any significant differences in the size of this curvilinear effect (Brain area [linear] x Frequency [order 5] x Stop-Go [linear], F (1, 4) = 0.335, *p* = 0.594). This suggest that conflict effects of PCS was similar between OFC, HPC and STN.

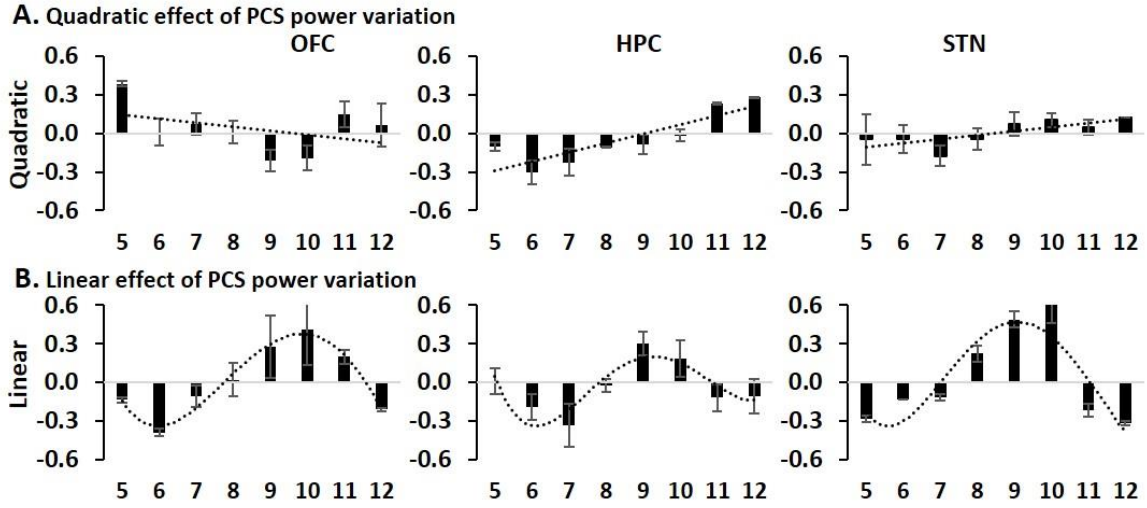

Figure 6.2 Power in Stop trials relative to Go trials.

Curves represent significant trends from ANOVA. A. Frequency variation in goal-conflict specific power, estimated as the difference between power in the intermediate trials and the average power of the low and high correct trials (quadratic) B. Goal-conflict specific power calculated as linear (difference between high and low correct trials). PCS: percent correct stopping. Trend lines show significant linear differences in frequency trend in A and significant common curvilinear effect that did not differ across brain areas in B.

6.3.3 Mean coherence of OFC, HPC and STN theta LFPs at three correct stopping values (25%, 50%, 75%) during the SST

Figure 6.3 shows coherence between HPC-STN, OFC-HPC and OFC-STN during correct Stop (left panel), correct Go (centre panel) and their difference (right panel) at low, intermediate and high PCS. The Stop-Go power differences showed clear mean coherence differences between the three types of PCS. Coherence interactions between pairs of structures showed similar coherence patterns i.e. greater coherence during intermediate stopping. The coherent activity during Stop-Go difference for intermediate stopping between HPC pairs

(HPC-STN and OFC-HPC) appeared greater at low theta frequencies (5-6 Hz) (Figure 6.3A and B, right panel). In contrast, OFC-STN shows at 8-10 Hz (Figure 6.3C). Further, we carried out a focused analysis on the quadratic effect of PCS to determine conflict-specific effects.

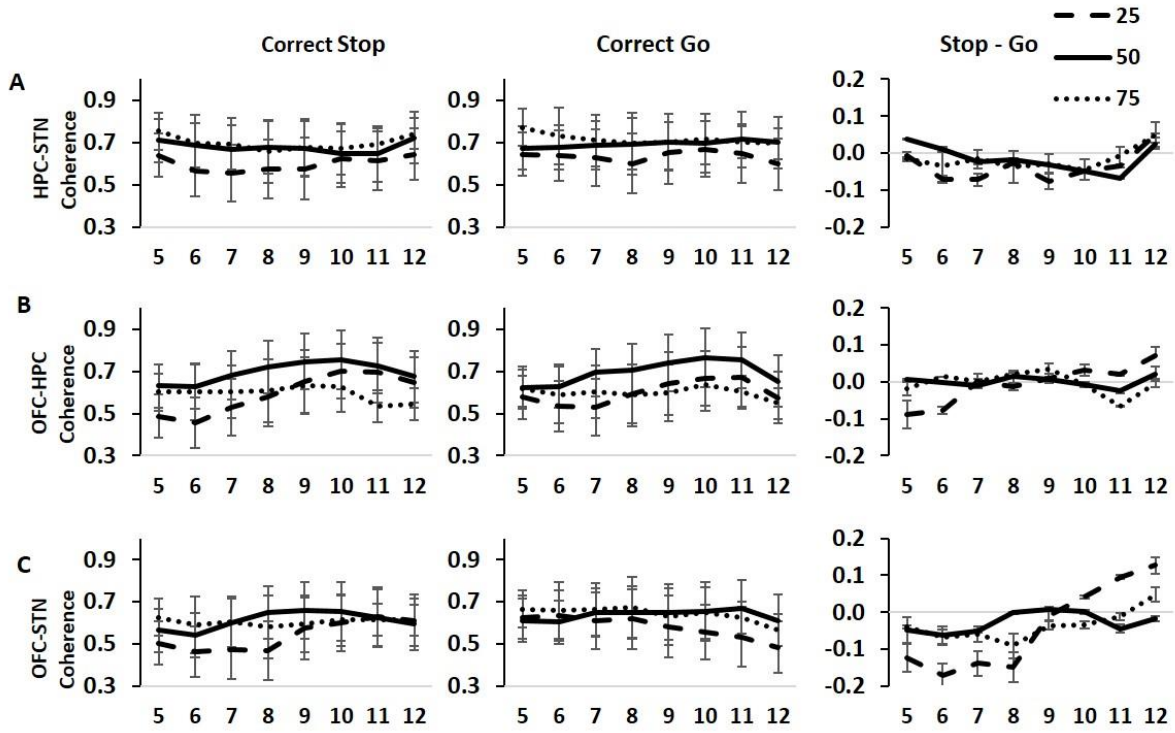

Figure 6.3 mean theta coherence during correct Stop, correct Go and Stop-Go differences.

75% Correct Stopping (66-97%), 50% Correct Stopping (40-58%) and 25% Correct Stopping (14-38%). (A) HPC-STN (B) OFC-HPC and (C) OFC-STN.

6.3.4 Quadratic and linear effects of percent correct stopping on coherence

In this analysis, the conflict effect was again represented by a quadratic effect (see section 6.3.2). Figure 6.4A shows the quadratic trend variation between HPC-STN, OFC-HPC and OFC-STN coherence at 5-12 Hz frequency. The conflict induced coherence effect was greatest at 8 Hz for OFC-STN while HPC-STN and OFC-HPC coherence was seen at 6 Hz and 5 Hz respectively. Overall, all brain regions showed conflict-related coherence at low frequencies. As can be seen in Figure 6.4A, OFC-HPC coherence is significantly different in the form of the frequency function from the average of the two STN pairs (Circuit [quadratic] x Frequency [order5] x Stop-Go [linear] x PCS [quadratic], F (1, 4) = 36.830, p = 0.004) i.e.

effects of conflict (as determined by quadratic contrast) on coherence shows greater coherence interaction between OFC-HPC compared to OFC-STN and HPC-STN. Conversely, the two STN pairs (HPC-STN and OFC-STN) did not differ from each other (Circuit [linear] x Frequency [order5] x Stop-Go [linear] x PCS [quadratic], F (1, 4) = 0.517, p = 0.512). Both of the STN circuits show a nonlinear trend with a decrease in coherence at 11-12 Hz.

We also calculated the linear contrast among PCS to assess proportionate variation with the three levels of PCS (see figure 6.4B). Activity reduces steadily from the lower to the higher frequencies (Frequency [linear] x PCS [linear], F (1, 4) = 11.571, p = 0.027) (Figure 6.4B). The slope of the HPC-STN (see 6.4B, left panel) seems different from other two but is equally linear in frequency trend (Circuit [linear] x PCS [linear], F (1, 4) = 0.106, p = 0.761). This suggests that the brain structures were not reliably different and the activity decreased to the higher frequencies.

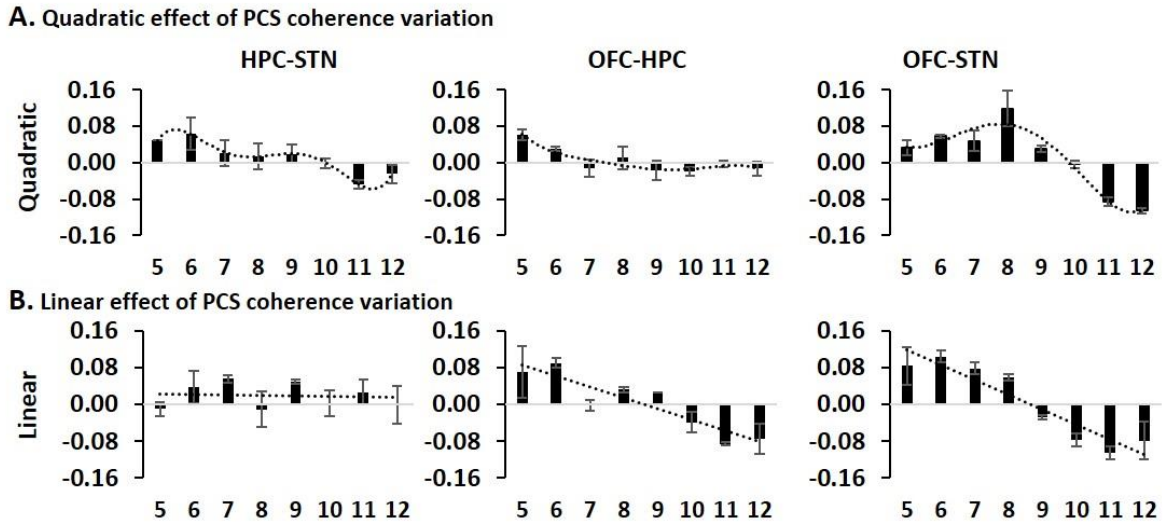

Figure 6.4 Coherence in Stop trials relative to Go trials.

A. Frequency variation in goal-conflict specific coherence, estimated as the difference between coherence in the intermediate trials and the average coherence of the low and high correct trials (quadratic) B. Goal-conflict specific coherence calculated as linear (difference between high and low correct trials). PCS: percent correct stopping.

6.4 Discussion

In this experiment, the SST was used to assess the detailed relations of activations of OFC, HPC and STN to behaviour and the varying conflict load. We measured power and coherence in the 5-12 Hz range during goal-conflict across the brain areas. Trials were divided into three groups based on percent correct stopping separately; 75% correct stopping (66-97%), 50% correct stopping (40-58%) and 25% (14-38%) correct stopping for each individual rat to give low, intermediate and high percent correct stopping groups. Then, goal-conflict activity was assessed as the difference between theta power and coherence at intermediate PCS and the average of the activity at low and high PCS trials across HPC, OFC and STN.

6.4.1 Goal-conflict related HPC, OFC and STN theta power

Stop-Go activation was examined as the difference between correct Stop and latency matched correct Go trials. We assume this process would cancel out the common processes that are linked with the presentation of the Go signal such as preparation, execution of the Go response, anticipation of the Stop response. Our results suggest that the conflict related effect in the intermediate correct stopping condition is greatest, relative to low conflict stopping. Interestingly, overall, all brain regions show conflict related effects at higher frequencies of 11 and 12 Hz. In the HPC and STN, the conflict effect was high only at the higher frequency of 11-12 Hz. In contrast OFC shows a conflict effect both at lower frequencies (5 and 7 Hz) and a small effect at higher theta frequencies 11-12 Hz.

We showed activation of OFC due to conflict at low theta frequencies at 5 and 7 Hz. This is in line with the previous conflict studies on humans that report Stop-Go LFP activity averaged across electrodes at medial right frontal cortex (equivalent to OFC) in the intermediate trials showed an increase in power at 7 Hz (Neo et al., 2011; Shadli et al., 2015). Also, a human study recently found increased mPFC activity in the theta frequency band (4-8 Hz) during conflict (Zavala et al., 2014).

6.4.2 Goal-conflict related HPC, OFC and STN theta coherence

Overall, all the circuits show conflict-related coherence in the low frequency theta band. Recent studies in rodents have reported theta phase coherence between frontal cortex and HPC involved in a conflict situation (Jacinto et al., 2016). Consistent with this, we found that during intermediate correct stopping, conflict induced coherence between OFC-HPC was greater at low theta frequencies (5-6 Hz). Indeed, the OFC receives a direct projection from the HPC (Cavada et al., 2000) and has been implicated beyond reward-related processing to encode conflict information (Mansouri et al., 2014).

Similarly, previous findings on the role of theta oscillation (4-8 Hz) demonstrated that high conflict trials in humans produced greater theta coherence between medial frontal cortex and STN (Zavala et al., 2016). In line with this finding, our data show that during intermediate stopping, conflict induced coherence effect was greater at lower theta (5-8 Hz) between two pairs of STN structures (HPC-STN and OFC-STN). Interestingly, the observed coherences between these pairs was not significantly different from each other. Earlier studies have separately reported conflict induced theta coherence between mPFC-HPC (Jacinto et al., 2016) and mPFC-STN (Zavala et al., 2014). In our study, we simultaneously recorded LFPs from all three brain areas and found an elevation of activity at low frequency. This implicates that three areas could become functionally connected during conflict. Taken as a whole, with these findings and frontal cortex driving STN during conflict (Zavala et al., 2014) suggest that OFC could utilize conflict information provided by the HPC to STN and shows evidence of functional interaction between HPC and STN during conflict-related processing at low theta frequency.

The experiments in this Chapter had two objectives. The first one was to investigate the interaction between HPC, OFC and STN to test the neural effects of goal-conflict. Our data demonstrate a modulation of theta power and theta coherence in these brain areas to process

conflict-specific information. The second aim was to see if HPC-STN coherence increased during goal conflict. The hypothesis here was high conflict trials would increase theta coherence between HPC and STN. The results show that theta coherence between cortical and subcortical structures may play role in goal-conflict. In the next and final Chapter, I summarize findings from all the experimental Chapters (4, 5 and 6) to assess the role of cortico-basal ganglia-limbic systems in behavioural inhibition.

Chapter 7. General Discussion

Suppression of behaviour that is no longer required or inappropriate in given situation is hallmark of cognitive control. In this thesis, I have presented a literature review and experimental data aimed at understanding how the BG (particularly the STR and STN) and limbic system (particularly HPC and OFC) support inhibitory cognitive control.

In Chapter 1, I explained why inhibitory processes are important for adaptive behaviour. Failure to inhibit unwanted action, thoughts or emotion could lead to psychological disorders. Previous lesion studies in rodents and humans discussed the neural basis of inhibitory function (Abela et al., 2013; Bari & Robbins, 2013; Boucher, Palmeri, Logan, & Schall, 2007; Davidson & Jarrard, 2004; Erika-Florence, Leech, & Hampshire, 2014; Gauggel, Rieger, & Feghoff, 2004). Specifically, inhibitory control functions are associated with fronto-basal ganglia circuitry. Dysfunction in the cortico-basal ganglia circuitry results in impaired stopping, which could therefore affect impulsivity (Bari & Robbins, 2013; Jentsch & Taylor, 1999; Knyazev, Levin, & Savostyanov, 2008). However, my argument was that adaptive behaviour in response to changing situations not only includes cortico-basal ganglia circuitry but also engages limbic structures. In particular, interaction between these systems influences goals or plans in a way that supports flexible and adaptive responses.

Given this starting point, my experiments set out to assess the possible interactions between BG and limbic circuits in the generation of inhibitory control. My experiments explored the contribution of the BG and limbic system to the acquisition of motor learning, to simple response inhibition, and to more complex behavioural inhibition. In the next sections, I summarise the findings from the experimental Chapters in relation to each of these types of process.

7.1 Electrophysiology of STR, OFC and HPC during simple motor learning/ approach behaviour

In Chapter 4, I first talk about simple motor learning (a Go task that is also the initial part of the SST) and examine the role of STR (the primary input stage of the BG), OFC, and HPC in acquisition of motor learning and reward delivery. I made an argument that STR sends information to HPC during initial learning of motor behaviour. Additionally, expectancy of reward outcome increases synchronisation between OFC-HPC. In the next section, I report the main results from multi-electrode recording in the cortico-basal ganglia and hippocampal network of freely behaving rats learning and performing a Go task.

7.1.1 The role of STR in simple motor learning

I have discussed the STR and its role in simple motor learning earlier in the introduction. Briefly, STR, classically thought as a movement regulating structure and recently has a role in cognitive functions, in particular associative learning (Ashby, Turner, & Horvitz, 2010; Balleine et al., 2007; Featherstone & McDonald, 2004; Powers, Somerville, Kelley, & Heatherton, 2016). Dorsal STR has been mainly implicated in stimulus-response association learning (Featherstone & McDonald, 2004). During initial learning, memory will be encoded and stored into parallel memory systems. Thus, stored memory will be selected depending on the situation for the control of behavioural. For adaptive behaviour it is important to learn to make associations between stimuli and responses. The aim of the Go task was to teach rats to make an association between light to food. Here, the rat has to run towards S1 and then moves to L5 to trigger S5 (Go response). Rats were motivated to trigger S5 to get the food reward (by triggering S0).

We found that the STR talks to the HPC in the early phase of motor learning and task performance. This could be because STR has long been implicated in associative learning. Striatal dopaminergic neurons encode reward that drives learning. STR receives inputs from

HPC and OFC. Earlier studies viewed both STR and HPC as a learning and memory system of different behaviour types. For instance, STR has a role in procedural learning and HPC is involved in episodic memory, complex learning such as spatial or complex maze (DeCoteau et al., 2007a; Gengler, Mallot, & Holscher, 2005; Graybiel & Grafton, 2015; Packard & Knowlton, 2002). Additionally we saw that after the task is learned, HPC-STR coherence reduced. This is in line with a previous study that showed that once the task is learned STR is mainly involved to maintain the motor behaviour (Wickens, Reynolds, & Hyland, 2003).

7.1.2 The role of OFC in simple motor learning

Reward motivates behaviour and is important for reinforcement learning. OFC has been long implicated in reward value, expected outcome and motivational learning. This could be because OFC receives sensory input from various sensory cortices (as explained and shown in Chapter 1) in which there is information about reward value, objects and stimulus response outcome (Rolls, 2004). In addition, lesion studies in rodents suggest that damage to OFC impairs learning of stimuli that are rewarding (Rolls, 2004).

We hypothesized that OFC-HPC coherence might increase during expectancy of reward outcome. Under this hypothesis, we saw OFC-HPC beta coherence before triggering S0. This could suggest that OFC beta oscillations might convey a reward signal to HPC (Lansink et al., 2016). During the Go task, we saw that before the rat the triggers S0, delta and beta power increases in OFC. Earlier studies showed low frequency (delta/theta) OFC oscillations for integrative processing while higher frequencies (beta and gamma bands) are linked to cognitive function (Buschman & Miller, 2014). Our results are consistent with findings that OFC plays a vital role in reward expectancy and information signaling reward (Riceberg & Shapiro, 2012; van Wingerden et al., 2010).

7.1.3 HPC involvement in simple motor learning

Our results showed theta coherence between STR and HPC as the rat triggers S1 and runs towards S5 (Go response). During early period, the coherence was stronger during simple running. This may be related to running and motivation towards reward. It is possibly because the behaviour (running) is motivated by reward. The reason for theta coherence between STR-HPC could be STR sending "efference copy" information to HPC and the fact that theta rhythm is activated by motor activity in the HPC. The sending of such "efference copy" information does not entail that HPC is functionally involved in simple motor skills. The literature suggests that damage to the medial temporal lobe does not affect simple learning (Chun & Phelps, 1999; Poldrack et al., 2001).

Taken together, these findings suggest that HPC receives reward and/or motivation-related information (during early learning) about ongoing actions from STR but may not be functionally involved in the control of those actions in simple learning paradigms; and does not receive response-related information once responding is habitual.

7.2 Electrophysiology of STN, OFC and HPC during simple response inhibition (stopping)

I have provided a detailed review on the role of the three brain areas during simple response inhibition (stopping) to support flexible and goal directed behaviour in Chapter 1. Furthermore, I have highlighted the importance of these brain areas in response inhibition. Many of these studies suggest that the frontal cortex, BG, in particular the STN, and HPC provides a type of inhibitory signal that suppress unwanted actions, emotions, motivations (Aron et al., 2007; Chambers et al., 2009; Fernandes, Moscovitch, Ziegler, & Grady, 2005; Isoda & Hikosaka, 2008) and such control is necessary for adaptive behaviour.

The aim of the experiment in Chapter 5 was to evaluate how oscillatory activity in the STN, OFC and HPC responds to the termination of actions as required in the SST. Most

importantly, we asked how inhibitory control is mediated by cortico-hippocampal-striatal circuitry. The hypothesis here was that successful stopping would increase theta and beta power in STN and increase coherence between OFC-STN. Also, we aimed to see if synchrosation between STN and HPC at theta frequencies occurs only after failure to stop simple, action inhibition.

7.2.1 STN and OFC involvement in response inhibition

In our experiment, during cancellation of the response, we found increased STN beta and OFC theta and beta power. OFC-STN coherence at low (delta/theta) and beta frequency was also observed. This possibly indicates that correct action stopping is accompanied by increased beta activity in STN as well as beta activity in OFC. This is in line with previous findings that correct stopping results in an increase in STN beta power (Kuhn et al., 2004; Ray et al., 2012) and OFC beta power (Leventhal et al., 2012). Another interesting finding we observed was that stop failure increased synchrosation between STN and HPC at theta frequencies. This observations is consistent with stop failure related modulation of low frequency (Friese et al., 2016).

These results suggest that OFC and STN are critical structures that work together in successful response inhibition. Additionally, while successful action inhibition does not involve HPC, Stop failure increased the theta phase synchrosation between HPC and STN. This suggests that these areas communicate recognition of failure to stop and no reward will be delivered. This is in line with a study that reported theta and beta activity in cortico-basal ganglia circuitry is involved in action inhibition (Emmons et al., 2016).

7.2.2 HPC involvement in response inhibition

Analysis of movement-related LFP oscillations suggested that functionally different anatomical structures are involved in synchronised activity in the beta band. We observed beta coherence between HPC-STN and HPC-OFC during stop failure but not increase in OFC-STN

coherence. This suggests that there may be communication among HPC, OFC and STN during stop failure. We also found increased gamma activity in HPC for following a stop failure. During the modulation of the goal directed action, the interaction between the frontal cortex and HPC is considered important. The HPC compares sensory information about the environment and intended movements and transmits an error signal to frontal cortex (Numan, 2015). These findings suggest that information about stop failure may be conveyed to frontal cortex. Our results are consistent with the findings that both delta and gamma frequency may support information processing between frontal cortex, BG and other brain regions including HPC (Fujisawa & Buzsaki, 2011) for response inhibition.

In the context of stopping an initiated action, interconnection between frontal cortex and the BG is considered vital (Aron & Poldrack, 2006; Hollerman, Tremblay, & Schultz, 2000; Wiecki & J., 2013). In addition, human fMRI data suggest three important areas for response inhibition: the preSMA, the rIFG and the STN (Aron et al., 2007; Eagle et al., 2008; Floden & Stuss, 2006). Our results suggest increases in STN and OFC theta and beta power and OFC-STN coherence at low (delta/theta) and beta frequencies indicating that theta and beta are linked to cognitive control.

In conclusion, LFP oscillatory activity in STN might be modulated by activity in both OFC and HPC that could vary with different frequency bands and behavioural states. For correct stopping theta and beta activity in cortico-basal ganglia circuitry is important. Similarly, beta and gamma frequency following stop failure. These functionally linked changes in coherence are consistent with different frequencies of rhythmicity binding groups of structures into different functional circuits as a result of task demands. Activity in this range may provide a means of synchronising frontal activity with other brain regions (Fujisawa and Buzsáki, 2011).

7.3 Electrophysiology of STN, OFC and HPC during complex inhibition (approach-avoidance / goal-conflict)

As previously described in Chapter 1, conflict processing has been separately reported to activate right frontal cortex, the septo-hippocampal system, and STN. However, it was not clear if their activation involves a specific goal-conflict component and in what ways they interact. Therefore, in Chapter 6, I examined activation of OFC, HPC and STN during goal-conflict processing.

There is a race between going (triggered by the Go stimulus) and stopping (triggered by the Stop signal) in the SST (Logan, Cowan, et al., 1984). The goal of the Go task and stop task is: "respond as quickly" as possible and "stop the response" respectively (Verbruggen & Logan, 2008b). For successful performance, monitoring and adjusting response strategies to Go and Stop stimulus is important. Subjects can stop the ongoing action successfully if the tone is presented close to the start of the go stimulus (low conflict). Similarly, going is successful if stop tone is presented close to completion of the Go task (low conflict). However, high conflict can occur when two goals (Go) and (Stop) are presented at the intermediate stop signal delay. Stop-Go activity in the intermediate stopping (50%), could reflect goal-conflict.

7.3.1 Conflict activations in OFC

In rats damage to OFC impairs stop-signal response inhibition (Eagle & Robbins, 2003a). OFC receives reinforcement information associated with the stimulus; encodes information and updates reinforcement expectancies (Wikenheiser & Schoenbaum, 2016). During conflict, OFC might be involved in evaluating and updating the available information to support conflict resolution (Mansouri et al., 2014). Our findings indicate that OFC power increased in the theta band (5 Hz) during intermediate correct stopping (designated as high conflict); and, therefore, might be involved in encoding and maintaining conflict information through to the time of behavioural goal achievement.

7.3.2 Conflict activations in HPC

As discussed in Chapter 1, information about goals encoded in cortical and subcortical structures is transmitted to the HF (Gray & McNaughton, 2000). HPC acts as a comparator for the detection of novelty (Vinogradova, 2001), response intention-response outcome working memory (Numan, 2015) and resolves goal conflict (Gray & McNaughton, 2000). In our study, we were interested in determining if activation of HPC occurs when it receives information about incompatible goals. We demonstrated that HPC power was greater during intermediate stopping (goal-conflict) at higher theta frequency (10-11 Hz). This result is in accordance with studies demonstrating the role of HPC theta in conflict in animals (Gray & McNaughton, 2000; Jacinto et al., 2016) and human (Neo et al., 2011). Additionally, limbic structures such as OFC and HPC can select the appropriate goals to reduce the goal conflict (Blair, 2007; Ito & Lee, 2016; Schumacher et al., 2018; Zavala et al., 2016).

7.3.3 Conflict activations in the STN

Initial evidence for this study was proposed by Neo et al. (2011), in human, who suggested that HPC might communicate with STN during behavioural inhibition. The present study was carried out to further assess conflict related LFP activity in HPC and STN during SST. Power analysis showed that goal-conflict effects were selective to the higher theta range (11-12 Hz). Specifically, theta power was increased during intermediate stopping, where two goals (going vs stopping) compete with each other. Additionally, we saw increased HPC-STN coherence at low theta frequency during intermediate PCS. An increase in coherence between structures within STN (HPC-STN and OFC-STN) during conflict allows these two structures to communicate prior to selection of action during conflict. These results, taken together suggest that theta coherence between cortical and subcortical structures may play a role in conflict related adaptation.

I proposed a model in Chapter 1 to show how BG, OFC and HPC could be functionally connected to support flexible and goal directed behaviour in response to changing environment. The results I have found are consistent with this previous literature and support the view that BG and limbic systems work in parallel for learning, response inhibition and goal-conflict. Taken together with the findings from this study, I present an updated tentative model (Figure 7.1) of the functional networks of the motor and limbic system building on that previously suggested by Gray and McNaughton (2000) and Neo et al. (2011). In the following section, I will describe how this model provides a framework of how BG and limbic network control the complex behavioural inhibition that guide motivation and movement.

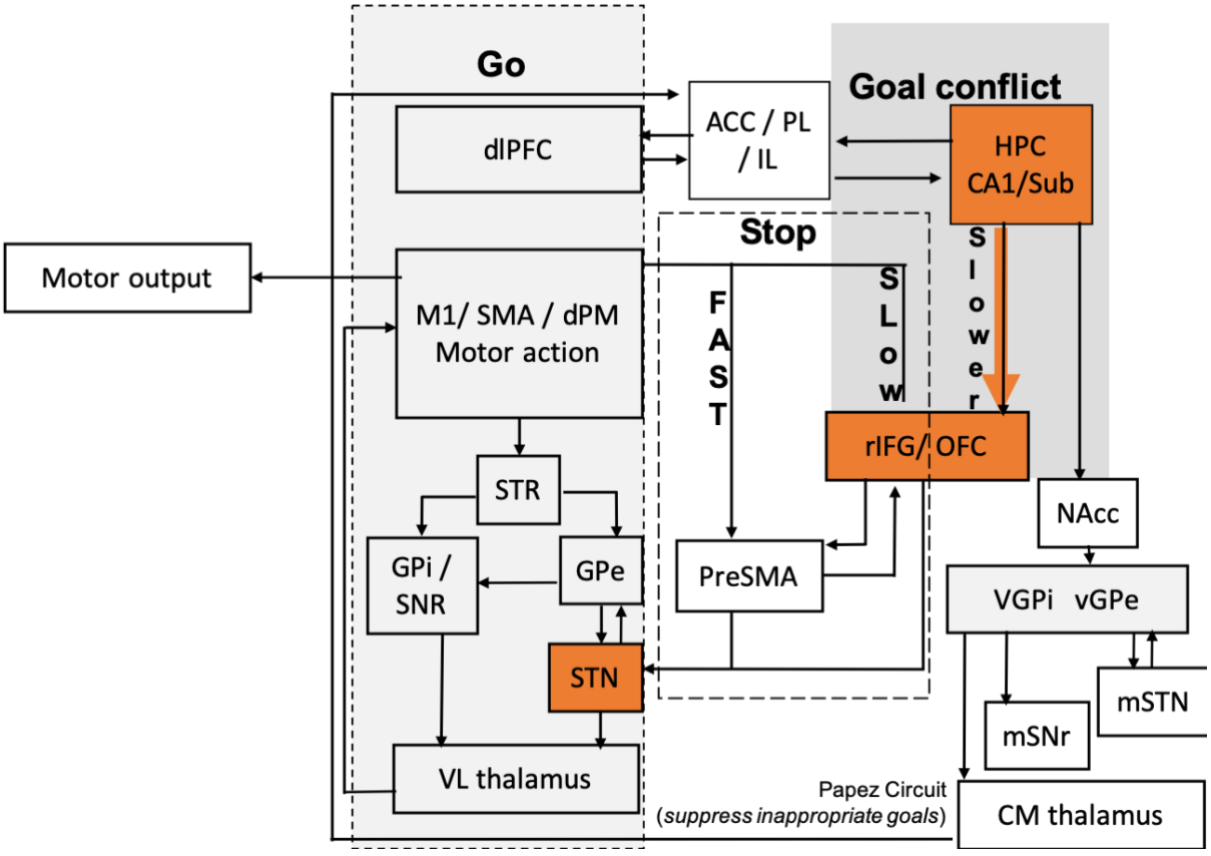

Figure 7.1 proposed neural connection between BG, OFC and STN for going and stopping and their links to the BIS (shaded box).

We propose that goal inhibition circuitry involves HPC and OFC, in addition to fast and slow routes motor inhibition circuits, to modulate the go circuit. To simplify the neural connections other structures in the BIS are omitted. ACC: anterior cingulate cortex; mOFC: medial orbitofrontal cortex; PL: prelimbic; IL: infralimbic, HPC:

hippocampus; STR: striatum; GPi/e: globus pallidus interna/externa; STN: subthalamic nucleus; dPM: dorsal premotor cortex; SMA: supplementary motor areas; preSMA: pre supplementary motor area; M1: primary motor cortex; rIFG: right inferior frontal gyrus; DLPFC: dorso lateral prefrontal cortex; SNr: substantia nigra pars reticulata; -vl: ventrolateral; -m: medial; CM: centromedial. Figure adapted from several previous Figures (Chambers et al., 2009; Haegelen et al., 2009; Neo et al., 2011)

7.4 Implications for motivation, response inhibition and behavioural inhibition

Cognitive functions depend on interconnected networks of anatomical components. Each network has a different role, with some components more central to network function. Earlier studies have shown that motivation could have effects on reward, brain activation, behaviour and overall cognitive control. In this study, we focused on understanding how motivation, simple inhibition and complex behaviour impacts brain regions and contribute to precise behaviour control.

7.4.1 Implications for motivation

Motivation is an important determinant of behaviour. In order to learn the task, one must be motivated to do it. In the behavioural approach process as described in Chapter 1, behaviour is directed by a delivery of PosR/rewarding stimuli or omission of NegR/punishing stimuli. Reward is the most important variable that makes the organism approach a response (Schultz, 2015). It provides a biological basis for the pairing of stimulus and response outcome. The subject learns the stimulus-reward association, encodes and represents the value of task events. Reward delivery makes strong associative connection between stimulus and specific response (Adcock, Thangavel, Whitfield-Gabrieli, Knutson, & Gabrieli, 2006; Rudebeck, Ripple, Mitz, Averbeck, & Murray, 2017). Nevertheless, reward processing involves other processes such as attention, anticipation, encoding value and recruits various brain regions (Critchley, Mathias, & Dolan, 2001; Oldham et al., 2018; Vartak, Jeurissen, Self, & Roelfsema, 2017), and involves other primary brain structures including STR, OFC and HPC. In our study we have examined the contribution of the STR, OFC and HPC to a simple motor task.

The left hand panel of Figure 7.1 shows the Go process that explicitly engages the motor system to organize and generate movements to respond appropriately to the environment. Various events or conditions including motivation, reward or association between stimuli could initiate action through cortico-basal ganglia integrative networks (Haber & Calzavara, 2009; Leisman et al., 2014; Mogenson, Jones, & Yim, 1980). STR is a key BG structure involved in motor system (Figure 7.1). It receives direct excitatory input from the cortex (mainly motor cortex, association cortex and limbic cortex particularly OFC) which mediate goal-directed actions (Haber & Calzavara, 2009). On a Go task, movement is initiated in motor cortical regions. Motor cortex sends excitatory signasl to STR and STN. The STR has direct inhibitory input to the GPe/i and selectively disinhibit the selected motor programme and enables response initiation (Chambers et al., 2009; Nambu et al., 2002). Different techniques including electrophysiological recordings have examined the STR's role for motor learning and reward delivery (Bergstrom et al., 2018; Featherstone & McDonald, 2004; Feingold et al., 2015; Yin et al., 2005).

The results of the current study suggest greater theta coherence between OFC-STR and HPC-STR during reward expectancy in a GO task. This suggest that both HPC and OFC code for expected reward outcome. HPC has a comparator function that means it is in checking mode for the anticipated outcome and actual outcome. On the other hand, OFC has been extensively studied in reward, motivation and acquisition of action outcome associative learning (Balleine et al., 2007; Dayan & Balleine, 2002; Yin et al., 2005). Increased theta coherence between OFC-STR could possible suggested that OFC may facilitate information about expected reward to STR as well as motivation related brain areas such as HPC during learning (van Wingerden et al., 2014; van Wingerden et al., 2010). Previous study have found learning-related higher level of HPC-STR theta coherence in a T-maze task (DeCoteau et al., 2007a). However, we

did not find such high coherence possibly because our task is a simple stimulus-response association task and may not require the same level of HPC involvement.

7.4.2 Implications for response inhibition

As explained in Chapter 1 section 1.6.2, with behavioural avoidance, behaviour is directed away from delivery of NegR or omission of PosR. For goal-directed behaviour, omission of an expected reward may have the same effects as a punishment (Kim, Shimojo, & O'Doherty, 2006; Purgert, Wheeler, McDannald, & Holland, 2012). In our experiment, animals are required to suppress or cancel the ongoing action when the stop tone is presented. Failure to do so will result in omission of expected reward delivery with a time out period. The stopping of ongoing motor activity could be considered as a relatively pure avoidance (simple, avoidance related activity) and mediates simple neural processing (action stopping recruiting frontal-basal ganglia circuitry). Successful stopping increased theta and beta power in STN as well as OFC. We observed increased theta coherence between OFC-STN. The increase in OFC-STN coherence could be because in rodents there is a projection from the OFC to the STN (Cavada et al., 2000; Haegelen et al., 2009) and this direct pathway may have been used to inhibit ongoing action.

The frontal cortex (OFC), BG (in particular the STN), and HPC provide a type of inhibitory signal that suppress the unwanted action, emotion and motivation (Aron et al., 2007; Chambers et al., 2009; Fernandes et al., 2005; Isoda & Hikosaka, 2008) and such control is necessary for adaptive behaviour. As can been seen in Figure 7.1 (middle panel), different areas of the fronto-basal ganglia network are involved in stopping. In rodent lesion studies, OFC and STN lesions impair stopping suggesting that the stopping process involves OFC and STN (Eagle et al., 2008; Eagle & Robbins, 2003b). Similarly, human imaging studies found that the SST activates rIFG (Aron et al., 2007; Aron & Poldrack, 2006; Aron, Robbins, & Poldrack, 2004). OFC in rodents may be considered homologous to rIFG in humans (Eagle et al., 2008).

Furthermore, human lesion studies suggested that right superior medial frontal lobe (mainly preSMA) slowed SSRT in SST (Floden & Stuss, 2006). These findings taken together suggest that OFC (rodents)/rIFG (humans) and preSMA are crucial to inhibitory control. However, the involvement of these areas for stopping differs with the Go speed. For example, when Go speed is *fast* (with no strategic slowing of go responses), preSMA may be recruited for the "kill switch" inhibitory system (Floden & Stuss, 2006); in contrast when Go speed is *slow* (strategic slowing of go response), more controlled stopping recruits rIFG (Aron, 2011; Aron et al., 2007).

When going versus stopping causes a conflict (usually at intermediate SSDs) HPC gets activated as a result of activation of BIS inputs. The SST may also activate motivational processes induced by goal conflict (Neo et al., 2011) involving slower responses. As explained earlier, action inhibition involves different pathways to stop the action depending on the GoRT. During goal-conflict processing, HPC may send signals to the motor system (STN) via right frontal regions (OFC in rodents) in a similar way to preSMA and rIFG and so inhibit the action (See Figure 7.1). Anatomical evidence supports that the HPC and OFC are reciprocally connected (Barbas & Blatt, 1995; J. J. Young & Shapiro, 2011). Thus HPC may be involved in action stopping for the *slower* go reaction time and need access to the motor control system.

7.4.3 Implications for complex behavioural inhibition (goal-conflict)

As described in the introduction and in Chapter 6, simple approach and simple avoidance are two responses for which immediate positive or negative reinforcement are available if these responses are previously associated with the reinforcer. The Go stimulus is required to make an approach response while the Stop signal was presented to inhibit/withhold the response. Therefore, these two processes each have a single goal either to approach (going) or avoid (stopping). Further, stop signals presented early or late should have low goal-conflict because Stop and Go activation predominate, respectively. On the contrary, goal-conflict

should be maximal at intermediate SSDs when Go and stop activation are approximately equal (as indexed by correct stopping occurring on about 50% of trials).

As explained earlier, the motor control system is involved in approach or avoidance behaviour. Motor control is processed by interacting levels of the frontal cortex including DLPFC, preSMA and area 8 (right hand side of Figure 7.1). In contrast, complex behavioural inhibition (goal-conflict) could be processed by a separate system– the BIS (see Figure 7.1, grey shaded box). In addition, Neo et al. (2011) have postulated that the right IFG and its related circuits could be recruited to inhibit relatively slow responses in the humans study. In their model, they proposed that the BIS operates in parallel with other inputs to rIFG to innervate the motor system.

In this rodent study, we therefore tested the neural effects of goal conflict to see if BIS could link to OFC. The increase in theta spectral power was used as a goal-conflict index and this increased theta power allowed us to evaluate goal-conflict specific activation in HPC, OFC and STN. The increased theta power in OFC due to conflict may be due the activation of motivational components of goal conflict. Conflict studies in humans report Stop-Go LFP activity at medial right frontal cortex (equivalent to OFC) in the intermediate trials showed an increase in theta power at 7-8 Hz (Neo et al., 2011; Shadli et al., 2015). Moreover, rodent and human studies have separately reported conflict induced theta coherence between mPFC-HPC (Jacinto et al., 2016) and mPFC-STN (Zavala et al., 2014). According to Zavala et al. (2014), "STN may be involved during conflict to adjust the 'evidence threshold' needed to prevent error and allowing time for right decision to make by corticostriatal pathway". The conflict induced coherence effect was observed at lower theta frequencies (5-8 Hz) between two pairs of STN-connected brain circuits (HPC-STN and OFC-STN). These coherences could be because of anatomical and functional connection that exist between OFC and STN. For instance, STN receives projections from limbic cortical structures such as medial frontal cortex

(Smith, Bevan, Shink, & Bolam, 1998). Taken as a whole, activation of HPC, OFC and STN during conflict suggests that OFC could utilize conflict information provided by the HPC to STN – evidence of functional interaction between HPC and STN during conflict-related processing at low theta frequency. The data as a whole imply that these three areas could become *functionally* connected during goal-conflict.

Overall, from those results we can conclude that the coherence between limbic structures, particularly OFC and HPC makes contributions to motivation and representation of reward and value. The BG (particularly STR and STN) are involved in action outcome associative learning, motivation and stopping of unwanted actions respectively. Additionally, we observed increased theta activity in the HPC, OFC and STN and in particular, increase theta coherence between structures during goal-conflict. Hence, interaction between BG and limbic structures may be important for complex behavioural inhibition.

7.5 Implications for the future research

A limitation of the standard SST is that it does not explicitly involve complex goals for instance, environmental features, distance and size of the object/stimulus – nor more complex stopping requirements. Future studies are needed to test that if the same brain circuitry is implemented during complex inhibition when the HPC is functionally involved (Eagle & Baunez, 2010). Furthermore, studies are needed to find out the actual neurobiological mechanism and precise role of these areas in behavioural inhibition. Although we provided an interplay between brain regions for inhibitory control using a behavioural and *in vivo* electrophysiological approach, advanced cell-type specific techniques, functional brain mapping and pharmacological approaches could be used to measure and manipulate the neural activity to better understand the neural circuitry. Unfortunately our pilot experiments (Chapter 2, section 2.1) indicated significant technical problems with appropriate stimulation of STN for testing its theta-frequency involvement in the SST.

Importantly, action inhibition is supported by cortico-fronto-basal ganglia-thalamic circuitry and behavioural inhibition by the interaction between OFC and HPC with this circuitry. The cortico-basal ganglia circuitry, particularly STN, appears to be an important and a common node in both action inhibition and behavioural inhibition. Critically, understanding the neurobiological basis of action and behavioural inhibition will allow researchers to examine the important neural structures and its sub component involved in various inhibition related disorders including impulsivity, ADHD, depression, anxiety etc. LFP and behavioural measures of action inhibition and goal inhibition could be used as a marker of treatment use. The current findings from our study may help us to broaden our understanding of neural mechanisms for processing of inhibitory control, in particular, complex behavioural inhibition in the brain. Future research could be carried out considering the detailed interaction between these systems and its sub components to isolate the parallel neurobiology of inhibitory control.

7.6 Final remarks

The current results from the different experiments suggests that BG (particularly STR and STN), OFC and HPC interact dynamically during learning, activation of approach, activation of avoidance (action inhibition) and in goal-conflict situations. As I discussed in detail in Chapter 1, different types of inhibition exist and engage distinct areas of frontal cortex, including OFC. The neural network involved in different forms of inhibition differ accordingly. My aim was to examine how simple inhibitory control (simple avoidance related) differed from complex behavioural inhibition (goal-conflict related). To answer this question, first I assessed the brain areas that have been implicated for simple learning and simple stopping, for instance frontocortico-BG circuitry. In addition to this circuitry, I also included the HPC to see if it modulates simple avoidance. Then, I studied similar areas to differentiate the simple inhibition from complex behavioural inhibition.

I showed that limbic structures, especially HPC, while not functionally involved in simple motor learning, may receive sensory and motor information form STR and OFC. In the context of simple stopping, contextual information for performing the task may be detected by HPC. That means goal relevant information is provided to HPC and this information is available for upcoming demands. However, the functional role of HPC depends on the type of goal information it receives. Simple avoidance focuses on a network connecting cortex with BG, which mediates inhibitory control of both action and goals; while, during complex inhibition, HPC detects goal-conflicts between concurrently activated goals for goal inhibition. However, goal inhibition needs access to circuits involved in simple stopping as its first step is to block prepotent action. This suggest that HPC output could couple to recursive networks that link to cortico-basal ganglia-thalamocortical loops through OFC.

I demonstrated that goal-conflict activates OFC and STN in addition to the HPC during high conflict situation. A previous study in humans from our lab reported goal-conflict specific theta activation at rIFG could be a conflict detector. Interestingly, we now report goal conflict theta activation in OFC (rodents OFC is considered to be homologues to rIFC in human). Additionally, we also found HPC-STN coherence at lower theta frequencies (5-8 Hz) during goal-conflict activation. This represents a separate pathway how the output from complex goal inhibition (HPC) could be relayed into action stopping circuitry during goal conflict resolution. The findings also showed that the rat brain can be activated like the human brain during goal-conflict. The current findings raise the possibility that, in addition to HPC, both OFC and STN could be important modules in the circuits mediating complex behavioural inhibition. These functional connections (limbic and BG) provides an adaptive control, such as selection of goal (limbic structures) and a motor program to execute that action (BG).

References

Abela, A. R., Dougherty, S. D., Fagen, E. D., Hill, C. J., & Chudasama, Y. (2013). Inhibitory control deficits in rats with ventral hippocampal lesions. *Cerebral Cortex, 23*(6), 1396-1409. doi:10.1093/cercor/bhs121

Adcock, R. A., Thangavel, A., Whitfield-Gabrieli, S., Knutson, B., & Gabrieli, J. D. (2006). Reward-motivated learning: mesolimbic activation precedes memory formation. *Neuron, 50*(3), 507-517. doi:10.1016/j.neuron.2006.03.036

Albin, R. L., Young, A. B., & Penney, J. B. (1989). The functional anatomy of basal ganglia disorders. *Trends in Neurosciences, 12*(10), 366-375. doi:10.1016/0166-2236(89)90074-X

Albouy, G., Sterpenich, V., Balteau, E., Vandewalle, G., Desseilles, M., Dang-Vu, T., . . . Maquet, P. (2008). Both the hippocampus and striatum are involved in consolidation of motor sequence memory. *Neuron, 58*(2), 261-272. doi:10.1016/j.neuron.2008.02.008

Albouy, G., Sterpenich, V., Vandewalle, G., Darsaud, A., Gais, S., Rauchs, G., . . . Maquet, P. (2013). Interaction between hippocampal and striatal systems predicts subsequent consolidation of motor sequence memory. *Plos One, 8*(3), e59490. doi:10.1371/journal.pone.0059490

Aron, A. R. (2011). From reactive to proactive and selective control: Developing a richer model for stopping inappropriate responses. *Biological Psychiatry, 69*(12), E55-E68. doi:10.1016/j.biopsych.2010.07.024

Aron, A. R., Durston, S., Eagle, D. M., Logan, G. D., Stinear, C. M., & Stuphorn, V. (2007). Converging evidence for a fronto-basal-ganglia network for inhibitory control of action and cognition. *The Journal of Neuroscience, 27*(44), 11860-11864. doi:10.1523/JNEUROSCI.3644-07.2007

Aron, A. R., & Poldrack, R. A. (2006). Cortical and subcortical contributions to Stop signal response inhibition: role of the subthalamic nucleus. *The Journal of Neuroscience, 26*(9), 2424-2433. doi:10.1523/JNEUROSCI.4682-05.2006

Aron, A. R., Robbins, T. W., & Poldrack, R. A. (2004). Inhibition and the right inferior frontal cortex. *Trends in cognitive sciences, 8*(4), 170-177. doi:10.1016/j.tics.2004.02.010

Ashby, F. G., Turner, B. O., & Horvitz, J. C. (2010). Cortical and basal ganglia contributions to habit learning and automaticity. *Trends in cognitive sciences, 14*(5), 208-215. doi:10.1016/j.tics.2010.02.001

Baldo, B. A., Pratt, W. E., Will, M. J., Hanlon, E. C., Bakshi, V. P., & Cador, M. (2013). Principles of motivation revealed by the diverse functions of neuropharmacological and neuroanatomical substrates underlying feeding behavior. *Neuroscience & Biobehavioral Reviews, 37*(9 Pt A), 1985-1998. doi:10.1016/j.neubiorev.2013.02.017

Balleine, B. W., Delgado, M. R., & Hikosaka, O. (2007). The role of the dorsal striatum in reward and decision-making. *The Journal of Neuroscience, 27*(31), 8161-8165. doi:10.1523/JNEUROSCI.1554-07.2007

Band, G. P. H., & van Boxtel, G. J. M. (1999). Inhibitory motor control in stop paradigms: review and reinterpretation of neural mechanisms. *Acta Psychologica, 101*(2–3), 179-211. doi:10.1016/S0001-6918(99)00005-0

Barbas, H., & Blatt, G. J. (1995). Topographically specific hippocampal projections target functionally distinct prefrontal areas in the rhesus monkey. *Hippocampus, 5*, 511-533. doi:10.1002/hipo.450050604

Bari, A., & Robbins, T. W. (2013). Inhibition and impulsivity: behavioral and neural basis of response control. *Progress in Neurobiology, 108*, 44-79. doi:10.1016/j.pneurobio.2013.06.005

Battaglia, F. P., Benchenane, K., Sirota, A., Pennartz, C. M., & Wiener, S. I. (2011). The hippocampus: hub of brain network communication for memory. *Trends in cognitive sciences, 15*(7), 310-318. doi:10.1016/j.tics.2011.05.008

Baufreton, J., Atherton, J. F., Surmeier, D. J., & Bevan, M. D. (2005). Enhancement of excitatory synaptic integration by GABAergic inhibition in the subthalamic nucleus. *The Journal of Neuroscience, 25*(37), 8505-8517. doi:10.1523/JNEUROSCI.1163-05.2005

Benchenane, K., Peyrache, A., Khamassi, M., Tierney, P. L., Gioanni, Y., Battaglia, F. P., & Wiener, S. I. (2010). Coherent theta oscillations and reorganization of spike timing in the hippocampal- prefrontal network upon learning. *Neuron, 66*(6), 921-936. doi:10.1016/j.neuron.2010.05.013

Bergstrom, H. C., Lipkin, A. M., Lieberman, A. G., Pinard, C. R., Gunduz-Cinar, O., Brockway, E. T., . . . Holmes, A. (2018). Dorsolateral striatum engagement interferes with early discrimination learning. *Cell Reports, 23*(8), 2264-2272. doi:10.1016/j.celrep.2018.04.081

Berke, J. D., Okatan, M., Skurski, J., & Eichenbaum, H. B. (2004). Oscillatory entrainment of striatal neurons in freely moving rats. *Neuron, 43*(6), 883-896. doi:10.1016/j.neuron.2004.08.035

Bird, C. M., & Burgess, N. (2008). The hippocampus and memory: insights from spatial processing. *Nature reviews neuroscience, 9*(3), 182-194. doi:10.1038/nrn2335

Birrell, J. M. , & Brown, V. J. (2000). Medial frontal cortex mediates perceptual attentional set shifting in the rat. *The Journal of Neuroscience, 20*(11), 4320-4324. doi:10.1523/JNEUROSCI.20-11-04320.2000

Blair, R. J. (2007). Dysfunctions of medial and lateral orbitofrontal cortex in psychopathy. *Annals of the New York Academy of Sciences, 1121*, 461-479. doi:10.1196/annals.1401.017

Boschin, E. A., Brkic, M. M., Simons, J. S., & Buckley, M. J. (2017). Distinct roles for the anterior cingulate and dorsolateral prefrontal cortices during conflict between abstract rules. *Cerebral Cortex, 27*(1), 34-45. doi:10.1093/cercor/bhw350

Botvinick, M. M., Cohen, J. D., & Carter, C. S. (2004). Conflict monitoring and anterior cingulate cortex: an update. *Trends in cognitive sciences, 8*(12), 539-546. doi:10.1016/j.tics.2004.10.003

Boucher, L., Palmeri, T. J., Logan, G. D., & Schall, J. D. (2007). Inhibitory control in mind and brain: an interactive race model of countermanding saccades. *Psychological Review, 114*(2), 376-397. doi:10.1037/0033-295X.114.2.376

Brian, B. H. (1986). The physiology and pharmacology of hippocampal formation theta rhythms *Progress in Neurobiology, 26*, 1-54. doi:10.1016/0301-0082(86)90019-5

Brittain, J. S., Watkins, K. E., Joundi, R. A., Ray, N. J., Holland, P., Green, A. L., . . . Jenkinson, N. (2012). A role for the subthalamic nucleus in response inhibition during conflict. *The Journal of Neuroscience, 32*(39), 13396-13401. doi:10.1523/JNEUROSCI.2259-12.2012

Brown, T. I., Ross, R. S., Tobyne, S. M., & Stern, C. E. (2012). Cooperative interactions between hippocampal and striatal systems support flexible navigation. *Neuroimage, 60*(2), 1316-1330. doi:10.1016/j.neuroimage.2012.01.046

Bryden, D. W., & Roesch, M. R. (2015). Executive control signals in orbitofrontal cortex during response inhibition. *The Journal of Neuroscience, 35*(9), 3903-3914. doi:10.1523/JNEUROSCI.3587-14.2015

Burgess, N., & O'Keefe, J. (2011). Models of place and grid cell firing and theta rhythmicity. *Current Opinion in Neurobiology, 21*(5), 734-744. doi:10.1016/j.conb.2011.07.002

Buschman, T. J., & Miller, E. K. (2014). Goal-direction and top-down control. *Philosophical Transactions of The Royal Society B Biological Sciences, 369*(1655). doi:10.1098/rstb.2013.0471

Buzsáki, G. (2002). Theta Oscillations in the Hippocampus. *Neuron, 33*, 325–340. doi:10.1016/S0896-6273(02)00586-X

Buzsaki, G., Anastassiou, C. A., & Koch, C. (2012). The origin of extracellular fields and currents--EEG, ECoG, LFP and spikes. *Nature reviews neuroscience, 13*(6), 407-420. doi:10.1038/nrn3241

Buzsáki, G., & Watson, B. O. (2012). Brain rhythms and neural syntax: implications for efficient coding of cognitive content and neuropsychiatric disease. *Dialogues in Clinical Neuroscience, 14*(4), 345-367.

Cannon, J., McCarthy, M. M., Lee, S., Lee, J., Borgers, C., Whittington, M. A., & Kopell, N. (2014). Neurosystems: brain rhythms and cognitive processing. *European Journal of Neuroscience, 39*(5), 705-719. doi:10.1111/ejn.12453

Cavada, Carmen, Company, Teresa, Tejedor, Jaime, Cruz-Rizzolo, Roelf J., & Reinoso-Suarez, Fernando. (2000). The anatomical connections of the macaque monkey orbitofrontal cortex. A review. *Cerebral Cortex, 10*(3), 220-242. doi:10.1093/cercor/10.3.220

Cavanagh, J. F., Wiecki, T. V., Cohen, M. X., Figueroa, C. M., Samanta, J., Sherman, S. J., & Frank, M. J. (2011). Subthalamic nucleus stimulation reverses mediofrontal influence over decision threshold. *Nature Neuroscience, 14*(11), 1462-1467. doi:10.1038/nn.2925

Cenquizca, L, A., & Swanson, L, W. (2007). Spatial organization of direct hippocampal field CA1 axonal projections to the rest of the Cerebral Cortex. *Brain Research Reviews, 56*(1), 1-26. doi:10.1016/j.brainresrev.2007.05.002

Chambers, C. D., Garavan, H., & Bellgrove, M. A. (2009). Insights into the neural basis of response inhibition from cognitive and clinical neuroscience. *Neuroscience and Biobehavioral Reviews, 33*, 631-646. doi:10.1016/j.neubiorev.2008.08.016

Cherubini, E., & Miles, R. (2015). The CA3 region of the hippocampus: how is it? What is it for? How does it do it? *Frontiers in Cellular Neuroscience, 9*, 19. doi:10.3389/fncel.2015.00019

Chudasama, Y., Doobay, V. M., & Liu, Y. (2012). Hippocampal-prefrontal cortical circuit mediates inhibitory response control in the rat. *The Journal of Neuroscience, 32*(32), 10915-10924. doi:10.1523/JNEUROSCI.1463-12.2012

Chun, M. M., & Phelps, E. A. (1999). Memory deficits for implicit contextual inofrmation in amnesic subjects with hippocampal damage. *Nature Neuroscience, 2*(9), 844-847. doi:10.1038/12222

Critchley, H. D., Mathias, C. J., & Dolan, R. J. (2001). Neural activity in the human brain relating to uncertainty and arousal during anticipation. *Neuron, 29*, 537–545. doi:10.1016/S0896-6273(01)00225-2

Dalley, J. W., & Roiser, J. P. (2012). Dopamine, serotonin and impulsivity. *Neuroscience, 215*, 42-58. doi:10.1016/j.neuroscience.2012.03.065

Davidson, T. L., & Jarrard, L. E. (2004). The hippocampus and inhibitory learning: a 'Gray' area? *Neuroscience & Biobehavioral Reviews, 28*(3), 261-271. doi:10.1016/j.neubiorev.2004.02.001

Day, N. F., & Nick, T. A. (2013). Rhythmic cortical neurons increase their oscillations and sculpt basal ganglia signaling during motor learning. *Developmental Neurobiology, 73*(10), 754-768. doi:10.1002/dneu.22098

Dayan, P., & Balleine, B. W. (2002). Reward, motivation and reinforcement learning. *Neuron, 35*, 285-298. doi:10.1016/S0896-6273(02)00963-7

DeCoteau, W. E., Thorn, C., Gibson, D. J., Courtemanche, R., Mitra, P., Kubota, Y., & Graybiel, A. M. (2007a). Learning-related coordination of striatal and hippocampal theta rhythms during acquisition of a procedural maze task. *Proceedings of the National Academy of Sciences of the United States of America, 104*(13), 5644-5649. doi:10.1073/pnas.0700818104

DeCoteau, W. E., Thorn, C., Gibson, D. J., Courtemanche, R., Mitra, P., Kubota, Y., & Graybiel, A. M. (2007b). Oscillations of local field potentials in the rat dorsal striatum during spontaneous and instructed behaviors. *Journal of Neurophysiology, 97*(5), 3800-3805. doi:10.1152/jn.00108.2007

DeLong, N. D., Kirby, M. S., Blitz, D. M., & Nusbaum, M. P. (2009). Parallel regulation of a modulator-activated current via distinct dynamics underlies comodulation of motor circuit output. *The Journal of Neuroscience, 29*(39), 12355-12367. doi:10.1523/JNEUROSCI.3079-09.2009

Devan, B. D., Hong, N. S., & McDonald, R. J. (2011). Parallel associative processing in the dorsal striatum: segregation of stimulus-response and cognitive control subregions. *Neurobiology of Learning and Memory, 96*(2), 95-120. doi:10.1016/j.nlm.2011.06.002

Dillon, D. F., & Pizzagalli, D. A. (2007). Inhibition of action, thought, and emotion: A selective neurobiological review. *Applied & Preventive Psychology, 12*(3), 99-114. doi:10.1016/j.appsy.2007.09.004

Duzel, E., Penny, W. D., & Burgess, N. (2010). Brain oscillations and memory. *Current Opinion in Neurobiology, 20*(2), 143-149. doi:10.1016/j.conb.2010.01.004

Eagle, D. M., & Baunez, C. (2010). Is there an inhibitory-response-control system in the rat? Evidence from anatomical and pharmacological studies of behavioral inhibition. *Neuroscience & Biobehavioral Reviews, 34*(1), 50-72. doi:10.1016/j.neubiorev.2009.07.003

Eagle, D. M., Baunez, C., Hutcheson, D. M., Lehmann, O., Shah, A. P., & Robbins, T. W. (2008). Stop-signal reaction-time task performance: role of prefrontal cortex and subthalamic nucleus. *Cerebral Cortex, 18*(1), 178-188. doi:10.1093/cercor/bhm044

Eagle, D. M., & Robbins, T. W. (2003a). Inhibitory control in rats performing a stop-signal reaction-time task: effects of lesions of the medial striatum and d-amphetamine. *Behavioral Neuroscience, 117*(6), 1302-1317. doi:10.1037/0735-7044.117.6.1302

Eagle, D. M., & Robbins, T. W. (2003b). Lesions of the medial prefrontal cortex or nucleus accumbens core do not impair inhibitory control in rats performing a stop-signal reaction time task. *Behavioural Brain Research, 146*(1-2), 131-144. doi:10.1016/j.bbr.2003.09.022

Ekstrom, A. D., & Watrous, A. J. (2014). Multifaceted roles for low-frequency oscillations in bottom-up and top-down processing during navigation and memory. *Neuroimage, 85 Pt 2*, 667-677. doi:10.1016/j.neuroimage.2013.06.049

Elliott, R., Dolan, R. J., & Frith, C. D. (2000). Dissociable Functions in the Medial and Lateral Orbitofrontal Cortex: Evidence from Human Neuroimaging Studies. *Cerebral Cortex, 10*, 308-317.

Emmons, E. B., Ruggiero, R. N., Kelley, R. M., Parker, K. L., & Narayanan, N. S. (2016). Corticostriatal field potentials are modulated at delta and theta frequencies during

Interval-timing task in rodents. *Behavioural Brain Research, 7*, 459. doi:10.3389/fpsyg.2016.00459

Erika-Florence, M., Leech, R., & Hampshire, A. (2014). A functional network perspective on response inhibition and attentional control. *Nature Communications, 5*, 4073. doi:10.1038/ncomms5073

Fauth-Buhler, M., de Rover, M., Rubia, K., Garavan, H., Abbott, S., Clark, L., . . . Robbins, T. W. (2012). Brain networks subserving fixed versus performance-adjusted delay stop trials in a stop signal task. *Behavioural Brain Research, 235*(1), 89-97. doi:10.1016/j.bbr.2012.07.023

Featherstone, R. E., & McDonald, R. J. (2004). Dorsal striatum and stimulus-response learning: lesions of the dorsolateral, but not dorsomedial, striatum impair acquisition of a stimulus-response-based instrumental discrimination task, while sparing conditioned place preference learning. *Neuroscience, 124*(1), 23-31. doi:10.1016/j.neuroscience.2003.10.038

Feingold, J., Gibson, D. J., DePasquale, B., & Graybiel, A. M. (2015). Bursts of beta oscillation differentiate postperformance activity in the striatum and motor cortex of monkeys performing movement tasks. *Proceedings of the National Academy of Sciences of the United States of America, 112*(44), 13687-13692. doi:10.1073/pnas.1517629112

Fernandes, M. A., Moscovitch, M., Ziegler, M., & Grady, C. (2005). Brain regions associated with successful and unsuccessful retrieval of verbal episodic memory as revealed by divided attention. *Neuropsychologia, 43*(8), 1115-1127. doi:10.1016/j.neuropsychologia.2004.11.026

Fife, K. H., Gutierrez-Reed, N. A., Zell, V., Bailly, J., Lewis, C. M., Aron, A. R., & Hnasko, T. S. (2017). Causal role for the subthalamic nucleus in interrupting behavior. *Elife, 6*. doi:10.7554/eLife.27689

Fischer, P., Pogosyan, A., Herz, D. M., Cheeran, B., Green, A. L., Fitzgerald, J., . . . Tan, H. (2017). Subthalamic nucleus gamma activity increases not only during movement but also during movement inhibition. *Elife, 6*. doi:10.7554/eLife.23947

Floden, D., & Stuss, D.T. (2006). Inhibitory control is slowed in patients with right superior medial frontal damage. *Journal of cognitive Neuroscience, 18*(11), 1843-1849. doi:10.1162/jocn.2006.18.11.1843

Flynt, J. (2017). Polylactic Acid (PLA): The Environment-friendly Plastic. Retrieved from http://3dinsider.com/what-is-pla/

Fox, C., Humphries, M., Mitchinson, B., Kiss, T., Somogyvari, Z., & Prescott, T. (2009). Technical integration of hippocampus, Basal Ganglia and physical models for spatial navigation. *Frontiers in Neuroinformatics, 3*, 6. doi:10.3389/neuro.11.006.2009

Frank, M. J. (2006). Hold your horses: a dynamic computational role for the subthalamic nucleus in decision making. *Neural Networks, 19*(8), 1120-1136. doi:10.1016/j.neunet.2006.03.006

Friese, U., Daume, J., Goschl, F., Konig, P., Wang, P., & Engel, A. K. (2016). Oscillatory brain activity during multisensory attention reflects activation, disinhibition, and cognitive control. *Scientific Reports, 6*, 32775. doi:10.1038/srep32775

Fujisawa, S., & Buzsaki, G. (2011). A 4 Hz oscillation adaptively synchronizes prefrontal, VTA, and hippocampal activities. *Neuron, 72*(1), 153-165. doi:10.1016/j.neuron.2011.08.018

Fumagalli, M., Giannicola, G., Rosa, M., Marceglia, S., Lucchiari, C., Mrakic-Sposta, S., . . . Priori, A. (2011). Conflict-dependent dynamic of subthalamic nucleus oscillations during moral decisions. *Social Neuroscience, 6*(3), 243-256. doi:10.1080/17470919.2010.515148

Furtak, S. C., Cho, C. E., Kerr, K. M., Barredo, J. L., Alleyne, J. E., Patterson, Y. R., & Burwell, R. D. (2009). The Floor Projection Maze: A novel behavioral apparatus for presenting visual stimuli to rats. *The Journal of Neuroscience Methods, 181*(1), 82-88. doi:10.1016/j.jneumeth.2009.04.023

Fuster, J. M. (2001). The Prefrontal Cortex—An update: time is of the essence. *Neuron, 30*, 319-333. doi:10.1016/S0896-6273(01)00285-9

Galvan, A., Kuwajima, M., & Smith, Y. (2006). Glutamate and GABA receptors and transporters in the basal ganglia: What does their subsynaptic localization reveal about their function? *Neuroscience, 143*(2), 351-375. doi:10.1016/j.neuroscience.2006.09.019

Gauggel, S., Rieger, M., & Feghoff, T-A. (2004). Inhibition of ongoing responses in patients with Parkinson's disease. *Journal of Neurology, Neurosurgery and Psychiatry, 75*, 539-544.

Gengler, S., Mallot, H. A., & Holscher, C. (2005). Inactivation of the rat dorsal striatum impairs performance in spatial tasks and alters hippocampal theta in the freely moving rat. *Behavioural Brain Research, 164*(1), 73-82. doi:10.1016/j.bbr.2005.06.009

Gould, T. D., Rowe, W. B., Heman, K. L., Mesches, M. H., Young, D. A., Rose, G. M., & Bickford, P.C. (2002). Effects of hippocampal lesions on patterned motor learning in the rat. *Brain Research Bulletin, 58*(6), 581-586. doi:10.1016/S0361-9230(02)00832-8

Goutagny, R., Jackson, J., & Williams, S. (2009). Self-generated theta oscillations in the hippocampus. *Nature Neuroscience, 12*(12), 1491-1493. doi:10.1038/nn.2440

Gray, J. A. (1982). Précis of The neuropsychology of anxiety: An enquiry into the functions of the septo-hippocampal system. *Behavioral and Brain Sciences, 5*, 469-534. doi:10.1017/s0140525x00013066

Gray, J. A. (1987). Perspective on anxiety and impulsivity: A commentary. *Journal of Research in Personality, 21*, 493-509. doi:10.1016/0092-6566(87)90036-5

Gray, J. A., & McNaughton, N. (1983). Comparison between the behavioural effets of septal and hippocampal lesions: A review. *Neuroscience & Biobehavioral Reviews, 7*, 119-188. doi:10.1016/0149-7634(83)90014-3

Gray, J. A., & McNaughton, N. (2000). *The Neuropsychology of Anxiety* (second ed.). New York: Oxford University Press.

Graybiel, A. M., & Grafton, S. T. (2015). The striatum: where skills and habits meet. *Cold Spring Harbor Perspectives in Biology, 7*(8), a021691. doi:10.1101/cshperspect.a021691

Gu, B. M., Kukreja, K., & Meck, W. H. (2018). Oscillation patterns of local field potentials in the dorsal striatum and sensorimotor cortex during the encoding, maintenance, and decision stages for the ordinal comparison of sub- and supra-second signal durations. *Neurobiology of Learning and Memory*. doi:10.1016/j.nlm.2018.05.003

Guridi, J., & Obeso, J. A. (2001). The subthalamic nucleus, hemiballismus and Parkinson's disease: reappraisal of a neurosurgical dogma. *Brain, 124*, 5-19.

Haber, S. N. (2003). The primate basal ganglia: parallel and integrative networks. *Journal of Chemical Neuroanatomy, 26*(4), 317-330. doi:10.1016/j.jchemneu.2003.10.003

Haber, S. N., & Calzavara, R. (2009). The cortico-basal ganglia integrative network: the role of the thalamus. *Brain Research Bulletin, 78*(2-3), 69-74. doi:10.1016/j.brainresbull.2008.09.013

Haegelen, C., Rouaud, T., Darnault, P., & Morandi, X. (2009). The subthalamic nucleus is a key-structure of limbic basal ganglia functions. *Medical Hypotheses, 72*, 421-426. doi:10.1016/j.mehy.2008.07.065

Hangya, B., Borhegyi, Z., Szilagyi, N., Freund, T. F., & Varga, V. (2009). GABAergic neurons of the medial septum lead the hippocampal network during theta activity. *The Journal of Neuroscience, 29*(25), 8094-8102. doi:10.1523/JNEUROSCI.5665-08.2009

Harlow, J. M. (1993). Recovery from the passage of an iron bar through the head. *History of Psychiatry, 4*(14), 274-281. doi:10.1177/0957154x9300401407

Harper, J., Malone, S. M., Bachman, M. D., & Bernat, E. M. (2016). Stimulus sequence context differentially modulates inhibition-related theta and delta band activity in a go/no-go task. *Psychophysiology, 53*(5), 712-722. doi:10.1111/psyp.12604

Hasselmo, M. E., & Eichenbaum, H. (2005). Hippocampal mechanisms for the context-dependent retrieval of episodes. *Neural Networks, 18*(9), 1172-1190. doi:10.1016/j.neunet.2005.08.007

Hilario, M., Holloway, T., Jin, X., & Costa, R. M. (2012). Different dorsal striatum circuits mediate action discrimination and action generalization. *European Journal of Neuroscience, 35*(7), 1105-1114. doi:10.1111/j.1460-9568.2012.08073.x

Hollerman, J. R., Tremblay, L., & Schultz, W. (2000). Involvement of basal ganglia and orbitofrontal cortex in goal-directed behavior. *Progress in Brain Research, 126*, 193-215. doi:10.1016/S0079-6123(00)26015-9

Holsheimer, J. (1982). Generation of theta activity (RSA) in the Cingulate Cortex of the rat. *Experimental brain research, 47*, 309-312. doi:10.1007/BF00239391

Howe, M. W., Atallah, H. E., McCool, A., Gibson, D. J., & Graybiel, A. M. (2011). Habit learning is associated with major shifts in frequencies of oscillatory activity and synchronized spike firing in striatum. *Proceedings of the National Academy of Sciences of the United States of America, 108*(40), 16801-16806. doi:10.1073/pnas.1113158108

Humphries, M. D., & Prescott, T. J. (2010). The ventral basal ganglia, a selection mechanism at the crossroads of space, strategy, and reward. *Progress in Neurobiology, 90*(4), 385-417. doi:10.1016/j.pneurobio.2009.11.003

Hyman, J. M., Zilli, E. A., Paley, A. M., & Hasselmo, M. E. (2010). Working memory performance correlates with prefrontal-hippocampal theta interactions but not with prefrontal neuron firing rates. *Frontiers in Integrative Neuroscience, 4*, 2. doi:10.3389/neuro.07.002.2010

Immordino-Yang, M. H., & Singh, V. (2013). Hippocampal contributions to the processing of social emotions. *Human Brain Mapping, 34*(4), 945-955. doi:10.1002/hbm.21485

Insausti, R., Marcos, M. P., Mohedano-Moriano, A., Arroyo-Jiménez, M. M., Córcoles-Parada, M., Artacho-Pérula, E., . . . Muñoz-López, M. (2017). The Nonhuman Primate Hippocampus: Neuroanatomy and Patterns of Cortical Connectivity. In Deborah E. Hannula & Melissa C. Duff (Eds.), *The Hippocampus from Cells to Systems: Structure, Connectivity, and Functional Contributions to Memory and Flexible Cognition* (pp. 3-36). Cham: Springer International Publishing.

Ishikawa, A., & Nakamura, S. (2003). Convergence and Interaction of Hippocampal and Amygdalar Projections within the Prefrontal Cortex in the Rat. *The Journal of Neuroscience, 23*(31), 9987-9995. doi:10.1523/JNEUROSCI.23-31-09987.2003

Isoda, M., & Hikosaka, O. (2008). Role for subthalamic nucleus neurons in switching from automatic to controlled eye movement. *The Journal of Neuroscience, 28*(28), 7209-7218. doi:10.1523/JNEUROSCI.0487-08.2008

Ito, R., & Lee, A. C. (2016). The role of the hippocampus in approach-avoidance conflict decision-making: Evidence from rodent and human studies. *Behavioural Brain Research, 313*, 345-357. doi:10.1016/j.bbr.2016.07.039

Jacinto, Luis R., Cerqueira, João J., & Sousa, Nuno. (2016). Patterns of theta activity in limbic anxiety circuit preceding exploratory behavior in approach-avoidance conflict. *Frontiers in Behavioral Neuroscience, 10*. doi:10.3389/fnbeh.2016.00171

Jacobs, J. (2014). Hippocampal theta oscillations are slower in humans than in rodents: implications for models of spatial navigation and memory. *Philosophical Transactions of The Royal Society B Biological Sciences, 369*(1635), 20130304. doi:10.1098/rstb.2013.0304

Jacobson, T. K., Gruenbaum, B. F., & Markus, E. J. (2012). Extensive training and hippocampus or striatum lesions: effect on place and response strategies. *Physiology & Behavior, 105*(3), 645-652. doi:10.1016/j.physbeh.2011.09.027

Jahanshahi, M., Obeso, I., Rothwell, J. C., & Obeso, J. A. (2015). A fronto-striato-subthalamic-pallidal network for goal-directed and habitual inhibition. *Nature reviews neuroscience, 16*(12), 719-732. doi:10.1038/nrn4038

James, W. . (1890). *The principles of psychology* (Vol. II). New York: Henry Holt.

Jarrard, L. E. (1993). On the role of the hippocampus in learning and memory in the rat *Behavioral and Neural Biology, 60*, 9-26. doi:10.1016/0163-1047(93)90664-4

Jentsch, J. D., & Taylor, J. R. (1999). Impulsivity resulting from frontostriatal dysfunction in drug abuse: implications for the control of behavior by reward-related stimuli. *Psychopharmacology (Berl), 146*(4), 373-390.

Jin, J., & Maren, S. (2015). Prefrontal-hippocampal interactions in memory and emotion. *Frontiers in Systems Neuroscience, 9*, 170. doi:10.3389/fnsys.2015.00170

Jones, M. W., & Wilson, M. A. (2005a). Phase precession of medial prefrontal cortical activity relative to the hippocampal theta rhythm. *Hippocampus, 15*(7), 867-873. doi:10.1002/hipo.20119

Jones, M. W., & Wilson, M. A. (2005b). Theta rhythms coordinate hippocampal-prefrontal interactions in a spatial memory task. *PLoS Biology, 3*(12), e402. doi:10.1371/journal.pbio.0030402

Kahana, M. J. (2006). The cognitive correlates of human brain oscillations. *The Journal of Neuroscience, 26*(6), 1669-1672. doi:10.1523/JNEUROSCI.3737-05c.2006

Kalivas, P. W., & Volkow, N. D. (2005). The neural basis of addiction: A pathology of motivation and choice. *American Journal of Psychiatry, 162*, 1403-1413. doi:10.1176/appi.ajp.162.8.1403

Kaplan, R., Doeller, C. F., Barnes, G. R., Litvak, V., Duzel, E., Bandettini, P. A., & Burgess, N. (2012). Movement-related theta rhythm in humans: coordinating self-directed hippocampal learning. *PLoS Biol, 10*(2), e1001267. doi:10.1371/journal.pbio.1001267

Kay, K., Sosa, M., Chung, J. E., Karlsson, M. P., Larkin, M. C., & Frank, L. M. (2016). A hippocampal network for spatial coding during immobility and sleep. *Nature, 531*(7593), 185-190. doi:10.1038/nature17144

Kim, H., Shimojo, S., & O'Doherty, J. P. (2006). Is avoiding an aversive outcome rewarding? Neural substrates of avoidance learning in the human brain. *PLoS Biol, 4*(8), e233. doi:10.1371/journal.pbio.0040233

Kirk, I.J. , & McNaughton, N. (1991). Supramammillary cell firing and hippocampal rhythmical slow activity. *Neuroreport, 2*(11), 723-725.

Knyazev, G. G., Levin, E. A., & Savostyanov, A. N. (2008). Impulsivity, anxiety, and individual differences in evoked and induced brain oscillations. *International Journal of Psychophysiology, 68*(3), 242-254. doi:10.1016/j.ijpsycho.2008.02.010

Kramis, R., Vanderwolf, C. H., & Bland, B. H. (1975). Two types of hippocampal rhythmical slow activity in both the rabbit and the rat: relations to behaviour and effects of atropine,

diethy ether, yrethane and pentobarbitol. *Experimental Neurology, 49*, 58-85. doi:10.1016/0014-4886(75)90195-8

Kringelbach, M. L. (2005). The human orbitofrontal cortex: linking reward to hedonic experience. *Nature reviews neuroscience, 6*(9), 691-702. doi:10.1038/nrn1747

Kuhn, A., D., Williams., Kupsch, A., Limousin, P., Hariz, M., Schneider, G. H., . . . Brown, P. (2004). Event-related beta desynchronization in human subthalamic nucleus correlates with motor performance. *Brain, 127*, 735-746. doi:10.1093/brain/awh106

Lanciego, J. L., Luquin, N., & Obeso, J. A. (2012). Functional neuroanatomy of the basal ganglia. *Cold Spring Harbor Perspectives in Medicine, 2*(12), a009621. doi:10.1101/cshperspect.a009621

Lansink, C. S., Meijer, G. T., Lankelma, J. V., Vinck, M. A., Jackson, J. C., & Pennartz, C. M. (2016). Reward expectancy strengthens CA1 theta and beta band synchronization and hippocampal-ventral striatal coupling. *The Journal of Neuroscience, 36*(41), 10598-10610. doi:10.1523/JNEUROSCI.0682-16.2016

Lavallee, C. F., Meemken, M. T., Herrmann, C. S., & Huster, R. J. (2014). When holding your horses meets the deer in the headlights: time-frequency characteristics of global and selective stopping under conditions of proactive and reactive control. *Frontiers in Human Neuroscience, 8*, 994. doi:10.3389/fnhum.2014.00994

Lee, I., & Byeon, J. S. (2014). Learning-dependent changes in the neuronal correlates of response inhibition in the prefrontal cortex and hippocampus. *Experimental Neurobiology, 23*(2), 178-189. doi:10.5607/en.2014.23.2.178

Leisman, G., Braun-Benjamin, O., & Melillo, R. (2014). Cognitive-motor interactions of the basal ganglia in development. *Frontiers in Systems Neuroscience, 8*, 16. doi:10.3389/fnsys.2014.00016

Leung, L. W. S., & Borst, J. G. G. (1987). Electrical activity of the cingulate cortex. I. Generating mechanisms and relations to behavior. *Brain Research, 407*(1), 68-80. doi:10.1016/0006-8993(87)91220-0

Leventhal, D. K., Gage, G. J., Schmidt, R., Pettibone, J. R., Case, A. C., & Berke, J. D. (2012). Basal ganglia beta oscillations accompany cue utilization. *Neuron, 73*(3), 523-536. doi:10.1016/j.neuron.2011.11.032

Liljeholm, M., & O'Doherty, J. P. (2012). Contributions of the striatum to learning, motivation, and performance: an associative account. *Trends in cognitive sciences, 16*(9), 467-475. doi:10.1016/j.tics.2012.07.007

Logan, G. D., Cowan, W. B., & Davis, K. A. (1984). On the ability to inhibit simple and choice reaction time responses: a model and a method. *Journal of Experimental Psychology: Human Perception and Performance, 10*(2), 276-291. doi:10.1037/0096-1523.10.2.276

Logan, G. D., Van Zandt, T., Verbruggen, F., & Wagenmakers, E. J. (1984). On the ability to inhibit thought and action: general and special theories of an act of control. *Psychological Review, 121*(3), 295-327. doi:10.1037/a0035230

Luks, T. L., Simpson, G. V., Dale, C. L., & Hough, M. G. (2007). Preparatory allocation of attention and adjustments in conflict processing. *Neuroimage, 35*(2), 949-958. doi:10.1016/j.neuroimage.2006.11.041

Mallet, L., Schupbach, M., N'Diaye, K., Remy, P., Bardinet, E., Czernecki, V., . . . Yelnik, J. (2007). Stimulation of subterritories of the subthalamic nucleus reveals its role in the integration of the emotional and motor aspects of behavior. *Proceedings of the National Academy of Sciences of the United States of America, 104*(25), 10661-10666. doi:10.1073/pnas.0610849104

Manes, Jordan L., Parkinson, Amy L., Larson, Charles R., Greenlee, Jeremy D., Eickhoff, Simon B., Corcos, Daniel M., & Robin, Donald A. (2014). Connectivity of the

subthalamic nucleus and globus pallidus pars interna to regions within the speech network: A meta-analytic connectivity study. *Human Brain Mapping, 35*(7), 3499-3516. doi:10.1002/hbm.22417

Mansouri, F. A., Buckley, M. J., & Tanaka, K. (2014). The essential role of primate orbitofrontal cortex in conflict-induced executive control adjustment. *The Journal of Neuroscience, 34*(33), 11016-11031. doi:10.1523/JNEUROSCI.1637-14.2014

Mar, A. C., Walker, A. L., Theobald, D. E., Eagle, D. M., & Robbins, T. W. (2011). Dissociable effects of lesions to orbitofrontal cortex subregions on impulsive choice in the rat. *The Journal of Neuroscience, 31*(17), 6398-6404. doi:10.1523/JNEUROSCI.6620-10.2011

Marx, C., Lex, B., Calaminus, C., Hauber, W., Backes, H., Neumaier, B., . . . Endepols, H. (2012). Conflict Processing in the Rat Brain: Behavioral Analysis and Functional muPET Imaging Using [F]Fluorodeoxyglucose. *Frontiers in Behavioral Neuroscience, 6*, 4. doi:10.3389/fnbeh.2012.00004

Maviel, T., Durkin, T.P., Menzaghi, F., & Bontempi, B. (2004). Sites of neocortical neorganization nritical for remote spatial memory. *Science, 305*, 96-99. doi:10.1126/science.1098180

McKenzie, S., & Eichenbaum, H. (2011). Consolidation and reconsolidation: two lives of memories? *Neuron, 71*(2), 224-233. doi:10.1016/j.neuron.2011.06.037

McNaughton, N. (2014). Development of a theoretically-derived human anxiety syndrome biomarker. *Translational Neuroscience, 5*(2). doi:10.2478/s13380-014-0220-z

McNaughton, N., & Corr, P. J. (2004). A two-dimensional neuropsychology of defense: fear/anxiety and defensive distance. *Neuroscience & Biobehavioral Reviews, 28*(3), 285-305. doi:10.1016/j.neubiorev.2004.03.005

McNaughton, N., & Corr, P. J. (2014). Approach, avoidance, and their conflict: the problem of anchoring. *Frontiers in Systems Neuroscience, 8*, 124. doi:10.3389/fnsys.2014.00124

McNaughton, N., DeYoung, C.G., & Corr, P.J. (2016). *Approach/Avoidance*: Elsevier.

McNaughton, N., & Gray, J. A. (2000). Anxiolytic action on the behavioural inhibition system implies multiple types of arousal contribute to anxiety. *Journal of Affective Disorders, 61*(3), 161-176. doi:10.1016/s0165-0327(00)00344-x

McNaughton, N., Ruan, M., & Woodnorth, M. A. (2006). Restoring theta-like rhythmicity in rats restores initial learning in the Morris water maze. *Hippocampus, 16*(12), 1102-1110. doi:10.1002/hipo.20235

McNaughton, N., Swart, C., Neo, P., Bates, V., & Glue, P. (2013). Anti-anxiety drugs reduce conflict-specific "theta"--a possible human anxiety-specific biomarker. *Journal of Affective Disorders, 148*(1), 104-111. doi:10.1016/j.jad.2012.11.057

Michell, Susan J., & Ranck, James B. (1980). Generation of theta rhythm in medial entorhinal cortex of freely moving rats. *Brain Research, 189*, 49-66.

Miller, E. K., & Cohen, J. D. (2001). An intergrative theory of prefrontal cortex function. *Annual Review of Neuroscience, 24*, 167-202. doi:10.1146/annurev.neuro.24.1.167

Mogenson, G. J., Jones, D. L., & Yim, C. Y. (1980). From motivation to action: Functional interface between the limbic system and the mot. *Progress in Neurobiology, 14*(69-97). doi:10.1016/0301-0082(80)90018-0

Morgane, P. J., Galler, J. R., & Mokler, D. J. (2005). A review of systems and networks of the limbic forebrain/limbic midbrain. *Progress in Neurobiology, 75*(2), 143-160. doi:10.1016/j.pneurobio.2005.01.001

Moser, E. I., Roudi, Y., Witter, M. P., Kentros, C., Bonhoeffer, T., & Moser, M. B. (2014). Grid cells and cortical representation. *Nature reviews neuroscience, 15*(7), 466-481. doi:10.1038/nrn3766

Nacher, V., Ledberg, A., Deco, G., & Romo, R. (2013). Coherent delta-band oscillations between cortical areas correlate with decision making. *Proceedings of the National*

Academy of Sciences of the United States of America, 110(37), 15085-15090. doi:10.1073/pnas.1314681110

Nambu, A., Tokuno, H., & Takada, M. (2002). Functional significance of the cortico-subthalamo-pallidal 'hyperdirect' pathway. *Neuroscience Research, 43,* 111-117. doi:10.1016/S0168-0102(02)00027-5

Neo, P. S., Thurlow, J. K., & McNaughton, N. (2011). Stopping, goal-conflict, trait anxiety and frontal rhythmic power in the stop-signal task. *Cognitive, Affective, & Behavioral Neuroscience, 11*(4), 485-493. doi:10.3758/s13415-011-0046-x

Nogueira, R., Abolafia, J. M., Drugowitsch, J., Balaguer-Ballester, E., Sanchez-Vives, M. V., & Moreno-Bote, R. (2017). Lateral orbitofrontal cortex anticipates choices and integrates prior with current information. *Nature Communications, 8,* 14823. doi:10.1038/ncomms14823

Numan, R. (2015). A Prefrontal-Hippocampal Comparator for Goal-Directed Behavior: The Intentional Self and Episodic Memory. *Frontiers in Behavioral Neuroscience, 9,* 323. doi:10.3389/fnbeh.2015.00323

O'Keefe, J., & Nadel, L. (1978). *The Hippocampus as a Cognitive Map*: Oxford: Clarendon Press.

O'Mara, S. (2005). The subiculum: what it does, what it might do, and what neuroanatomy has yet to tell us. *Journal of Anatomy, 207*(3), 271-282. doi:10.1111/j.1469-7580.2005.00446.x

O'Neil, E. B., Newsome, R. N., Li, I. H., Thavabalasingam, S., Ito, R., & Lee, A. C. (2015). Examining the Role of the Human Hippocampus in Approach-Avoidance Decision Making Using a Novel Conflict Paradigm and Multivariate Functional Magnetic Resonance Imaging. *The Journal of Neuroscience, 35*(45), 15039-15049. doi:10.1523/JNEUROSCI.1915-15.2015

O'Neill, P. K., Gordon, J. A., & Sigurdsson, T. (2013). Theta oscillations in the medial prefrontal cortex are modulated by spatial working memory and synchronize with the hippocampus through its ventral subregion. *The Journal of Neuroscience, 33*(35), 14211-14224. doi:10.1523/JNEUROSCI.2378-13.2013

Obeso, I., Wilkinson, L. , Rodríguez-Oroz, M. , Obeso, J.A., & Jahanshahi, M. (2013). Bilateral stimulation of the subthalamic nucleus has differential effects on reactive and proactive inhibition and conflict-induced slowing in Parkinson's disease. *Experimental brain research*. doi:10.1007/s00221-013-3457-9)

Ojemann, G. A., Ojemann, J., & Ramsey, N. F. (2013). Relation between functional magnetic resonance imaging (fMRI) and single neuron, local field potential (LFP) and electrocorticography (ECoG) activity in human cortex. *Frontiers in Human Neuroscience, 7*, 34. doi:10.3389/fnhum.2013.00034

Oldham, S., Murawski, C., Fornito, A., Youssef, G., Yucel, M., & Lorenzetti, V. (2018). The anticipation and outcome phases of reward and loss processing: A neuroimaging meta-analysis of the monetary incentive delay task. *Human Brain Mapping, 39*(8), 3398-3418. doi:10.1002/hbm.24184

Packard, M. G., & Knowlton, B. J. (2002). Learning and memory functions of the Basal Ganglia. *Annual Review of Neuroscience, 25*, 563-593. doi:10.1146/annurev.neuro.25.112701.142937

Pani, P., Di Bello, F., Brunamonti, E., D'Andrea, V., Papazachariadis, O., & Ferraina, S. (2014). Alpha- and beta-band oscillations subserve different processes in reactive control of limb movements. *Frontiers in Behavioral Neuroscience, 8*, 383. doi:10.3389/fnbeh.2014.00383

Pare, D., & Collins, D. R. (2000). Neuronal correlates of fear in the lateral amygdala: Multiple extracellular reordings in conscious cats. *The Journal of Neuroscience, 20*(7), 2. doi:10.1523/JNEUROSCI.20-07-02701.2000

Paxinos, G., & Watson, C. (2007). *The rat brain in sterotaxic coordinates* (6th ed.). London: Academic Press.

Pignatelli, M., Beyeler, A., & Leinekugel, X. (2012). Neural circuits underlying the generation of theta oscillations. *Journal of Physiology-Paris, 106*(3-4), 81-92. doi:10.1016/j.jphysparis.2011.09.007

Poldrack, R. A., Clark, J., Pare-Blagoev, E. J., Shohamy, D., Moyano, J. C, Myers, c., . . . 414. (2001). Interactive memory systems in the human brain. *Nature, 414*, 546-550. doi:doi: 10.1038/35107080

Powers, K. E., Somerville, L. H., Kelley, W. M., & Heatherton, T. F. (2016). Striatal Associative Learning Signals Are Tuned to In-groups. *Journal of cognitive Neuroscience, 28*(9), 1243-1254. doi:10.1162/jocn_a_00971

Purgert, R. J., Wheeler, D. S., McDannald, M. A., & Holland, P. C. (2012). Role of amygdala central nucleus in aversive learning produced by shock or by unexpected omission of food. *The Journal of Neuroscience, 32*(7), 2461-2472. doi:10.1523/JNEUROSCI.5090-11.2012

Ray, N. J., Brittain, J. S., Holland, P., Joundi, R. A., Stein, J. F., Aziz, T. Z., & Jenkinson, N. (2012). The role of the subthalamic nucleus in response inhibition: evidence from local field potential recordings in the human subthalamic nucleus. *Neuroimage, 60*(1), 271-278. doi:10.1016/j.neuroimage.2011.12.035

Redgrave, P., Prescott, T. J., & Gurney, K. (1999). The basal ganglia: A vertebrate solution to the selection problem? *Neuroscience, 89*(4), 1009-1023. doi:10.1016/S0306-4522(98)00319-4

Riceberg, J. S., & Shapiro, M. L. (2012). Reward stability determines the contribution of orbitofrontal cortex to adaptive behavior. *The Journal of Neuroscience, 32*(46), 16402-16409. doi:10.1523/JNEUROSCI.0776-12.2012

Roberts, A. C., Tomic, D. L., Parkinson, C. H., Roeling, T. A., Cutter, D. J., Robbins, T. W., & Everitt, B. J. (2007). Forebrain connectivity of the prefrontal cortex in the marmoset monkey (Callithrix jacchus): an anterograde and retrograde tract-tracing study. *The Journal of Comparative Neurology, 502*(1), 86-112. doi:10.1002/cne.21300

Rolls, E. T. (2004). The functions of the orbitofrontal cortex. *Brain and Cognition, 55*(1), 11-29. doi:10.1016/s0278-2626(03)00277-x

Rolls, E. T., & Grabenhorst, F. (2008). The orbitofrontal cortex and beyond: from affect to decision-making. *Progress in Neurobiology, 86*(3), 216-244. doi:10.1016/j.pneurobio.2008.09.001

Rolls, E. T., & Xiang, J.Z. (2005). Reward–Spatial View Representations and Learning in the Primate Hippocampus. *The Journal of Neuroscience, 25*(26), 6167-6174. doi:10.1523/JNEUROSCI.1481-05.2005

Ross, R. S., Sherrill, K. R., & Stern, C. E. (2011). The hippocampus is functionally connected to the striatum and orbitofrontal cortex during context dependent decision making. *Brain Research, 1423*, 53-66. doi:10.1016/j.brainres.2011.09.038

Rothenhoefer, K. M., Costa, V. D., Bartolo, R., Vicario-Feliciano, R., Murray, E. A., & Averbeck, B. B. (2017). Effects of Ventral Striatum Lesions on Stimulus-Based versus Action-Based Reinforcement Learning. *The Journal of Neuroscience, 37*(29), 6902-6914. doi:10.1523/JNEUROSCI.0631-17.2017

Rubin, R. D., Watson, P. D., Duff, M. C., & Cohen, N. J. (2014). The role of the hippocampus in flexible cognition and social behavior. *Frontiers in Human Neuroscience, 8*, 742. doi:10.3389/fnhum.2014.00742

Rudebeck, P. H., Ripple, J. A., Mitz, A. R., Averbeck, B. B., & Murray, E. A. (2017). Amygdala Contributions to Stimulus-Reward Encoding in the Macaque Medial and Orbital Frontal Cortex during Learning. *The Journal of Neuroscience, 37*(8), 2186-2202. doi:10.1523/JNEUROSCI.0933-16.2017

Rudebeck, P. H., Walton, M. E., Smyth, A. N., Bannerman, D. M., & Rushworth, M. F. (2006). Separate neural pathways process different decision costs. *Nature Neuroscience, 9*(9), 1161-1168. doi:10.1038/nn1756

Sainsbury, R.S. (1998). Hippocampal Theta: a Sensory-inhibition Theory of Function. *Neuroscience & Biobehavioral Reviews, 22*(2), 237-241. doi:10.1016/S0149-7634(97)00011-0

Sakimoto, Y., & Sakata, S. (2015). Change in hippocampal theta activity during behavioral inhibition for a stimulus having an overlapping element. *Behavioural Brain Research, 282*, 111-116. doi:10.1016/j.bbr.2014.12.041

Schmidt, R., Leventhal, D. K., Mallet, N., Chen, F., & Berke, J. D. (2013). Canceling actions involves a race between basal ganglia pathways. *Nature Neuroscience, 16*(8), 1118-1124. doi:10.1038/nn.3456

Schmidtke, K., Manner, H., Kaufmann, R., & Schmolck, H. (2002). Cognitive procedural learning in patients with fronto-striatal lesions. *Learning & Memory, 9*(6), 419-429. doi:10.1101/lm.47202

Schultz, W. (2015). Neuronal Reward and Decision Signals: From Theories to Data. *Physiological Reviews, 95*(3), 853-951. doi:10.1152/physrev.00023.2014

Schumacher, A., Villaruel, F. R., Ussling, A., Riaz, S., Lee, A. C. H., & Ito, R. (2018). Ventral Hippocampal CA1 and CA3 Differentially Mediate Learned Approach-Avoidance Conflict Processing. *Current Biology*. doi:10.1016/j.cub.2018.03.012

Sesack, S. R., & Grace, A. A. (2010). Cortico-Basal Ganglia reward network: microcircuitry. *Neuropsychopharmacology, 35*(1), 27-47. doi:10.1038/npp.2009.93

Shadli, S. M., Glue, P., McIntosh, J., & McNaughton, N. (2015). An improved human anxiety process biomarker: characterization of frequency band, personality and pharmacology. *Translational Psychiatry, 5*, e699. doi:10.1038/tp.2015.188

Shan, Q., Ge, M., Christie, M. J., & Balleine, B. W. (2014). The acquisition of goal-directed actions generates opposing plasticity in direct and indirect pathways in dorsomedial striatum. *The Journal of Neuroscience, 34*(28), 9196-9201. doi:10.1523/JNEUROSCI.0313-14.2014

Sharott, Andrew. (2014). Local Field Potential, Methods of Recording. 1-3. doi:10.1007/978-1-4614-7320-6_723-1

Shiflett, M. W., & Balleine, B. W. (2010). At the limbic-motor interface: disconnection of basolateral amygdala from nucleus accumbens core and shell reveals dissociable components of incentive motivation. *European Journal of Neuroscience, 32*(10), 1735-1743. doi:10.1111/j.1460-9568.2010.07439.x

Silkis, I. G. (2008). A mechanism for influencing the septo-hippocampal theta rhythm by dopamine through the basal ganglia. *Neurochemical Journal, 2*(3), 157-163. doi:10.1134/s1819712408030045

Smith, Y., Bevan, M. D. , Shink, E., & Bolam, J. P. (1998). Microcircuitry of the direct and indirect pathways of the basal ganglia. *Neuroscience, 86*, 353–387. doi:10.1016/S0306-4522(98)00004-9

Stalnaker, T. A., Cooch, N. K., & Schoenbaum, G. (2015). What the orbitofrontal cortex does not do. *Nature Neuroscience, 18*(5), 620-627. doi:10.1038/nn.3982

Temel, Y., Blokland, A., Steinbusch, H. W., & Visser-Vandewalle, V. (2005). The functional role of the subthalamic nucleus in cognitive and limbic circuits. *Progress in Neurobiology, 76*(6), 393-413. doi:10.1016/j.pneurobio.2005.09.005

Thut, G., Miniussi, C., & Gross, J. (2012). The functional importance of rhythmic activity in the brain. *Current Biology, 22*(16), R658-663. doi:10.1016/j.cub.2012.06.061

Tommasi, G., Fiorio, M., Yelnik, J., Krack, P., Sala, F., Schmitt, E., . . . Chelazzi, L. (2015). Disentangling the Role of Cortico-Basal Ganglia Loops in Top-Down and Bottom-Up Visual Attention: An Investigation of Attention Deficits in Parkinson Disease. *Journal of cognitive Neuroscience, 27*(6), 1215-1237. doi:10.1162/jocn_a_00770

Tort, A. B., Kramer, M. A., Thorn, C., Gibson, D. J., Kubota, Y., Graybiel, A. M., & Kopell, N. J. (2008). Dynamic cross-frequency couplings of local field potential oscillations in rat striatum and hippocampus during performance of a T-maze task. *Proceedings of the National Academy of Sciences of the United States of America, 105*(51), 20517-20522. doi:10.1073/pnas.0810524105

Tricomi, E., & Lempert, K. M. (2015). Value and probability coding in a feedback-based learning task utilizing food rewards. *Journal of Neurophysiology, 113*(1), 4-13. doi:10.1152/jn.00086.2014

van der Meer, M. A., & Redish, A. D. (2009). Low and High Gamma Oscillations in Rat Ventral Striatum have Distinct Relationships to Behavior, Reward, and Spiking Activity on a Learned Spatial Decision Task. *Frontiers in Integrative Neuroscience, 3*, 9. doi:10.3389/neuro.07.009.2009

van Strien, N. M., Cappaert, N. L., & Witter, M. P. (2009). The anatomy of memory: an interactive overview of the parahippocampal-hippocampal network. *Nature reviews neuroscience, 10*(4), 272-282. doi:10.1038/nrn2614

van Wijk, B. C., Beek, P. J., & Daffertshofer, A. (2012). Neural synchrony within the motor system: what have we learned so far? *Frontiers in Human Neuroscience, 6*, 252. doi:10.3389/fnhum.2012.00252

van Wingerden, M., van der Meij, R., Kalenscher, T., Maris, E., & Pennartz, C. M. (2014). Phase-amplitude coupling in rat orbitofrontal cortex discriminates between correct and incorrect decisions during associative learning. *The Journal of Neuroscience, 34*(2), 493-505. doi:10.1523/JNEUROSCI.2098-13.2014

van Wingerden, M., Vinck, M., Lankelma, J., & Pennartz, C. M. (2010). Theta-band phase locking of orbitofrontal neurons during reward expectancy. *The Journal of Neuroscience, 30*(20), 7078-7087. doi:10.1523/JNEUROSCI.3860-09.2010

Vandecasteele, M., Varga, V., Berenyi, A., Papp, E., Bartho, P., Venance, L., . . . Buzsaki, G. (2014). Optogenetic activation of septal cholinergic neurons suppresses sharp wave ripples and enhances theta oscillations in the hippocampus. *Proceedings of the National Academy of Sciences of the United States of America, 111*(37), 13535-13540. doi:10.1073/pnas.1411233111

Vartak, D., Jeurissen, D., Self, M. W., & Roelfsema, P. R. (2017). The influence of attention and reward on the learning of stimulus-response associations. *Scientific Reports, 7*(1), 9036. doi:10.1038/s41598-017-08200-w

Verbruggen, F., & Logan, G. D. (2008a). Automatic and controlled response inhibition: associative learning in the go/no-go and stop-signal paradigms. *Journal of experimental psychology. General, 137*(4), 649-672. doi:10.1037/a0013170

Verbruggen, F., & Logan, G. D. (2008b). Response inhibition in the stop-signal paradigm. *Trends in cognitive sciences, 12*(11), 418-424. doi:10.1016/j.tics.2008.07.005

Verbruggen, F., & Logan, G. D. (2009). Models of response inhibition in the stop-signal and stop-change paradigms. *Neuroscience & Biobehavioral Reviews, 33*(5), 647-661. doi:10.1016/j.neubiorev.2008.08.014

Vertes, R. P., Hoover, W. B., & Viana Di Prisco, G. (2004). Theta rhythm of the hippocampus: subcortical control and functional significance. *Behavioral and Cognitive Neuroscience Reviews, 3*(3), 173-200. doi:10.1177/1534582304273594

Vinogradova, O.S. (2001). Hippocampus as comparator: Role of the two input and two output systems of the hippocmapus in selection and registration of inofrmation. *Hippocampus, 11*, 578-598. doi:10.1002/hipo.1073

Wang, C. H., Chang, C. C., Liang, Y. M., Shih, C. M., Chiu, W. S., Tseng, P., . . . Juan, C. H. (2013). Open vs. closed skill sports and the modulation of inhibitory control. *Plos One, 8*(2), e55773. doi:10.1371/journal.pone.0055773

Wang, S. H., & Morris, R. G. (2010). Hippocampal-neocortical interactions in memory formation, consolidation, and reconsolidation. *Annual Review of Psychology, 61*, 49-79, C41-44. doi:10.1146/annurev.psych.093008.100523

Wessel, J. R., & Aron, A. R. (2017). On the Globality of Motor Suppression: Unexpected Events and Their Influence on Behavior and Cognition. *Neuron, 93*(2), 259-280. doi:10.1016/j.neuron.2016.12.013

Wessel, J. R., Jenkinson, Ned, Brittain, John-Stuart, Voets, Sarah H. E. M., Aziz, Tipu Z., & Aron, Adam R. (2016). Surprise disrupts cognition via a fronto-basal ganglia suppressive mechanism. *Nature Communications, 7*. doi:10.1038/ncomms11195

Wickens, Jeffery R., Reynolds, John N. J., & Hyland, Brian I. (2003). Neural mechanisms of reward-related motor learning. *Current Opinion in Neurobiology, 13*(6), 685-690. doi:10.1016/j.conb.2003.10.013

Wiecki, T. V., & J., Frank M. (2013). A computational model of inhibitory control in frontal cortex and basal ganglia. *Psychological Review, 120*(2), 329-355. doi:10.1037/a0031542.supp

Wikenheiser, A. M., & Schoenbaum, G. (2016). Over the river, through the woods: cognitive maps in the hippocampus and orbitofrontal cortex. *Nature reviews neuroscience, 17*(8), 513-523. doi:10.1038/nrn.2016.56

Winstanley, C. A., Theobald, D. E., Cardinal, R. N., & Robbins, T. W. (2004). Contrasting roles of basolateral amygdala and orbitofrontal cortex in impulsive choice. *The Journal of Neuroscience, 24*(20), 4718-4722. doi:10.1523/JNEUROSCI.5606-03.2004

Yin, H. H., Ostlund, S. B., Knowlton, B. J., & Balleine, B. W. (2005). The role of the dorsomedial striatum in instrumental conditioning. *European Journal of Neuroscience, 22*(2), 513-523. doi:10.1111/j.1460-9568.2005.04218.x

Yordanova, J., Kolev, V., & Kirov, R. (2012). Brain oscillations and predictive processing. *Behavioural Brain Research, 3*, 416. doi:10.3389/fpsyg.2012.00416

Young, C. K., & Eggermont, J. J. (2009). Coupling of mesoscopic brain oscillations: Recent advances in analytical and theoretical perspectives. *Progress in Neurobiology*, *89*(1), 61-78. doi:10.1016/j.pneurobio.2009.06.002

Young, J. J., & Shapiro, M. L. (2011). The orbitofrontal cortex and response selection. *Annals of the New York Academy of Sciences, 1239*, 25-32. doi:10.1111/j.1749-6632.2011.06279.x

Zahm, D. S. (2000). An integrative neuroanatomical perspective on some subcortical substrates of adaptive responding with emphasis on the nucleus accumbens. *Neuroscience and Biobehavioral Reviews, 24*, 85-105. doi:10.1016/S0149-7634(99)00065-2

Zavala, B., Tan, H., Ashkan, K., Foltynie, T., Limousin, P., Zrinzo, L., . . . Brown, P. (2016). Human subthalamic nucleus-medial frontal cortex theta phase coherence is involved in

conflict and error related cortical monitoring. *Neuroimage, 137*, 178-187. doi:10.1016/j.neuroimage.2016.05.031

Zavala, B., Tan, H., Little, S., Ashkan, K., Hariz, M., Foltynie, T., . . . Brown, P. (2014). Midline frontal cortex low-frequency activity drives subthalamic nucleus oscillations during conflict. *The Journal of Neuroscience, 34*(21), 7322-7333. doi:10.1523/JNEUROSCI.1169-14.2014

Zavala, B., Zaghloul, K., & Brown, P. (2015). The subthalamic nucleus, oscillations, and conflict. *Movement Disorders, 30*(3), 328-338. doi:10.1002/mds.26072

Appendix 1

Animal Welfare Score Sheet for Rodents

One sheet per animal to record parameters listed below

Animal/Species # _____ **Date of Treatment/Operation:-**_____

Pre-study Bodyweight: _____ **Surgeon:** _____ **AEC #:** _____

Date												
Day												

BODY WEIGHT & B.A.R. SCORE

Body wt yesterday												
Body wt today												
Body wt change												
BAR (bright, alert, responsive)												
Approach response (inquisitive behaviour investigates your presence)												

GENERAL CLINICAL SIGNS

Inactive												
Hunched posture												
Coat rough , fur on end												
Red eye/nose discharges												
Pink staining of neck												
Dehydration - Skin turgor test (see reverse)												

BEHAVIOURAL SIGNS OF PAIN IN RATS ***each time when sign is observed)***

Back arch Hunched up with arched back												
Belly press Presses belly to cage floor												
Writhe Twisting of body or flank												
Stagger Sudden loss of balance /gait												
Twitch Sudden spasm of flank muscles												
Fall Rat falls over												

WATER BALANCE *(Healthy animals drink approx 10% body wt per day, e.g. a 300gm rat should drink 30mls every 24hrs)*

Start weight of bottle (A)												
Current weight of bottle (B)												
Water intake (A-B) mls												

OPERATION SITE

Wound OK												
Bleeding												
Sutures/clips OK												

POST-OP SUPPORT - Analgesic Administration

Drug												
Dose												
Fluids by SC injection												
Other drugs												
Signature												

Appendix 2

Design of jig and jig base used in the thesis